AD_____

Award Number: DAMD17-00-1-0454

TITLE: Assessment of the Activation of Rho Family GTP-Binding Proteins in Breast Cancer Cells and Specimens

PRINCIPAL INVESTIGATOR: Yi Zheng, Ph.D.

CONTRACTING ORGANIZATION: University of Tennessee, Memphis
Memphis, Tennessee 38163

REPORT DATE: August 2001

TYPE OF REPORT: Annual

PREPARED FOR: U.S. Army Medical Research and Materiel Command
Fort Detrick, Maryland 21702-5012

REPORT DOCUMENTATION PAGE

Form Approved
OMB No. 074-0188

1. AGENCY USE ONLY (Leave blank)	2. REPORT DATE	3. REPORT TYPE AND DATES COVERED
	August 2001	Annual (3 Jul 00 - 2 Jul 01)

4. TITLE AND SUBTITLE
Assessment of the Activation of Rho Family GTP-Binding Proteins in Breast Cancer Cells and Specimens

5. FUNDING NUMBERS
DAMD17-00-1-0454

6. AUTHOR(S)
Yi Zheng, Ph.D.

7. PERFORMING ORGANIZATION NAME(S) AND ADDRESS(ES)
University of Tennessee, Memphis
Memphis, Tennessee 38163

E-Mail: Yxheng@utmem.edu

8. PERFORMING ORGANIZATION REPORT NUMBER

9. SPONSORING / MONITORING AGENCY NAME(S) AND ADDRESS(ES)
U.S. Army Medical Research and Materiel Command
Fort Detrick, Maryland 21702-5012

10. SPONSORING / MONITORING AGENCY REPORT NUMBER

11. SUPPLEMENTARY NOTES
Report contains color photos.

12a. DISTRIBUTION / AVAILABILITY STATEMENT
Approved for Public Release; Distribution Unlimited

12b. DISTRIBUTION CODE

13. ABSTRACT ***(Maximum 200 Words)***

Rho GTPases have begun to be appreciated to play roles in breast carcinogenesis. To establish a causal link between activation of individual Rho signaling events and certain aspects of breast cancer development, we have started to search for direct effect on Rho GTPases in mitogenic conditions and in various physiological situations that may be connected to mammary cell transformation. As stated in this first annual report, we have established a method using the Rho GTPase-interactive effector domains of WASP, PAK1, and Rhotekin to quantitatively define the activation-states of Rho family members Cdc42, Rac, and Rho in cells, and applied this method to four cellular conditions which are related to mammary tumorigenesis. These studies are significant since the findings further confirmed the involvement of Rho GTPases in diverse physiological situations that may contribute to oncogenesis, and have paved the way for us to examine the endogenous Rho family GTPases in mitogen-stimulated or oncogene-transformed mammary cells and in breast cancer specimens. The results obtained also strengthened our working hypothesis that certain Rho GTPases are activated in breast cancer cells and tissues and that exploration of the role Rho proteins in breast may lead to novel anti-cancer therapeutics.

14. SUBJECT TERMS	15. NUMBER OF PAGES
Cancer biology, Cell signaling, GTP-Binding proteins, Rho/Rac/Cdc42, Effector targets	112
	16. PRICE CODE

17. SECURITY CLASSIFICATION OF REPORT	18. SECURITY CLASSIFICATION OF THIS PAGE	19. SECURITY CLASSIFICATION OF ABSTRACT	20. LIMITATION OF ABSTRACT
Unclassified	Unclassified	Unclassified	Unlimited

Table of Contents

Introduction

The Rho family small GTPases function as molecular switches that control the signal flows from a variety of cell surface receptors. Among the panel of receptors that require Rho family GTPases to relay signals leading to mammary cell transformation and metastasis, the epidermal growth factor receptor, the erbB-2 gene product, the colony stimulating factor-1 receptor, and the cell adhesion receptor integrins are the prominent ones. Overexpression or mutation of these receptors and many signal transducers downstream of these receptors are known to correlate with breast carcinogenesis. We hypothesize that in breast cancer cells overexpressing or bearing mutations of one of the oncogenic receptors, Ras proteins, or Rho-specific activators, a higher percentage of Rho family members, Rho, Rac or Cdc42, are in the active state. Determination of the activation states of these GTPases in breast tumors and defining which tumor types show increased Rho, Rac, or Cdc42 activation will lead the way in the search for a direct connection between Rho pathways and breast cancer genesis, and may provide novel treatment strategies targeted at the Rho signaling components. We have utilized a novel method to measure the activation state of endogenous Rho family GTPases in the oncogenic and mitogenic pathways of model cell systems and will further extend it to examine the activation state of the Rho family members, Rho, Rac, Cdc42, in breast cancer cells and specimens.

Body

The first two aims (task 1 and task 2) were proposed for months 1-10 and months 6-24 of the funding period, which overlap in this first annual report. Specifically, we have proposed to determine which p21-binding domains (PBDs) of effectors are most suitable for the detection of activated RhoA and Rac1 (task 1) and to begin to apply the efector PBD-binding assay to the examination of endogenous Rho family GTPases in mitogen-stimulated or oncogene-transformed cells. Such studies are necessary for later investigation of the potential involvement of Rho pathways in transducing mitogenic/oncogenic signals in mammary cells and in breast cancer specimens. To this end, we have mostly completed the tasks we set out before, and we do not expect any major changes to the original Statement of Work. The results are summarized below.

1. Activation and translocation of Cdc42 and Rac1 by mitogenic and adhesion signals.

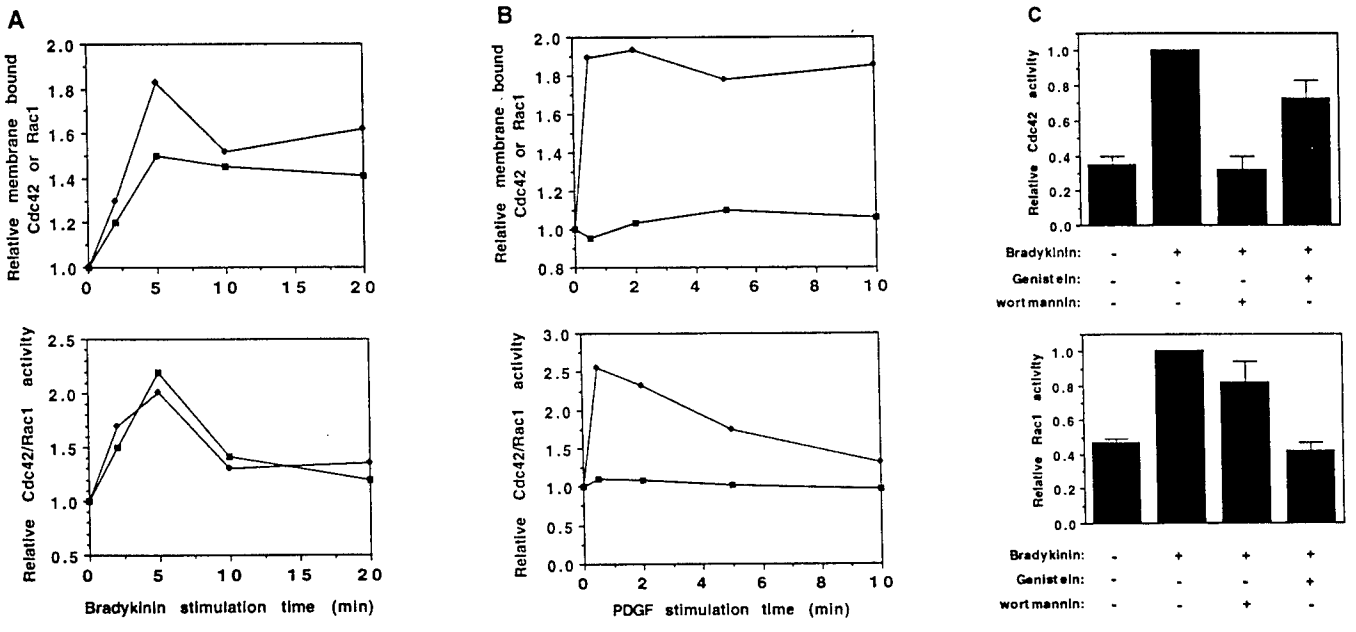

Figure 1. Effect of bradykinin and PDGF on the cellular distribution and activation of Cdc42 and Rac1. Swiss 3T3 cells were serum starved overnight before challenged with 100 ng/ml bradykinin (A) or 50 ng/ml PDGF (B) for the indicated times. The cells were lysed and fractionated as described (84) and the cytosol and high speed membranes were analyzed for total Cdc42 or Rac1 as well as for the active, GTP-bound Cdc42 or Rac1 by Western blotting of the proteins with or without GST-PAK1 pull-down treatment. Square symbols, Cdc42; triangles, Rac1. C, Cdc42 and Rac1 activation stimulated by bradykinin in cells pretreated with tyrosine kinase and PI 3-kinase inhibitors. 100 μM genistein or 30 nM wortmannin were added to the cells in the serum-free medium for 30 min at 37 °C. Cells were then stimulated with 100ng/ml bradykinin for 5 min before the addition of ice-cold lysis buffer. Cell lysates were subjected to GST-PAK1 affinity precipitation analysis.

The Rho family GTPases Cdc42 and Rac1 are important signal transducers of many receptor-initiated pathways (1, 2) and are regulated by mitogenic signals such as bradykinin and PDGF as well as by adhesion (3, 4, 5). We have investigated the relationship between membrane translocation and activation of endogenous Cdc42 and Rac1 in response to mitogenic and integrin stimulation. The mitogen bradykinin induced translocation of Cdc42 and Rac1 to a membrane fraction of Swiss 3T3 cells within two minutes, which correlated with the activation kinetics of the GTPases (Fig. 1A). PDGF treatment of the cells induced rapid translocation and activation of Rac1 but not Cdc42 within 30 seconds (Fig. 1B). The activation of Cdc42 and Rac1 appeared to precede actin microspike formation or membrane ruffle induction of the cells. However, the translocated GTPases were found to remain membrane bound for a much longer time course than their activation status, suggesting that a deactivation event occurs at the membrane level. Cell adhesion on fibronectin matrix resulted in transient activation of both Cdc42 and Rac1, and caused a partial inhibition of bradykinin or PDGF effect on the small G-proteins. Pretreatment of the cells with genistein or wortmannin significantly reduced the bradykinin, PDGF, or fibronectin stimulated Cdc42 or Rac1 activity (Fig. 1C), indicating that both tyrosine kinase and PI3 kinase are required elements of the small G-protein pathways. Finally, Cdc42 and Rac1 activation by bradykinin were abolished by pertussis toxin treatment, whereas the outcome by the PDGF or integrin treatment was unaffected. These results suggest that mitogenic agonist and integrin mediated signals are integrated at the small G-protein level, and tyrosine kinase, PI3 kinase, and/or heterotrimeric G-proteins are intimately involved in the Cdc42 and Rac1 activation process.

2. Genetic deletion of the Pten tumor suppresor gene promotes cell motility by activation of Rac1 and Cdc42 GTPases.

Pten is a recently identified tumor suppressor gene which is deleted or mutated in a variety of primary human cancers including breast cancer (6). Pten has been implicated in controlling cell migration, among other functions, but the exact mechanism is not very clear (7). In collaboration with Dr. Hong Wu's laboratory (UCLA), we have shown that *Pten* deficiency led to increased cell motility (8). Significant increases in the endogenous activities of Rac1 and cdc42, two small GTPases involved in regulating the actin cytoskeleton, were observed in Pten-/- cells. Overexpression of dominant negative mutant forms of Rac1 and cdc42 reversed the cell migration phenotype of Pten-/- cells. These studies suggest that Pten negatively controls cell motility by down-regulating Rac1 and Cdc42 (reprint enclosed in Appendix).

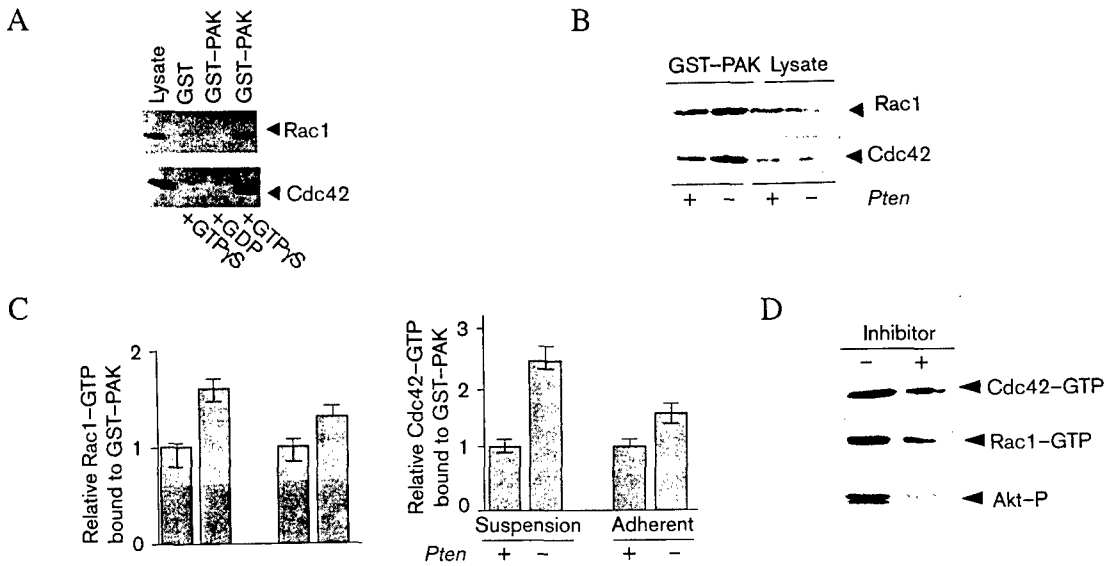

Figure 2. Pten deletion results in activation of Rac1 and Cdc42. A, GST-PAK binding is specific for GTP-bound Rac1 and Cdc42. Pten-/- fibroblast lysates were loaded with GTPgS or GDP prior to affinity precipitation with 10 μg GST or GST-PAK immobilized on glutathione agarose beads. The precipitated proteins were analyzed by Western blot with anti-Rac1 or anti-Cdc42 antibodies. B, The GST-PAK precipitates from wild type (+) and Pten-/- (-) fibroblasts under log phase growing conditions, along with cell lysates, were analyzed by western blots. C, Wild type or Pten-/- cells, either in suspension or adherent, were lysed and subjected to GST-PAK affinity precipitation. Rac1-GTP (left graph) or Cdc42-GTP (right graph) activities detected were normalized to the amount of Rac1 or Cdc42 in whole cell lysates. Results are means +/- SD from three experiments. D, Pten-/- cells were treated with 20 μM LY294002 (+) or 50 nM wortmannin (not shown) or DMSO vehicle control (-) for 6 hr before harvesting. Cell lysates were precipitated with GST-PAK and blotted with anti-Rac1 or anti-Cdc42. In parallel, aliquots of cell lysates were analyzed with anti-phospho-Akt antibody.

3. Examination of proto-Dbl guanine nucleotide exchange activity in cells.

The *dbl* oncogene encodes a prototype member of the Rho GTPase guanine nucleotide exchange factor (GEF) family (9). Oncogenic activation of proto-Dbl occurs through the truncation of N-terminal 497 residues (10). The C-terminal half of proto-Dbl includes residues 498-680 and 710-815 that fold into the Dbl homology (DH) domain and the pleckstrin homology (PH) domain, respectively, both of which are essential for cell transformation via the Rho GEF activity or cytoskeletal targeting function (11). We have investigated the mechanism of the apparent negative regulation of proto-Dbl imposed by the N-terminal sequences, employing the GST-effector pull down assays to detect the effect of various proto-Dbl constructs on the endogenous Rho GTPase activities (12). Deletion of the N-terminal 285 or C-terminal 100 residues of proto-Dbl did not significantly effect on either its transforming activity or GEF activity, while removal of the N-terminal 348 amino acids

resulted in a significant increase in both transformation and GEF potential. Together with other cell biology evidence, our findings unveiled an autoinhibitory mode of regulation of proto-Dbl that is mediated by the intramolecular interaction between its N-terminal sequences and PH domain, directly impacting on both the GEF function and intracellular distribution (reprint enclosed in Appendix).

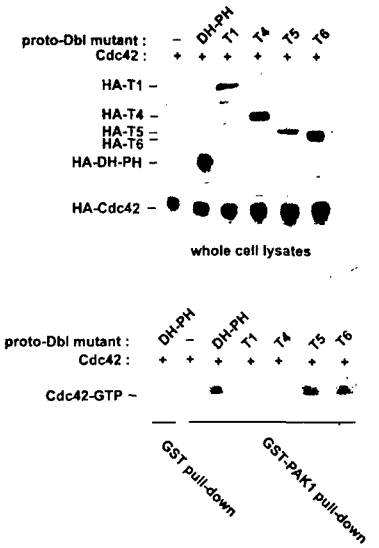

Figure 3. Detection of the Cdc42 exchange potential by the proto-Dbl mutants in cells. $(HA)_3$-Cdc42 was expressed alone or together with HA-DH-PH, HA-T1, HA-T4, HA-T5, or HA-T6 in Cos-7 cells. The cell lysates were probed with anti-HA antibody in a Western blot. The cell lysates were subjected to GST or GST-PAK1 pull-down assay, and the glutathione agarose co-precipitates were detected by anti-HA Western blotting to reveal the relative amount of Cdc42-GTP in cells.

4. Modulation of RhoA activity in epithelial cells by Na,K-ATPase.

The mechanism by which the formation of tight junctions and desmosomes are regulated in polarized epithelial cells are not well understood (13-14). Such mechanism may be tightly associated with mammary epithelial transformation (15). In collaboration with Dr. A. K. Rajasekaran's laboratory (UCLA), we have investigated the involvement of RhoA GTPase in Na,K-ATPase mediated assembly of tight junctions and desmosomes in MDCK cells (16). We found that an increased sodium level caused by the inhibition of Na,K-ATPase prevents the formation of tight junctions and desmosomes and this effect is negatively correlated with the endogenous RhoA activity. The results indicate that the intracellular sodium level maintained by the N,K-ATPase is an upstream regulator of RhoA GTPase function in epithelial cells and might play a crucial role in the biogenesis of polarized epithelia (see Appendix for details).

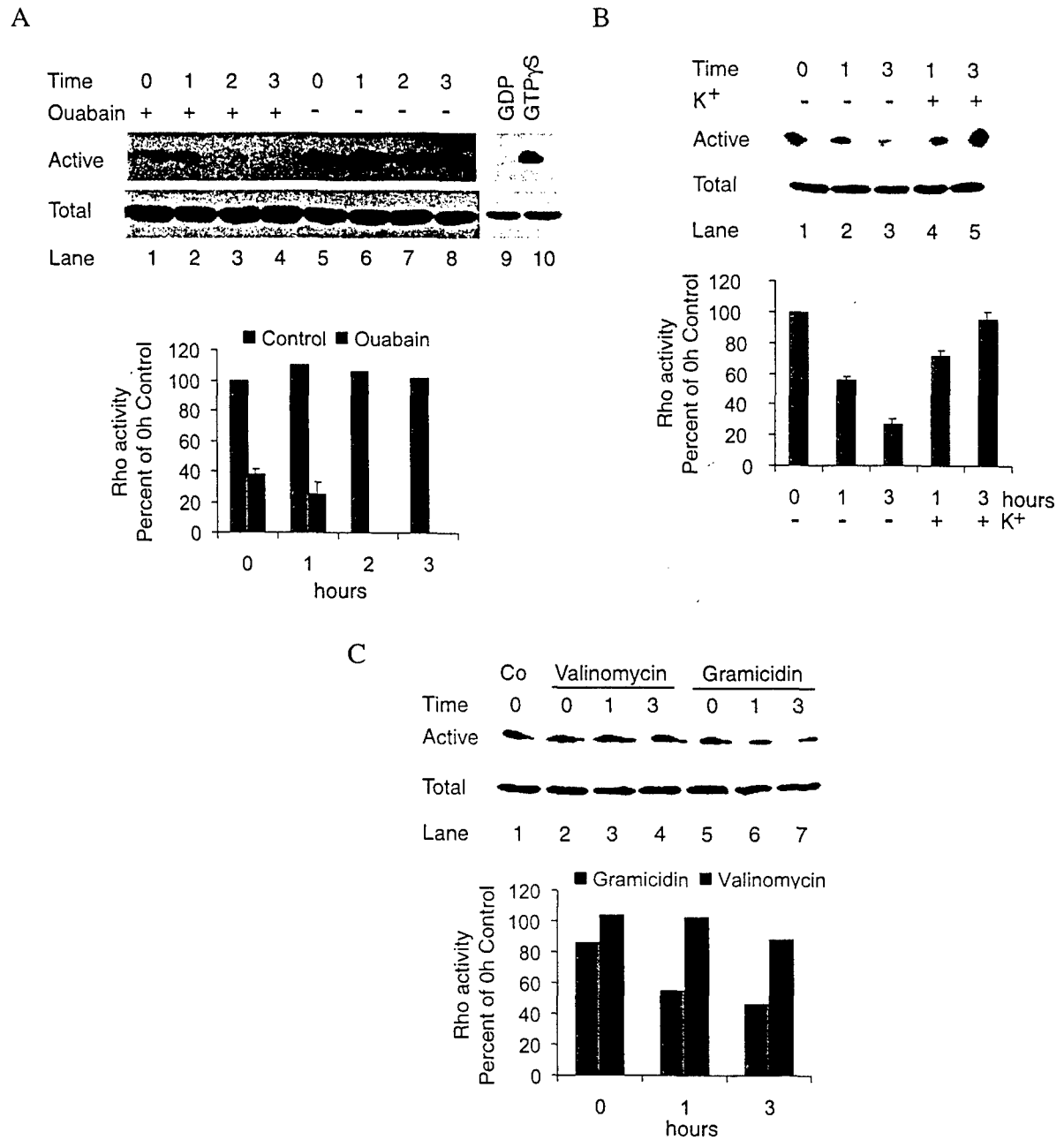

Figure 4. Inhibition of Na,K-ATPase led to down-regulation of RhoA activity in MDCK cells. A, effect of ouabain treatment on RhoA activity. Immunoblots show active and total RhoA in ouabain and control cells. The immunobloting results were quantified to yield the bar graph. B, effect of K^+ depletion and repletion on RhoA activity. Immunoblots of active and total RhoA are quantified and represent the mean of two independent experiments. C, effect of gramicidin and valinomycin on RhoA activity.

Key Research Accomplishments

- Established that the Rho GTPase-interactive effector domains of WASP, PAK1, and Rhotekin constitute the activation-state specific probes for Cdc42, Rac, and Rho that can be utilized to detect endogenous Cdc42-GTP, Rac1-GTP, and RhoA-GTP species, respectively.

- Applied GST-PAK1 probe to Swiss 3T3 model cell system to determine the activation kinetics of endogenous Cdc42 and Rac1 in response to the mitogen, bradykinin or PDGF, stimulation.

- Applied GST-PAK1 and GST-Rhotekin probes in NIH 3T3 cells transfected with various proto-Dbl oncogene products to reveal the activation states of Cdc42 and RhoA that were regulated by proto-Dbl derivatives, suggesting that residues 286 to 482 of proto-Dbl are involved in an autoinhibition mechanism.

- Applied GST-WASP, GST-PAK1, and GST-Rhotekin to the tumor-suppressor, Pten, knock-out mouse embryonic fibroblasts to determine that all three major Rho GTPases activities become upregulated in the system, which correlates with increase motility of the cells, suggesting that Pten negatively controls cell motility by down-regulating Rac1 and Cdc42.

- Applied GST-Rhotekin to an epithelial cell system to determine that inhibition of Na,K-ATPase negatively regulates RhoA activity, which may in turn affect the formation of tight junctions and desmosomes.

Reportable Outcomes

- Liliental, J., Moon, S. Y., Lesche, R., Mamillapalli, R., Gavrilova, N., **Zheng, Y.**, Sun, H., and Wu, H. (2000) Genetic deletion of the PTEN tumor suppresor gene promotes cell motility by activation of Rac1 and Cdc42 GTPases. *Curr. Biol.* 10, 401-404.

- Bi, F., Debreceni, B., Zhu, K., Salani, B., Eva, A, and **Zheng, Y.** (2001) Autoinhibition mechanism of proto-Dbl. *Mol. Cell. Biol.* 21, 1463-1474.

- Rajasekaran, S. A., Palmer, L. G., Moon, S. Y., Soler, A. P., Apodaca, G. L., Harper, J. F., **Zheng, Y.**, and Rajasekaran, A. K. (2001) Na,K-ATPase regulates the formation of tight junctions and desmosomes through RhoA GTPase. *Mol. Biol. Cell* submitted.

- **Zheng, Y.** (2001) Dbl family guanine nucleotide exchange factors for Rho GTPases. *Trends Biochem. Sci.* in press.

Conclusions

Rho GTPase signaling pathways have begun to be appreciated to play roles in breast carcinogenesis. To establish a causal link between activation of individual Rho signaling events and certain aspects of breast cancer development, we have started to search for direct effect on Rho GTPases in mitogenic conditions, and in various physiological situations that may be connected to mammary cell transformation and metastasis. As stated in this first annual report, we have established a method using the Rho GTPase-interactive effector domains of WASP, PAK1, and Rhotekin to quantitatively define the activation-states of Rho family members Cdc42, Rac, and Rho in cells, and applied this method to four cellular conditions which are all related to mammary tumorigenesis: (1) in a Swiss 3T3 model cell system to determine the activation kinetics of endogenous Cdc42 and Rac1 in response to the mitogen, bradykinin or PDGF, stimulation; (2) in NIH 3T3 cells transfected with various proto-Dbl oncogene products to reveal the activation states of Cdc42 and RhoA that were regulated by proto-Dbl derivatives, suggesting that residues 286 to 482 of proto-Dbl are involved in an autoinhibition mechanism; (3) in the tumor-suppressor, Pten, knock-out mouse embryonic fibroblasts to determine that all three major Rho GTPases activities become upregulated in the system, which correlates with increase motility of the cells, suggesting that Pten negatively controls cell motility by down-regulating Rac1 and Cdc42; and (4) in an epithelial cell system to determine that inhibition of Na,K-ATPase negatively regulates RhoA activity, which may in turn affect the formation of tight junctions and desmosomes. These studies are significant since the findings have further confirmed the involvement of Rho GTPases in diverse physiological situations that may contribute to oncogenesis, and have paved the way for us to examine the endogenous Rho family GTPases in mitogen-stimulated or oncogene-transformed mammary cells and in breast cancer specimens in the next funding period. The results obtained also strengthened our working hypothesis that certain Rho GTPases are activated in breast cancer cells and tissues, and exploration of the role Rho proteins in breast cancer development may lead to novel anti-cancer therapeutics.

References

1. Hall, A. (1998) Rho GTPases and the actin cytoskeleton. *Science* 279, 509-514.

2. van Aelst, L., and D'Souza-Schorey, C. (1997) Rho GTPases and signaling networks. *Genes & Dev.* 11, 2295-2322.

3. Zohn, I. M., Campbell, S. L., Khosravi-Far, R., Rossman, K. L., and Der, C. J. (1998) Rho family proteins and Ras transformation: the RHOad less traveled gets congested. *Oncogene* 13, 1415-1438.

4. Ridley, A. J. (1996) Rho: theme and variations. *Curr. Biol.* 6, 1256-1264.

5. Schwartz, M. A., and Shattil, S. J. (2000) Signaling networks linking integrins and Rho family GTPases. *Trends Biochem. Sci.* 25, 388-341.

6. Eng, C., Peacocke, M. (1998) Genetics of Cowden syndrome: through the looking glass of oncology. Int. J. Oncology 12, 701-710.

7. Tamura, M., Gu, J., Matsumoto, K., Aota, S., Parsons, R., Yamada, K. M. (1998) Inhibition of cell migration, spreading, and focal adhesions by tumor suppressor PTEN. *Science* 280, 1614-1617.

8. Liliental, J., Moon, S. Y., Lesche, R., Mamillapalli, R., Gavrilova, N., Zheng, Y., Sun, H., and Wu, H. (2000) Genetic deletion of the PTEN tumor suppresor gene promotes cell motility by activation of Rac1 and Cdc42 GTPases. *Curr. Biol.* 10, 401-404.

9. Zheng, Y. (2001) Dbl family guanine nucleotide exchange factors for Rho GTPases. *Trends Biochem. Sci.* in press.

10. Ron, D., Tronick, S. R., Aaronson, S. A., and Eva, A. (1998) Molecular cloning and characterization of the human dbl proto-oncogene: evidence that its overexppresion is sufficient to transform NIH3T3 cells. EMBO J. 7, 2465-2473.

11. Zheng, Y., Zangrilli, D., Cerione, R. A., and Eva, A. (1996) The pleckstrin homology domain mediates transformation by oncogenic Dbl through specific intracellular targeting. J. Biol. Chem. 271, 19017-19020.

12. Bi, F., Debreceni, B., Zhu, K., Salani, B., Eva, A, and Zheng, Y. (2001) Autoinhibition mechanism of proto-Dbl. *Mol. Cell. Biol.* 21, 1463-1474.

13. Yap, A. S., Brieher, W. M., and Gumbiner, B. M. (1997) Molecular and functional analysis of cadherin-based adherens junctions. Ann. Rev. Cell Dev. Biol. 13, 119-146.

14. Garrod, D., Chidgey, M., and North, A. (1996) Desmosomes: differentiation, development, dynamics, and disease. Curr. Opin. Cell Biol. 5, 670-678.

15. Keely, P., Parise, L., and Juliano, R. (1998) Integrins and GTPases in tumour cell growth, motility and invasion. *Trends Cell Biol.* 8, 101-106.

16. Rajasekaran, S. A., Palmer, L. G., Moon, S. Y., Soler, A. P., Apodaca, G. L., Harper, J. F., Zheng, Y., and Rajasekaran, A. K. (2001) Na,K-ATPase regulates the formation of tight junctions and desmosomes through RhoA GTPase. *Mol. Biol. Cell* submitted.

Appendices

Reprints and preprints of research work supported by the grant are enclosed. Four manuscripts described in Reportable Outcomes are included.

Genetic deletion of the *Pten* tumor suppressor gene promotes cell motility by activation of Rac1 and Cdc42 GTPases

Joanna Liliental*†, Sun Young Moon‡, Ralf Lesche*§, Ramanaiah Mamillapalli¶, Daming Li¶, Yi Zheng‡, Hong Sun¶ and Hong Wu*§

***Pten* (Phosphatase and tensin homolog deleted on chromosome 10) is a recently identified tumor suppressor gene which is deleted or mutated in a variety of primary human cancers and in three cancer predisposition syndromes [1]. Pten regulates apoptosis and cell cycle progression through its phosphatase activity on phosphatidylinositol (PI) 3,4,5-trisphosphate (PI(3,4,5)P_3), a product of PI 3-kinase [2–5]. Pten has also been implicated in controlling cell migration [6], but the exact mechanism is not very clear. Using the isogenic *Pten*$^{+/+}$ and *Pten*$^{-/-}$ mouse fibroblast lines, here we show that Pten deficiency led to increased cell motility. Reintroducing the wild-type *Pten*, but not the catalytically inactive *Pten* C124S or lipid-phosphatase-deficient *Pten* G129E mutant, reduced the enhanced cell motility of Pten-deficient cells. Moreover, phosphorylation of the focal adhesion kinase p125^{FAK} was not changed in *Pten*$^{-/-}$ cells. Instead, significant increases in the endogenous activities of Rac1 and Cdc42, two small GTPases involved in regulating the actin cytoskeleton [7], were observed in *Pten*$^{-/-}$ cells. Overexpression of dominant-negative mutant forms of Rac1 and Cdc42 reversed the cell migration phenotype of *Pten*$^{-/-}$ cells. Thus, our studies suggest that Pten negatively controls cell motility through its lipid phosphatase activity by down-regulating Rac1 and Cdc42.**

Addresses: *Howard Hughes Medical Institute, †Department of Microbiology and Molecular Immunology, and §Department of Molecular and Medical Pharmacology, University of California at Los Angeles School of Medicine, 650 Circle Drive South, Los Angeles, California 90095-1735, USA. ‡Department of Biochemistry, University of Tennessee, Memphis, Tennessee 38163, USA. ¶Department of Genetics, Yale University School of Medicine, 333 Cedar Street, New Haven, Connecticut 06520, USA.

Correspondence: Hong Wu
E-mail: hwu@mednet.ucla.edu

Received: **23 November 1999**
Revised: **4 January 2000**
Accepted: **21 January 2000**

Published: **24 March 2000**

Current Biology 2000, 10:401–404

0960-9822/00/$ – see front matter

Results and discussion

To test the role of Pten in cell migration, we established independent immortalized fibroblast lines from wild-type and *Pten* deficient (*Pten*$^{-/-}$) mice, using the 3T9 protocol [8]. Similar to primary mouse embryonic fibroblasts [4], the immortalized *Pten*$^{-/-}$ cell lines showed increased levels of phosphorylation of protein kinase B/Akt compared to their wild-type counterparts and were resistant to serum-deprivation induced apoptosis. In contrast to our observation with wild-type and *Pten*$^{-/-}$ embryonic stem cells [4], however, no significant differences in the rates of cell proliferation and the levels of the cyclin-dependent kinase inhibitor p27^{KIP1} could be detected between log-phase growing wild-type and *Pten*$^{-/-}$ fibroblast cells (data not shown).

Pten$^{-/-}$ fibroblasts have an increased cell motility, as shown by a classic 'wound healing' assay (Figure 1a, left panels) [9]. They were able to completely close the wound within 15 hours, whereas wild-type cells took almost 30 hours. To demonstrate that the increase in cell migration is an individual cell based and cell division-independent event, we employed a colloidal-gold based motility assay [10]. This assay revealed that *Pten*$^{-/-}$ fibroblasts could produce longer 'trails' than wild-type cells in a defined time period, indicating that *Pten*$^{-/-}$ cells indeed migrate faster than the wild-type cells (Figure 1a, middle panels). In order to obtain more quantitative measurements of the migration distance, we employed a modified 'wound healing' assay. In this assay, cells are first seeded on coverslips, and then transferred to a new plate coated with fibronectin. Upon transfer, cells migrate from the rim of the coverslip outwards onto the new plate. As shown in Figure 1a (right panels) and quantified in Figure 1b with independent cell lines, *Pten*$^{-/-}$ cells migrate almost twice as fast as wild-type cells. Moreover, careful observation of cell morphology revealed that *Pten*$^{-/-}$ fibroblasts appeared rounded and had intense cortical F-actin staining (Figure 1c). Together, these results suggest that Pten negatively regulates signaling pathways controlling cell migration.

In order to determine whether increased cell migration in *Pten*$^{-/-}$ cells is due to lack of the Pten phosphatase activity or if other structural motifs may play a role, we re-introduced either wild-type *Pten* or *Pten* C124S, a catalytically inactive mutant, into the *Pten*$^{-/-}$ cells by retrovirus infection [11]. We used a retroviral vector that expresses the gene of interest and the green fluorescent protein (GFP) as a bicistronic mRNA. GFP-positive, thus *Pten*-expressing, cells were sorted by fluorescence activated cell sorting (FACS) following retroviral infection. Wild-type *Pten* and the C124S mutant were expressed in comparable levels in the sorted populations (Figure 2c). As shown in Figure 2a

Figure 1

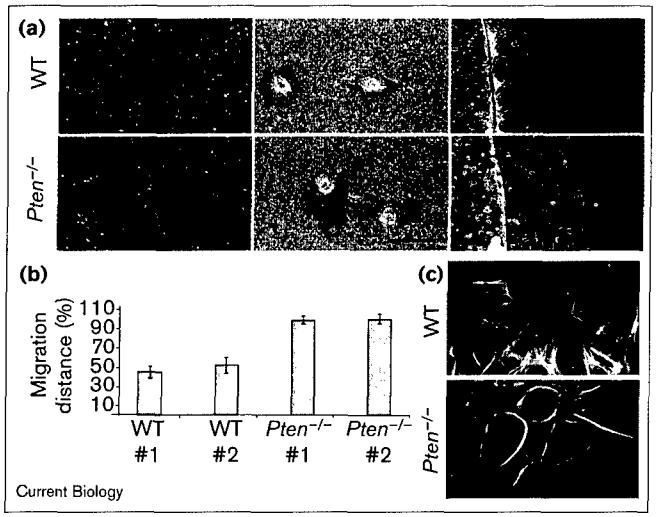

Pten-deficient fibroblasts migrate faster than wild type. **(a)** An equal number of wild-type (WT) or *Pten*$^{-/-}$ fibroblasts were seeded on a fibronectin-coated plate and cultured for 24 h. Migration into the wound is shown 15 h after the wound was introduced (left panels; open arrowheads point to the boundaries of the wound at time = 0). In the middle panel, 2×10^3 cells per well were seeded on colloidal gold-coated 6-well dishes in duplicates. Migration of wild-type or *Pten*$^{-/-}$ fibroblasts is shown at 24 h. The scale bar represents 10 μm. In the right panels, wild-type or *Pten*$^{-/-}$ fibroblasts grown on glass coverslips were placed onto 5 μg/ml fibronectin-coated dishes and cultured for 15 h. **(b)** Cell motility was assessed and compared using independent cell lines. Migration distances were determined by taking seven independent measurements from each coverslip. Each experiment was conducted in triplicate, and mean ± SD was calculated. The migration distance is normalized so that 100% represents migration distance of *Pten*$^{-/-}$ cells. **(c)** *Pten*$^{-/-}$ cells exhibited increased cortical actin polymerization as compared to the wild-type cells. Briefly, log-phase growing fibroblasts were cultured without serum for 20 h. After fixation in 4% paraformaldehyde, cells were permeabilized with 0.2% Triton X-100 and stained for F-actin using rhodamine–phalloidin (Molecular Probes).

Figure 2

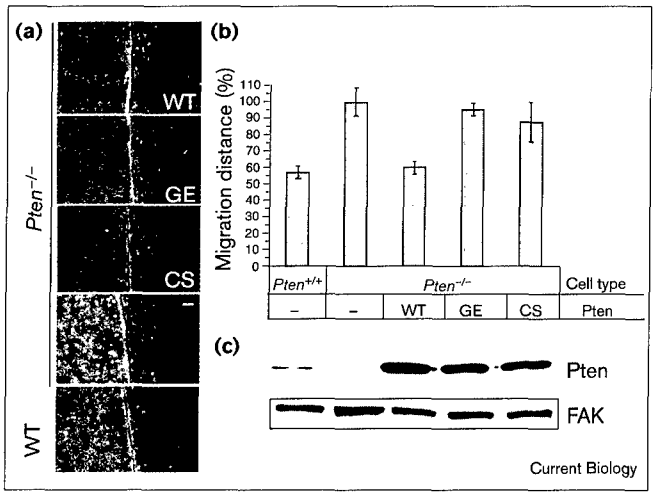

Increased cell motility in *Pten*$^{-/-}$ cells is due to the lack of lipid phosphatase activity of *Pten*. **(a)** *Pten*$^{-/-}$ cells were infected with retroviral GFP vectors containing wild-type *Pten* (WT), G129E (GE), or C124S (CS) *Pten* mutants. Control wild-type or *Pten*$^{-/-}$ cells were infected with viruses containing GFP only. 48 h later, GFP positive cells were sorted by fluorescence-activated cell sorting (FACS), seeded onto glass coverslips in triplicate, and grown for an additional 5 h. Cells on coverslips were then replaced onto a fibronectin-coated surface and incubated for 15 h. **(b)** Quantitative representation of (a). Cell migration is normalized so that 100% represents the migration distance of *Pten*$^{-/-}$ cells infected by empty vector. **(c)** Pten protein levels in uninfected and infected cells after FACS sorting. Western blots of total protein extracts were probed with an affinity-purified anti-Pten antibody. Blots were reprobed with anti-FAK antibody (Santa Cruz Biotechnology) to confirm equal loading.

and quantified in Figure 2b, wild-type *Pten*, but not the C124S mutant, could fully reverse the migration phenotype of *Pten*$^{-/-}$ cells, confirming that the enhanced motility is directly due to the lack of Pten phosphatase activity.

Recent studies suggested that PI(3,4,5)P_3 is a major substrate for Pten both *in vitro* [2] and *in vivo* [3,4]. Interestingly, *Pten* G129E is deficient for the phosphatase activity towards PI(3,4,5)P_3, while its activity towards synthetic protein substrates is unaffected [12]. Using the *Pten* G129E mutant, we further tested whether Pten controls cell migration through its lipid phosphatase activity or its protein phosphatase activities. *Pten* G129E behaved similarly to the C124S mutant as they were both unable to rescue the migration phenotype in this assay. This experiment suggests that the enhanced motility of *Pten*$^{-/-}$ cells is a result of the loss of Pten phosphatase activity, in particular, its lipid-phosphatase activity.

It has been suggested that Pten negatively regulates cell migration by directly dephosphorylating p125^{FAK} and changing mitogen-activated protein (MAP) kinase activity [6,13]. In order to test whether p125^{FAK} phosphorylation and MAP kinase activation are also affected by the loss of *Pten*, we examined the tyrosine phosphorylation status of these proteins. Whole cell lysates from log-phase growing wild-type or *Pten*$^{-/-}$ fibroblasts were immunoprecipitated with 4G10 anti-phosphotyrosine antibody and western blotted with anti-FAK antibody (Figure 3a, upper panel), or were immunoprecipitated with anti-FAK antibody and western blotted with 4G10 (Figure 3b, lower panel). In contrast to what would be predicted if Pten could directly dephosphorylate p125^{FAK}, no difference in tyrosine phosphorylation of p125^{FAK} could be detected in *Pten*$^{-/-}$ fibroblast lines compared to wild-type cells. The activation status of MAP kinases was not affected by the *Pten* deletion either, but the level of Akt phosphorylation was significantly increased in *Pten*$^{-/-}$ fibroblast cell lines (data not shown), similar to what we have observed previously in *Pten*$^{-/-}$ embryonic stem cells [4]. These results suggest that the enhanced cell motility caused by *Pten* deficiency may be mediated by effectors other than p125^{FAK} and MAP kinases.

Figure 3

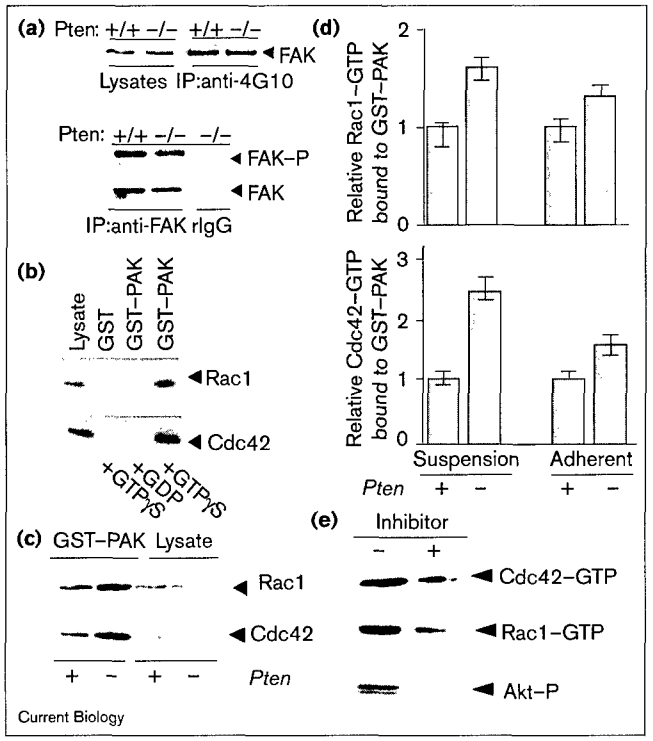

Pten deletion results in activation of Rac1 and Cdc42, but not FAK. **(a)** FAK phosphorylation is not affected by *Pten* deletion. Upper panel, equal amounts of proteins were immunoprecipitated with anti-phosphotyrosine antibody (4G10, Upstate Biotechnology). Western blots were probed with anti-FAK antibody. Bottom panel, anti-FAK immunoprecipitates were western blotted with 4G10 (for phosphorylated FAK, FAK–P) or an anti-FAK antibody. rIgG indicates immunoprecipitation with a rabbit isotype control antibody. **(b)** GST–PAK binding is specific for GTP. *Pten*$^{-/-}$ fibroblast lysates were loaded with GTPγS or GDP prior to affinity precipitation with GST or GST–PAK immobilized on 10 μg glutathione–agarose beads. The precipitated proteins were analyzed by western blot with anti-Rac1 (Upstate Biotechnology) or anti-Cdc42 (Santa Cruz Biotechnology) antibody, respectively. Results are representative of three independent experiments. **(c)** The GST–PAK precipitates from wild-type (+) and *Pten*$^{-/-}$ (–) fibroblasts under log phase growing conditions, along with total cell lysates, were analyzed by western blot with anti-Rac1 or anti-Cdc42 antibodies. **(d)** Wild-type or *Pten*$^{-/-}$ cells, either in suspension or adherent, were lysed and subjected to GST–PAK affinity precipitation analysis. The Rac1–GTP (upper graph) or Cdc42–GTP (lower graph) activities detected by western blot were normalized to the amount of Rac1 or Cdc42 in whole cell lysates. Results are means ± SD from three experiments. **(e)** *Pten*$^{-/-}$ cells were treated with 20 μM LY294002 (shown here, +), or 50 nM wortmannin (not shown), or DMSO vehicle control (–) for 6 h before harvesting. Cell lysates were precipitated with GST–PAK and blotted with anti-Rac1 or anti-Cdc42 antibodies, respectively. In parallel, aliquots of cell lysates were analyzed with anti-phospho-Akt antibody (New England Biolabs).

Figure 4

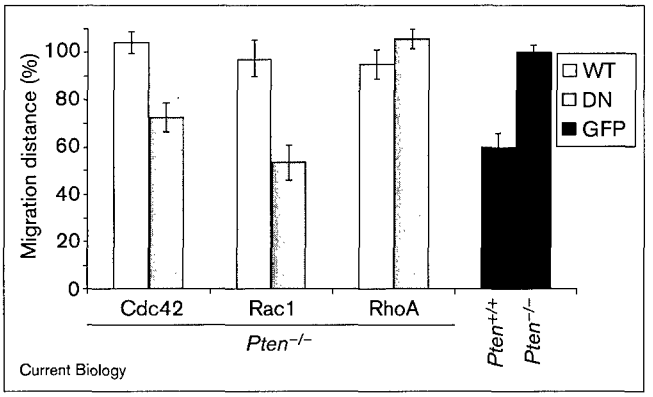

Increased motility of *Pten*$^{-/-}$ cells can be reversed by expression of dominant-negative (DN) Rac1 and Cdc42, but not RhoA. Cell motility was assessed by directly measuring the migration distance 15 h after plating, and presented as an average of three independent experiments. WT, wild-type constructs were expressed; GFP, a GFP-expressing vector only was expressed.

As increased cell motility is associated with a deficiency in Pten lipid-phosphatase activity, and cells in which *Pten* is genetically deleted contain elevated levels of PI(3,4,5)P_3 [3,4], we next examined whether activation of known downstream PI(3,4,5)P_3 effectors might be responsible for the increased cell migration phenotype in *Pten*$^{-/-}$ cells. Activation of Cdc42 and Rac1 has been implicated in promoting cell migration [7] and their GDP/GTP exchange factors (GEFs) can be activated in a PI(3,4,5)P_3-dependent manner [14,15]. We therefore examined whether Pten deficiency leads to changes in the Rac1 and Cdc42 activities. In this assay, the p21-binding domain of PAK1 was expressed as a GST-fusion protein. GST–PAK1 can specifically recognize Rac1–GTP or Cdc42–GTP forms, but not GDP-bound forms, suggesting that the affinity precipitation assay is specific and effective in assessing the activation states of Rac1 and Cdc42 (Figure 3b). We then examined the level of endogenous GTP-bound forms of Rac1 or Cdc42 in *Pten*$^{-/-}$ cells and wild-type cells. As shown in Figure 3c, there are marked increases of the GTP-bound forms of Rac1 and Cdc42 in logarithmically growing *Pten*$^{-/-}$ cells compared to wild-type cells, although the total protein levels are not affected by the *Pten* status. As PI(3,4,5)P_3 levels were highly sensitive to growth conditions [4], we also examined the Rac1 and Cdc42 activities in unfavorable confluent culture conditions. There is a notable ~30% increase in Rac1–GTP content and a ~50% increase in Cdc42–GTP content compared to the wild-type cells (Figure 3d). When similar assays were performed using suspended cell cultures which lack the adherent stimuli, ~60% and ~130% increases of Rac1–GTP and Cdc42–GTP forms, respectively, were observed (Figure 3d, suspension). The extent of elevation in the endogenous Cdc42 and Rac1 activities in *Pten*$^{-/-}$ cells were consistent when independent cell lines were used, and reintroducing wild-type *Pten* into *Pten*$^{-/-}$ cells led to a decrease in the GTP-bound forms of Rac1 and Cdc42 (data not shown).

Recent experiments demonstrated that a correlation exists between activation of the activity of PI 3-kinase and the activities of Rac1 and Cdc42 [14–17]. However, whether PI 3-kinase functions downstream or upstream of Rac1 and Cdc42 remains unclear. To test whether Rac1 and Cdc42 were activated in a PI 3-kinase dependent manner, we treated *Pten*$^{-/-}$ cells with the PI 3-kinase inhibitor LY294002 or wortmannin. Figure 3e shows that the activities of Rac1 and Cdc42 dramatically decrease upon treatment with PI 3-kinase inhibitors, indicating that similar to Akt, Rac1 and Cdc42 activation in *Pten*$^{-/-}$ cells is downstream of PI 3-kinase.

To formally prove that the elevated endogenous activities of Rac1 and Cdc42 in *Pten*$^{-/-}$ cells are responsible for the increased cell migration phenotype, we introduced either wild-type or dominant negative forms of Rac1 (N17Rac1) and Cdc42 (N17Cdc42) into *Pten*$^{-/-}$ cells by retroviral infection. These mutants are thought to act by sequestering specific GEFs necessary for activation of Rac1 and Cdc42, preventing their functions. Figure 4 shows that expression of N17Rac1 and N17Cdc42 in *Pten*$^{-/-}$ cells could reverse the cell migration phenotype by 100% and 50%, respectively. The less efficient reversion by N17Cdc42 is not due to the lower expression level (data not shown), but could reflect the suggested hierarchical relationship between Rac1 and Cdc42, where Cdc42 is thought to function upstream of Rac1 [7]. As a control for the specificity of these GTPases, we also expressed the dominant negative form of RhoA (N19RhoA), a GTPase involved in focal adhesion and stress fiber formation [18,19]. No effect on the migration of *Pten*$^{-/-}$ fibroblasts was observed with N19RhoA, or with the wild-type Rho GTPases (Figure 4). These results indicate that Rac1 and Cdc42 serve as downstream effectors of Pten in the regulation of cell migration.

In summary, we show that inactivation of the *Pten* tumor suppressor gene promotes cell motility in fibroblasts. In contrast to previous reports that Pten negatively regulates cell migration by directly dephosphorylating p125^{FAK} and changing MAP kinase activities, we demonstrate genetically that the tumor suppressor Pten controls cell motility by down regulating Rac1 and Cdc42 GTPases, and this negative regulation is dependent on the lipid phosphatase activity of Pten. In combination with our previous work and other studies, we suggest that Pten exerts its tumor suppressor function not only at the stage of tumor initiation, but also in tumor progression and metastasis.

Supplementary material

Supplementary material including additional methodological details is available at http://current-biology.com/supmat/supmatin.htm.

Acknowledgements

We thank H. Herschman, O. Witte, C. Sawyers, K. Shuai, X. Liu for critical reading of the manuscript. We thank X.L. Liu and H.L. Lodish of MIT for kindly providing pMX-IRES-GFP vector, and Jing Gao and Nadia Gavrilova for technical assistance. R.L. is supported by the Deutsche Forschungsgemeinschaft and a Carolan Seed grant (to H.W.). H.S. is a Pew Scholar in the Biomedical Sciences. H.W. is an Assistant Investigator of the Howard Hughes Medical Institute and V Foundation Scholar. This work was supported by the V foundation and a Carolan Seed grant (to H.W.); American Cancer Society (RPG-97-146) and National Institutes of Health grant (GM53943 to Y.Z.); Department of the Army (DAMD 17-98-1-8271) and National Institutes of Health grant (CA77695 to H.S.).

References

1. Eng C, Peacocke M: **Genetics of Cowden syndrome: through the looking glass of oncology.** *Int J Oncology* 1998, **12:**701-710.
2. Maehama T, Dixon JE: **The tumor suppressor, PTEN/MMAC1, dephosphorylates the lipid second messenger, phosphatidylinositol 3,4,5-trisphosphate.** *J Biol Chem* 1998, **273:**13375-13378.
3. Stambolic V, Suzuki A, de la Pompa JL, Brothers GM, Mirtsos C, Sasaki T, *et al.*: **Negative regulation of PKB/Akt-dependent cell survival by the tumor suppressor PTEN.** *Cell* 1998, **95:**29-39.
4. Sun H, Lesche R, Li DM, Liliental J, Zhang H, Gao J, *et al.*: **PTEN modulates cell cycle progression and cell survival by regulating phosphatidylinositol 3,4,5,-trisphosphate and Akt/protein kinase B signaling pathway.** *Proc Natl Acad Sci USA* 1999, **96:**6199-6204.
5. Cantley LC, Neel BG: **New insights into tumor suppression: PTEN suppresses tumor formation by restraining the phosphoinositide 3-kinase/AKT pathway.** *Proc Natl Acad Sci USA* 1999, **96:**4240-4245.
6. Tamura M, Gu J, Matsumoto K, Aota S, Parsons R, Yamada KM: **Inhibition of cell migration, spreading, and focal adhesions by tumor suppressor PTEN.** *Science* 1998, **280:**1614-1617.
7. Hall A: **Rho GTPases and the actin cytoskeleton.** *Science* 1998, **279:**509-514.
8. Kamijo T, Zindy F, Roussel MF, Quelle DE, Downing JR, Ashmun RA, *et al.*: **Tumor suppression at the mouse INK4a locus mediated by the alternative reading frame product p19ARF.** *Cell* 1997, **91:**649-659.
9. Xu W, Baribault H, Adamson ED: **Vinculin knockout results in heart and brain defects during embryonic development.** *Development* 1998, **125:**327-337.
10. Takaishi K, Sasaki T, Takai Y: **Cell motility assay and inhibition by Rho-GDP dissociation inhibitor.** *Methods Enzymol* 1995, **256:**336-347.
11. Grignani F, Kinsella T, Mencarelli A, Valtieri M, Riganelli D, Lanfrancone L, *et al.*: **High-efficiency gene transfer and selection of human hematopoietic progenitor cells with a hybrid EBV/retroviral vector expressing the green fluorescence protein.** *Cancer Res* 1998, **58:**14-19.
12. Myers MP, Pass I, Batty IH, Van der Kaay J, Stolarov JP, Hemmings BA, *et al.*: **The lipid phosphatase activity of PTEN is critical for its tumor suppressor function.** *Proc Natl Acad Sci USA* 1998, **95:**13513-13518.
13. Gu J, Tamura M, Yamada KM: **Tumor suppressor PTEN inhibits integrin- and growth factor-mediated mitogen-activated protein (MAP) kinase signaling pathways.** *J Cell Biol* 1998, **143:**1375-1383.
14. Van Aelst L, D'Souza-Schorey C: **Rho GTPases and signaling networks.** *Genes Dev* 1997, **11:**2295-2322.
15. Han J, Luby-Phelps K, Das B, Shu X, Xia Y, Mosteller RD, *et al.*: **Role of substrates and products of PI 3-kinase in regulating activation of Rac-related guanosine triphosphatases by Vav.** *Science* 1998, **279:**558-560.
16. Tolias KF, Cantley LC, Carpenter CL: **Rho family GTPases bind to phosphoinositide kinases.** *J Biol Chem* 1995, **270:**17656-17659.
17. Keely PJ, Westwick JK, Whitehead IP, Der CJ, Parise LV: **Cdc42 and Rac1 induce integrin-mediated cell motility and invasiveness through PI(3)K.** *Nature* 1997, **390:**632-636.
18. Nobes CD, Hall A: **Rho, rac, and cdc42 GTPases regulate the assembly of multimolecular focal complexes associated with actin stress fibers, lamellipodia, and filopodia.** *Cell* 1995, **81:**53-62.
19. Ridley AJ, Paterson HF, Johnston CL, Diekmann D, Hall A: **The small GTP-binding protein rac regulates growth factor-induced membrane ruffling.** *Cell* 1992, **70:**401-410.

MOLECULAR AND CELLULAR BIOLOGY, Mar. 2001, p. 1463–1474 Vol. 21, No. 5
0270-7306/01/$04.00+0 DOI: 10.1128/MCB.21.5.1463–1474.2001

Autoinhibition Mechanism of Proto-Dbl

FENG BI,[1] BALAZS DEBRECENI,[1] KEJIN ZHU,[1] BARBARA SALANI,[2] ALESSANDRA EVA,[2] AND YI ZHENG[1]*

Department of Molecular Sciences, University of Tennessee Health Science Center, Memphis, Tennessee 38163,[1] and Laboratorio di Bioligia Molecolare, Istituto G. Gaslini, 16148 Genoa, Italy[2]

Received 29 September 2000/Returned for modification 9 November 2000/Accepted 30 November 2000

The *dbl* oncogene encodes a prototype member of the Rho GTPase guanine nucleotide exchange factor (GEF) family. Oncogenic activation of proto-Dbl occurs through truncation of the N-terminal 497 residues. The C-terminal half of proto-Dbl includes residues 498 to 680 and 710 to 815, which fold into the Dbl homology (DH) domain and the pleckstrin homology (PH) domain, respectively, both of which are essential for cell transformation via the Rho GEF activity or cytoskeletal targeting function. Here we have investigated the mechanism of the apparent negative regulation of proto-Dbl imposed by the N-terminal sequences. Deletion of the N-terminal 285 or C-terminal 100 residues of proto-Dbl did not significantly affect either its transforming activity or GEF activity, while removal of the N-terminal 348 amino acids resulted in a significant increase in both transformation and GEF potential. Proto-Dbl displayed a mostly perinuclear distribution pattern, similar to a polypeptide derived from its N-terminal sequences, whereas onco-Dbl colocalized with actin stress fibers, like the PH domain. Coexpression of the N-terminal 482 residues with onco-Dbl resulted in disruption of its cytoskeletal localization and led to inhibition of onco-Dbl transforming activity. The apparent interference with the DH and PH functions by the N-terminal sequences can be rationalized by the observation that the N-terminal 482 residues or a fragment containing residues 286 to 482 binds specifically to the PH domain, limiting the access of Rho GTPases to the catalytic DH domain and masking the intracellular targeting function of the PH domain. Taken together, our findings unveiled an autoinhibitory mode of regulation of proto-Dbl that is mediated by the intramolecular interaction between its N-terminal sequences and PH domain, directly impacting both the GEF function and intracellular distribution.

The proto-Dbl protein is the prototype member of a large family of guanine nucleotide exchange factors (GEFs) for Rho GTPases (8, 50). Oncogenic activation of proto-Dbl occurs by truncation of the amino-terminal 497 residues (41), resulting in constitutively active carboxyl-terminal sequences that include a Dbl homology (DH) domain in tandem with a pleckstrin homology (PH) domain, the conserved motifs of the Dbl family. Many members of this family, including Vav, Ect2, Tim, Ost, Dbs, Lbc, Lfc, Lsc, and Net, possess transformation or invasion ability, similar to onco-Dbl upon activation. In many cases, the DH-PH module represents the minimum structural unit that is required for cell transformation (8, 50).

A large body of evidence has helped establish that the biological functions of Dbl family members are intimately dependent upon their ability to interact with and activate Rho GTPases and that the cellular effects of Dbl-like proteins, including actin cytoskeletal reorganization, cell growth stimulation, and transformation, are likely the consequences of coordinated action of their immediate downstream substrates, the Rho family GTPases (8, 47, 50). The evidence includes the findings that Dbl family oncoprotein-induced foci are morphologically similar to those transformed by constitutively activated Rho GTPases but distinct from that seen when cells are transformed by Ras, Raf, or Src (23); coexpression of Dbl family members with dominant negative mutants of Rho family GTPases blocks their transforming activity (20, 23, 32, 52); mutants of the GEFs that are no longer able to interact or activate Rho protein substrates behave dominant-negatively in cells (46, 54); and many cellular activities induced by Dbl family proteins, such as actin cytoskeleton reorganization, c-Jun kinase (JNK) activation, SRF transcriptional activation, and NF-κB activation, are associated with the activation of signaling pathways known to be mediated by the Rho GTPase effector targets (24, 30, 36, 48). Therefore, the ability to interact and activate Rho proteins is essential for Dbl family functions.

Current biochemical and structural data have pointed to the conserved structural motif of the Dbl family, the DH domain, as the primary interactive site with Rho GTPases (2, 20, 31, 44, 54). The DH domain does not have significant sequence homology with other subtypes of small GTPase activators such as the Cdc25 domain and Sec7 domain, which are specific to Ras and ARF, respectively (6, 14), indicating that the DH-Rho protein interaction employs a distinct mechanism (9). Deletions or mutations within the DH domain have been reported to result in loss of GEF activity and cellular functions by the GEFs (20, 40, 43, 54, 55), suggesting that an intact DH domain, likely its Rho GTPase-interactive ability, is critical for the cellular effects of Dbl family members.

The invariable location of a PH domain immediately C-terminal to the DH domain of the Dbl family GEFs suggests a functional interdependence between the two domains. Indeed, a regulatory role of the PH domain in the function of Dbl family members has been recognized. Derivatives of the Dbl family members onco-Dbl, Lbc, Lfc, and Dbs that are trun-

* Corresponding author. Mailing address: Department of Molecular Sciences, University of Tennessee, 858 Madison Avenue, Memphis, TN 38163. Phone: (901) 448-5138. Fax: (901) 448-7360. E-mail: yzheng@utmem.edu.

cated within the PH domain are impaired in their transforming activity (38, 48, 49, 53). In these cases, the PH domain was found to promote the translocation of the Dbl family proteins to the plasma membrane or cytoskeleton, where the Rho GTPase substrates reside. It is therefore likely that the PH domain of the Dbl proteins, acting similarly to the SH2/SH3 domains in the Ras pathway (10, 39), serves to bring the catalytic DH domain to specific intracellular locations to effectively activate the Rho GTPases.

Many members of the Dbl family appear to exist in an inactive, basal state prior to full activation. The incoming upstream signals, such as the heterotrimeric G-protein Gα and Gβγ subunits, protein tyrosine or serine/threonine kinases, adaptor or scaffolding proteins, and phosphoinositol lipids, may contribute in varying degrees to GEF activation processes (12, 13, 18, 19, 26, 34, 46). The best-understood example of self-regulation among the family members is the proto-Vav protein. The N-terminal autoinhibitory extension of proto-Vav forms an α-helix that binds in the DH domain active site through direct contact with the Rho GTPase binding pocket, blocking access to GTPases (3). Phosphorylation of Tyr174, which is an integral part of the autoinhibition interface, by Syk or Src-like kinases causes the N-terminal peptide to become unstructured and released from the DH domain, resulting in proto-Vav activation (3). The yeast Dbl family member Cdc24, which is a Cdc42-specific GEF, forms a protein complex with the scaffolding molecule Far1 and the Gβγ subunits to mediate the mating response of *Saccharomyces cerevisiae* (34). Mammalian p115RhoGEF becomes activated as a Rho GEF upon $G\alpha_{13}$ binding to its N-terminal RGS domain, suggesting that the coupling between a Gα and p115Rho GEF may relieve the intrinsic constraint of the DH domain (19). Moreover, phosphorylation of the Rac1-specific GEF Tiam1 by Ca^{2+}/calmodulin-dependent protein kinase II has been shown to lead to its translocation to the plasma membrane and activation (13), possibly by interference of the PH domain function of Tiam1, which has previously been demonstrated to determine its subcellular location (45). These cases suggest that the Dbl family GEFs employ a diverse range of self-regulatory mechanisms to maintain themselves in the basal state.

Proto-Dbl activation occurs through truncation of N-terminal 497 amino acids (42), suggesting that the N-terminal half of the molecule contains a negative regulatory element(s) for the C-terminal DH-PH functional module. A previous database search found limited similarities between the N terminus of proto-Dbl and the intermediate filament protein vimentin, spanning a 300-amino-acid region which was predicted to consist of an extended α-helical coiled-coil structure (41). However, where the inhibitory function resides upstream of the DH domain (residues 498 to 690) and how the N terminus exerts the inhibitory function remain unclear. In the present article, we report the finding that proto-Dbl protein involves an intramolecular interaction between the N terminus and the PH domain to maintain an autoinhibited, inactive state. The N- and C-terminal domain interaction effectively limits the access of the Rho GTPase substrates RhoA and Cdc42 to the catalytic site of the DH domain and masks the intracellular targeting function of the PH domain, resulting in suppression of its GEF function and a unique perinuclear localization pattern in cells. Such an autoinhibition state prevents proto-Dbl from transforming cells, and presents a basal mode that could be subject to modulation by a variety of upstream signals.

MATERIALS AND METHODS

Construction of mutant proto-Dbl cDNAs. Constructs pZipneo-onco-Dbl, pZipneoGST-DH-PH, pKH3-DH-PH, pKH3-Cdc42, and KH3-RhoA were generated as described before (54). Various proto-Dbl truncation mutants, including T1-T7, N1-N4, and the DH and PH domains (Fig. 1A), were generated by PCR cloning using the high-fidelity *Pfu* DNA polymerase (Stratagene) as described (28). The resulting constructs in the pZipneo vector were subsequently sequence proofed by automated fluorescence sequencing. The cDNAs encoding T1-T7, DH-PH, DH, or PH were subcloned into the pKH3 vector for expression as the trihemagglutinin (HA_3)-tagged proteins in Cos-7 cells. The Myc-tagged N2 and Flag-tagged N1 constructs were generated by subcloning the corresponding cDNA sequences to the pCMV6 and pCMV2B vectors, respectively. The *Bam*HI fragments encoding T1, N1, and the DH-PH module were also subcloned into the *Bgl*II and *Bam*HI sites of pVL1392 vector together with the cDNAs encoding the glutathione *S*-transferase (GST) or His_6 sequences for insect cell expression (51). The N2, N3, and N4 cDNAs were subcloned into the *Bam*HI and *Eco*RI sites of the pGEX-2T vector for expression in *Escherichia coli* as GST fusions. The pSR-lbc and pSR-v-ras plasmids used for the transformation assays were described before (52).

Expression of recombinant proteins in *E. coli* and insect cells. Expression and purification of GST fusion small GTP-binding proteins (GST-Cdc42, GST-RhoA, GST-N17Cdc42, and GST-N19RhoA) from pGEX vector-transformed *E. coli* were carried out as described previously (20). Production of GST-N2, -N3, and -N4 and the GST-PH domain of Dbl in *E. coli* was carried out similarly. Production and purification of the Sf9 insect cell expressed His_6-tagged T1, DH-PH module, or N1 polypeptide were performed as described (51). The concentration and integrity of purified proteins were estimated by Coomassie blue staining after sodium dodecyl sulfate-polyacrylamide gel electrophoresis (SDS-PAGE).

Cell culture and transfection. Cells were maintained in Dulbecco's modified Eagle's medium (DMEM) supplemented with 10% calf serum (NIH 3T3) or 10% fetal bovine serum (Cos-7). Transfections were carried out using the Lipofectamine reagent (Gibco Life Sciences, Inc.). To generate stable cell lines, NIH 3T3 cells were transfected with pZipneoGST constructs or a combination of the pKH3 construct with pCMV2B vector (Stratagene), which contains a neomycin resistance selection marker and were selected in DMEM supplemented with 5% calf serum and G418 (350 μg/ml). The drug-resistant colonies were cloned and subcultured in the same medium after 18 days.

To assay transforming activity, NIH 3T3 cells were transfected with the pZipneo-proto-Dbl constructs onco-Dbl and *lbc* or v-*ras* cDNA by the calcium phosphate method as described (53). For inhibition assays, different doses of the cDNAs encoding the N-terminal polypeptide N1 or N2 in the pCEFL vector or the pCEFL vector alone were cotransfected with onco-Dbl, *lbc*, or v-*ras* cDNAs into the cells. The transfected NIH 3T3 cells were fed every 2 days with fresh DMEM supplemented with 10% calf serum. At 12 to 14 days posttransfection, the cell culture dishes were either visualized directly under the microscope for focus formation or stained with a 2% solution of Giemsa for focus scoring (53).

In vitro GDP/GTP exchange assay. The time courses for [^{3}H]GDP/GTP exchange of Rho family GTPases in the presence and absence of purified His_6-tagged or HA_3-tagged proto-Dbl mutants were determined as previously described using the nitrocellulose filtration method (51). The GEF reaction buffer contains [^{3}H]GDP-loaded Cdc42 with 20 mM Tris-HCl (pH 7.6), 100 mM NaCl, 10 mM $MgCl_2$, 0.5 mM GTP, and 1 mM dithiothreitol (DTT) supplemented with various proto-Dbl mutants.

Complex formation and immunoprecipitation. Cos-7 cells were transfected with various proto-Dbl constructs or the N-terminal polypeptide N1 by the Lipofectamine method (54). At 48 h posttransfection, complex formation between the HA_3-tagged proto-Dbl mutants and GST-fused dominant negative Cdc42 (N17Cdc42) were carried out by incubation of the mutant proto-Dbl-expressing cell lysates with the immobilized GST fusion proteins (54). Complex formation between GST-N1, GST-N2, GST-N3, or GST-N4 and the DH-PH, DH, or PH protein or between the GST-PH domain and the HA_3-N1 polypeptide were carried out similarly. The coprecipitation complexes were probed with anti-HA monoclonal antibody and visualized with chemiluminiscence reagents (Amersham Pharmacia). To detect coimmunoprecipitation between the N2 polypeptide and various Dbl mutants, the Myc-N2-encoding cDNAs in vector pCMV6 were cotransfected with the DH-PH, DH, or PH construct in the pKH3 vector into Cos-7 cells, and the cell lysates were subjected to anti-HA immuno-

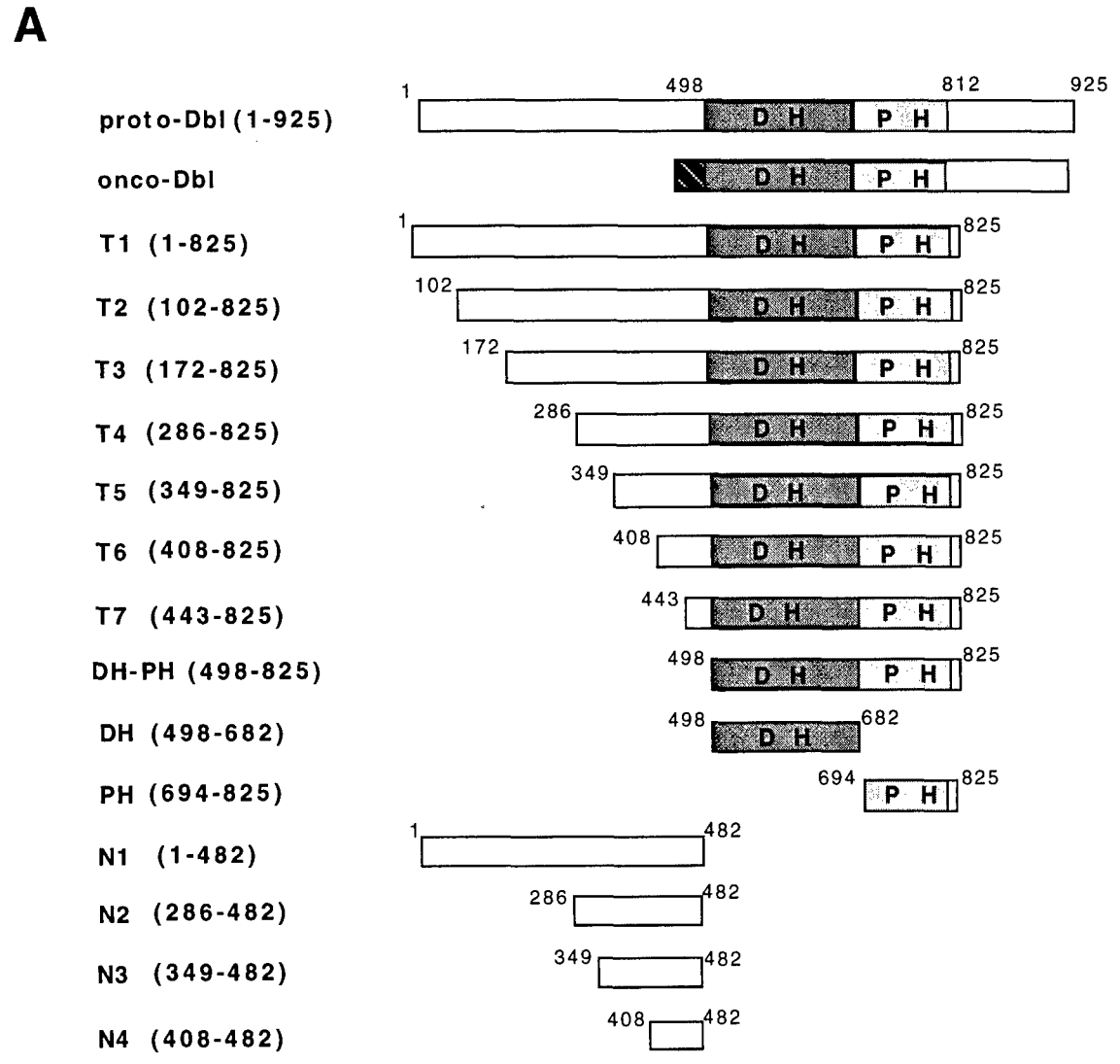

FIG. 1. N terminus of proto-Dbl contains an inhibitory motif for transforming activity. (A) Schematic representation of the structures of proto-Dbl, onco-Dbl, and various deletion mutants. Numbering refers to proto-Dbl sequences. (B) Focus-forming activities of various proto-Dbl constructs in NIH 3T3 cells. The cDNAs encoding various proto-Dbl mutants were cloned into plasmid pZipneo-GST and transfected into NIH 3T3 cells (0.1 μg/60-mm dish). At 14 days posttransfection, the number of foci was quantified visually after crystal violet staining.

precipitation with an anti-HA monoclonal antibody immobilized on agarose beads (Roche Biochemicals). The coprecipitates were washed three times before being probed with anti-HA or anti-Myc in Western blots.

In vivo Rho GTPase activation assay. The glutathione-agarose-immobilized GST-PAK1, which contains the p21-binding domain (PBD) of human PAK1 (residues 51 to 135), and GST-PKN, which contains the site required for RhoA-GTP recognition of protein kinase N (residues 1 to 128), were expressed and purified in *E. coli* by using the pGEX-KG vector as previously described (29). The active, GTP-bound form of Cdc42 or RhoA in fresh Cos-7 cell lysates coexpressing the small GTPase and various proto-Dbl constructs was captured by incubation with the GST-fused effector domains for 40 min at 4°C (54).

Fluorescence microscopy. Log-phase growing fibroblasts were seeded at a density of 3×10^4 cells per 12-mm round coverslip (Fisher Scientific) overnight before fixation in phosphate-buffered saline containing 4% paraformaldehyde for 10 min at room temperature. The cells were permeabilized in Tris-buffered saline containing 0.2% Triton X-100 for 5 min and double stained for HA-tagged protein and F-actin using anti-HA monoclonal antibody and rhodamine-phalloidin (Molecular Probes). Coverslips were mounted onto slides in 50% glycerol–Tris-buffered saline. Stained cells were analyzed with a conventional fluorescence microscope and a Zeiss confocal microscope (54).

RESULTS

Effect of deletion mutations on proto-Dbl transforming activity. To delineate a possible structural motif embedded within the N-terminal sequences that confers an inhibitory function, we generated a series of deletion mutants of proto-Dbl in which the N-terminal 101, 171, 285, 348, 407, 442, or 497 residues and/or the C-terminal 100 amino acids (T1 to T7 and DH-PH) were removed while leaving the DH-PH module intact (Fig. 1A). To evaluate the transforming potential of these proto-Dbl constructs, the respective cDNAs were cloned into the mammalian pZipneo vector and transfected into NIH 3T3 cells. As positive and negative controls, pZipneo-proto-Dbl, pZipneo-onco-Dbl, and the pZipneo vector alone were tested in parallel.

As shown in Fig. 1B, under assay conditions in which proto-Dbl displayed 1 to 2% of the transforming activity of onco-Dbl, the vector alone consistently yielded null foci. Deletion of the C-terminal 100 residues from proto-Dbl (T1) yielded a similar number of foci as proto-Dbl itself, indicating that the C-terminal sequences after the PH domain do not contribute directly to proto-Dbl regulation. Sequential removal of the N-terminal sequences, however, apparently unleashed the transforming activity in a two-step manner: the T2, T3, and T4 constructs, which lack the N-terminal 101, 171, and 285 residues, respectively, displayed a minor increase in transforming activity, with 7 to 9% of the transforming activity of onco-Dbl, whereas further truncation to residue 348, 407, or 442 (T5, T6, and T7, respectively) resulted in significant activation of transforming activity indistinguishable from that of onco-Dbl. Since the deletion mutants were expressed equally well in NIH 3T3 cells and Cos-7 cells, giving rise to polypeptides of the expected molecular weights (data not shown; see Western blots described below), the differences between the mutants in transformation are likely to reflect the true biological activities in cells rather than their differences in stability. Consistent with a previous observation (20), the DH-PH module (residues 498 to 825) behaved like onco-Dbl (Fig. 1B), implying that the DH and PH domains together constitute the structural module sufficient for maximum transforming activity. These results suggest that the extreme N terminus (residues 1 to 101) of proto-Dbl contains a minor negative regulatory element and that sequences between residues 286 and 348 contain an additional element(s) that is involved in imposing a major constraining effect on the oncogenic activity of the subsequent DH-PH module.

Effect of deletion mutations on the GEF activity of proto-Dbl protein. The transforming activity of onco-Dbl was found to correlate closely with its Rho GEF activity (54). We pondered whether proto-Dbl, under the constraint of the N-terminal sequences, is defective in functioning as a GEF for Cdc42 and RhoA, resulting in the apparent suppression of transforming activity. To this end, the T1 mutant, which bears the C-terminal 100-amino-acid truncation and functions like proto-Dbl in transformation assays, and the DH-PH module, which mimics onco-Dbl in both GEF catalysis and transformation ability (20), were expressed in Sf9 insect cells as His_6-tagged fusion proteins and purified by Ni^{2+}-agarose affinity chromatography. When equal molar amounts of His_6-T1 and His_6-DH-PH were assayed for the ability to stimulate [^{3}H]GDP/GTP exchange of Cdc42, we observed that while DH-PH was very efficient in accelerating the GEF reaction, such that over 90% of bound [^{3}H]GDP was dissociated from Cdc42 within 5 min under its stimulation, T1 was only marginally active in stimulating the GEF reaction, such that only ~10% of Cdc42-bound [^{3}H]GDP was replaced by GTP within the same time period compared with that in the absence of T1 (Fig. 2A). Thus, the N-terminal sequences of proto-Dbl negatively regulate the GEF activity of the DH-PH module.

Next, we examined the catalytic GEF activity of a panel of proto-Dbl mutants on Cdc42 in vitro. The T1, T4, T5, T6, and DH-PH cDNAs in the pKH3 vector, which provides an HA_3 tag at the N terminus, were transiently expressed in Cos-7 cells, and the proteins were purified by immunoprecipitation from the cell lysates by using anti-HA agarose beads. Upon elution by HA peptides, the purified deletion mutants were analyzed by anti-HA Western blot, and the amount of each protein was visualized by chemiluminiscence imaging of the blot (Fig. 2B). While the T5 and T6 mutants, which lacked the N-terminal 348 and 407 residues, respectively, showed activities in stimulating [^{3}H]GDP dissociation from Cdc42 similar to that of the DH-PH module, T1 and T4, which contain an intact N terminus or residues 286 to 825, respectively, were comparable in displaying a significantly weaker GEF activity at equal molar quantities (Fig. 2C). These results indicate that the N-terminal sequences directly impose an inhibitory effect on the GEF activity of the DH-PH module. To test if the N terminus interacts with the catalytic DH domain, resulting in inhibition, the N1 polypeptide encoding residues 1 to 482 was generated in Sf9 insect cells as a GST fusion and included in the GEF activity assays with the DH-PH module. As shown in Fig. 2D, no detectable effect was observed when a fourfold molar excess of GST-N1 was present together with the DH-PH module in stimulating [^{3}H]GDP dissociation from Cdc42 compared with DH-PH alone. We conclude that the N terminus of proto-Dbl interferes with the GEF function through a mechanism other than direct blockage of substrate binding to the DH domain as is the case with Vav (3).

To determine the Rho GTP ase exchange potential of the mutants in cells, the HA-tagged proto-Dbl mutants were transiently cotransfected with HA-tagged, wild-type Cdc42 or RhoA in Cos-7 cells. The expression level of the mutants and Cdc42 or RhoA could be directly compared (Fig. 3). The relative amounts of activated GTPases in the cell lysates were measured by GST-PAK1 or GST-PKN pull-down, which specifically recognizes and stabilizes the GTP-bound form of Cdc42 or RhoA (29). As shown in Fig. 3, both the T1 and T4 mutants demonstrated significantly lower Cdc42 activating potential, while T5 and T6 were similar to the DH-PH module in their ability to generate Cdc42-GTP. Similar observations were also made when RhoA was examined as an in vivo substrate (data not shown). These results indicate that the cellular Rho GTPase-activating potential of the proto-Dbl mutants correlates with their in vitro GEF activity. This pattern of GEF activity and the Rho protein-activating potential of the mutants are reminiscent of the above-described transforming abilities of the mutants (Fig. 1B). We deduce from these results that the sequences between residues 286 and 348 contain the critical structural element(s) that appears to hinder the GEF function of the DH-PH module and that the lack of transforming ac-

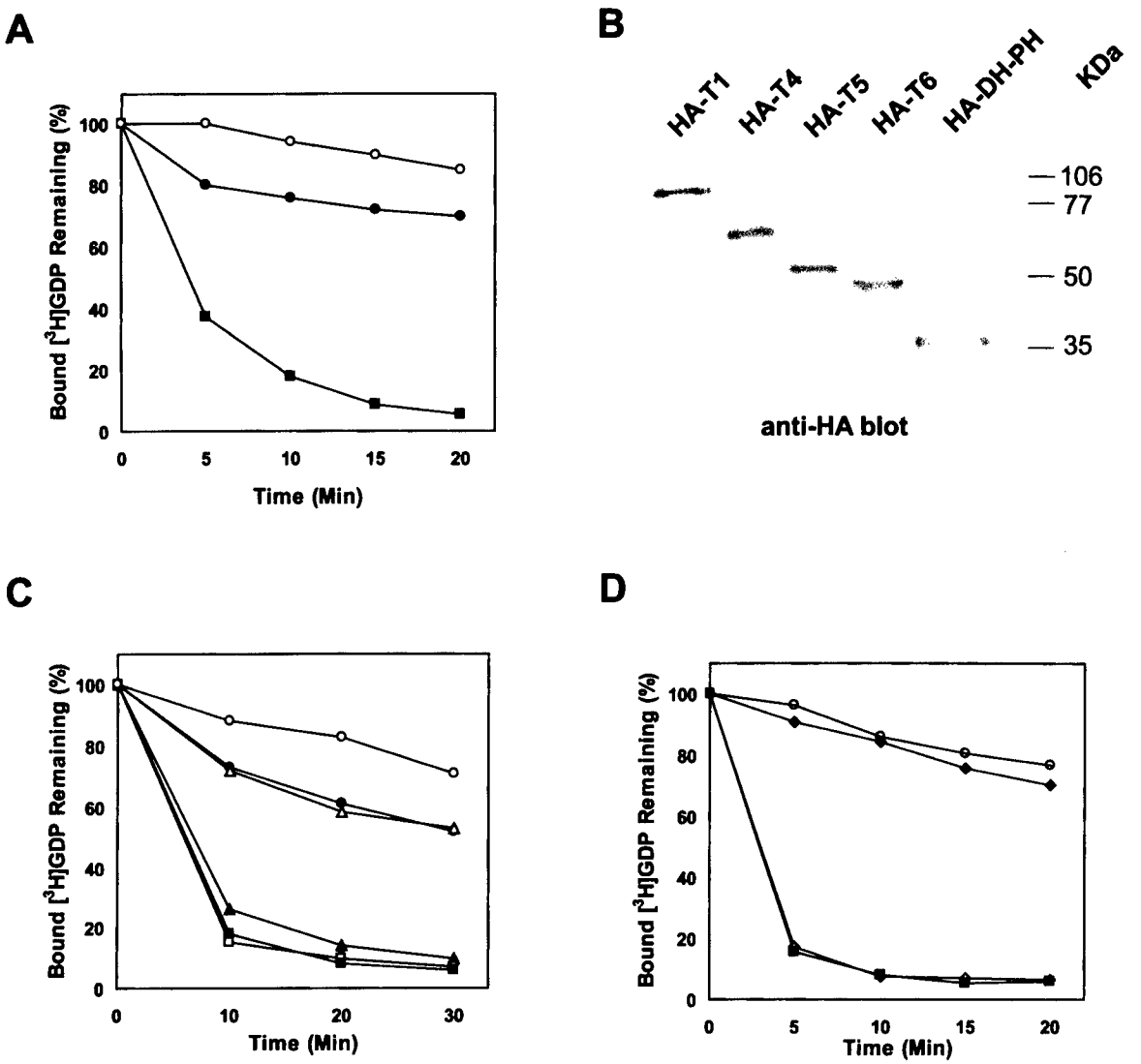

FIG. 2. GEF activity of proto-Dbl is negatively regulated by the presence of the N-terminal sequences. (A) Time courses of [^{3}H]GDP dissociation from Cdc42 catalyzed by T1 and the DH-PH module. The insect cell-expressed His_6-T1 and His_6-DH-PH were purified to homogeneity by Ni^{2+}-agarose affinity chromatography. Approximately 10 pmol of each (T1, solid circles; DH-PH, solid squares; buffer, open circles) was used to assay GEF activity on ~1 μg of Cdc42-[^{3}H]GDP in a buffer containing 20 mM Tris-HCl (pH 7.6), 100 mM NaCl, 10 mM $MgCl_2$, 0.5 mM GTP, and 1 mM DTT. The GEF reactions were terminated at the indicated time points by nitrocellulose filtration. (B) HA_3-tagged deletion mutants were purified from Cos-7 cell lysates by using the immobilized anti-HA antibody. After elution with 0.2 mM HA peptides, the mutants were analyzed by Western blot with anti-HA antibody. (C) Effect of deletion mutations on GEF activity. Approximately equal molar amounts of the mutants purified from Cos-7 cell lysates (20 μl) were assayed for the ability to stimulate [^{3}H]GDP dissociation from Cdc42 at various times. Open circles, buffer; solid circles, T1; open triangles, T4; solid triangles, T5; open squares, T6; solid squares, DH-PH. (D) Effect of isolated N-terminal peptide N1 on GEF activity of DH-PH. [^{3}H]GDP dissociation from Cdc42 was assayed in the presence (solid squares and open diamonds) or absence of His_6-DH-PH (open circles and solid diamonds) and an approximately fourfold molar excess of purified GST-N1 (diamonds) at various time points.

tivity of proto-Dbl reflects the suppressive effect on the catalytic GEF activity by the N-terminal negative regulatory constraint(s).

Rho GTPase-binding activities of deletion mutants of proto-Dbl. To further investigate the functional properties of the various deletion mutants of proto-Dbl, we next compared their abilities to directly bind to the Rho GTPase substrate Cdc42. Cos-7 cell lysates expressing similar amounts of HA-tagged T1, T4, T5, T6, and the DH-PH module (Fig. 4) were incubated with the glutathione-agarose-immobilized, GST-fused, dominant negative form of Cdc42, N17Cdc42, that is known to bind to the DH domain of onco-Dbl with high affinity (20). After extensive washing the coprecipitates of GST-N17Cdc42 were subjected to anti-HA Western blotting. Among the five HA-tagged polypeptides, T5, T6, and the DH-PH module displayed a similarly strong binding pattern to N17Cdc42. T4 bound significantly more weakly, and T1 binding was barely detectable (Fig. 4). These results are consistent with the relative effectiveness of the mutants in activating the guanine nucleotide exchange of Cdc42 in vitro and in vivo (Fig. 2 and 3) and coincide with the mutants' transformation abilities (Fig. 1B). They suggest that the N-terminal residues, particularly residues 285

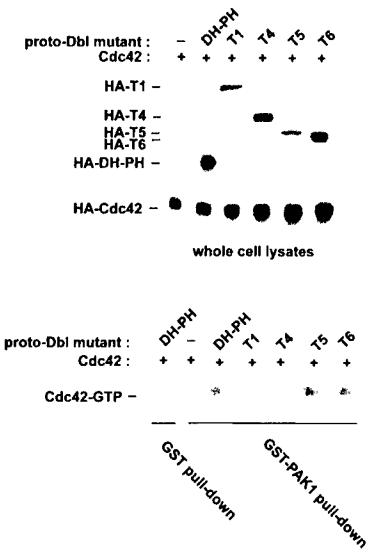

FIG. 3. Cdc42 exchange potential of proto-Dbl mutants in cells. HA_3-Cdc42 was expressed alone or together with HA-DH-PH, HA-T1, HA-T4, HA-T5, or HA-T6 in Cos-7 cells. The cell lysates were probed with anti-HA antibody in a Western blot. The cell lysates were subjected to a GST or GST-PAK1 pull-down assay, and the glutathione-agarose coprecipitates were detected by anti-HA Western blotting to reveal the relative amount of Cdc42-GTP in cells.

to 348, are involved in negative allosteric control of proto-Dbl activity by limiting the access of Rho GTPase to the catalytic site on the DH domain.

N-terminal sequences dictate the intracellular localization pattern of proto-Dbl. Onco-Dbl and the PH domain of Dbl were colocalized with Triton X-100-insoluble particulates in previous cell fractionation studies (53). Whether the N-terminal constraining sequences of proto-Dbl would interfere with the PH domain intracellular targeting function, thereby causing an alteration in the intracellular distribution pattern of

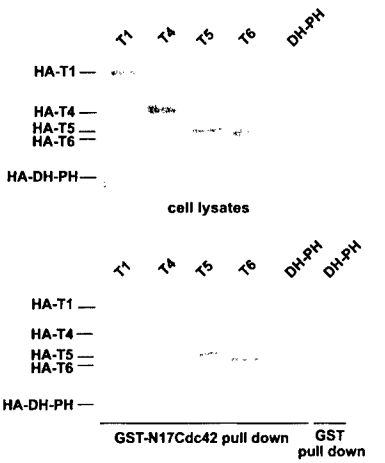

FIG. 4. In vitro binding activity of proto-Dbl mutants to GST-N17Cdc42. Various proto-Dbl constructs were expressed in Cos-7 cells by transient transfection. A portion of cell lysates was analyzed by anti-HA Western blotting. The cell lysates were incubated with 2 μg of GST or GST-Cdc42N17 immobilized on glutathione beads for 1 h at 4°C under constant agitation. After three washes, bound proteins were detected by immunoblotting with anti-HA antibody.

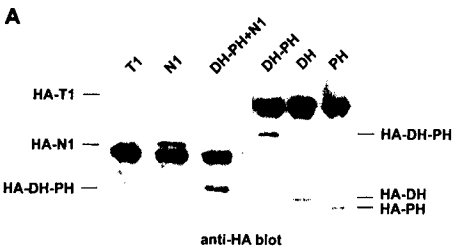

FIG. 5. Intracellular distribution patterns of proto-Dbl and various deletion mutants. (A) Stable transfectants of HA-tagged T1 (proto-Dbl), DH-PH module, DH domain, PH domain, N-terminal N1 polypeptide, or DH-PH module coexpressed with the N1 polypeptide were generated in NIH 3T3 cells by G418 selection. Cell lysates (~5×10^5 cells) of the G418-resistant clones were subjected to anti-HA immunoprecipitation followed by Western blotting with anti-HA antibody. (B) Fluorescence microscopy of the cellular localization patterns of the proto-Dbl mutants. Stably transfected cells were maintained in low serum (2%) overnight before being fixed and double stained as described in the text. The cells were analyzed by confocal microscopy with double filters for fluorescein and rhodamine. The overlap of fluorescein and rhodamine images is shown in yellow.

proto-Dbl from that of onco-Dbl, has not been assessed. To examine the effect of the N-terminal sequences on proto-Dbl cellular localization and to determine the contribution of individual structural motifs to the proto-Dbl localization pattern, we have generated stable transfectants of NIH 3T3 cells expressing the HA-tagged proto-Dbl (T1), DH-PH module, DH domain, PH domain, or the N1 polypeptide (residues 1 to 482), as well as a cell clone coexpressing Flag-tagged N1 together with HA-DH-PH (DH-PH+N1). Western blot analysis of the anti-HA immunoprecipitates from the respective cell lysates confirmed that HA-tagged polypeptides of the expected molecular sizes were expressed in the cell lines (Fig. 5A). In addition, an anti-Flag Western blot further confirmed that Flag-N1 was coexpressed with HA-DH-PH in the DH-PH+N1 cells (data not shown). After fixation, the cells were double stained with anti-HA monoclonal antibody plus fluorescein-labeled anti-mouse immunoglobulin antibody and rhodamine-labeled phalloidin to visualize HA-tagged polypeptide distribution and cellular actin structures. Under a confocal microscope, we found that proto-Dbl displayed a mostly perinuclear distribution pattern similar to that of the N1 polypeptide (Fig. 5B). The DH-PH module, on the other hand, was found to colocalize with actin stress fibers, like the PH domain alone, whereas the DH domain was mostly diffused throughout cells, with some degree of concentration around the nucleus (Fig. 5B). These results are consistent with the previous cell fractionation data showing a significant portion of the DH-PH module and the PH domain in the Triton X-100-insoluble fraction and the DH domain mostly in the cytosol (53) and suggest that the N-terminal sequences in proto-Dbl affect the cellular distribution pattern of proto-Dbl. In the N1 polypeptide-coexpressing cells, the actin-stress fiber colocalization pattern of DH-PH was disrupted and changed to the mostly perinuclear localization, similar to that of the N1 polypeptide alone (Fig. 5B). Thus, the N-terminal sequences of proto-Dbl contain the structural element(s) that dictates the intracellular distribution of proto-Dbl. This is likely due to the interference of the PH domain targeting function that de-

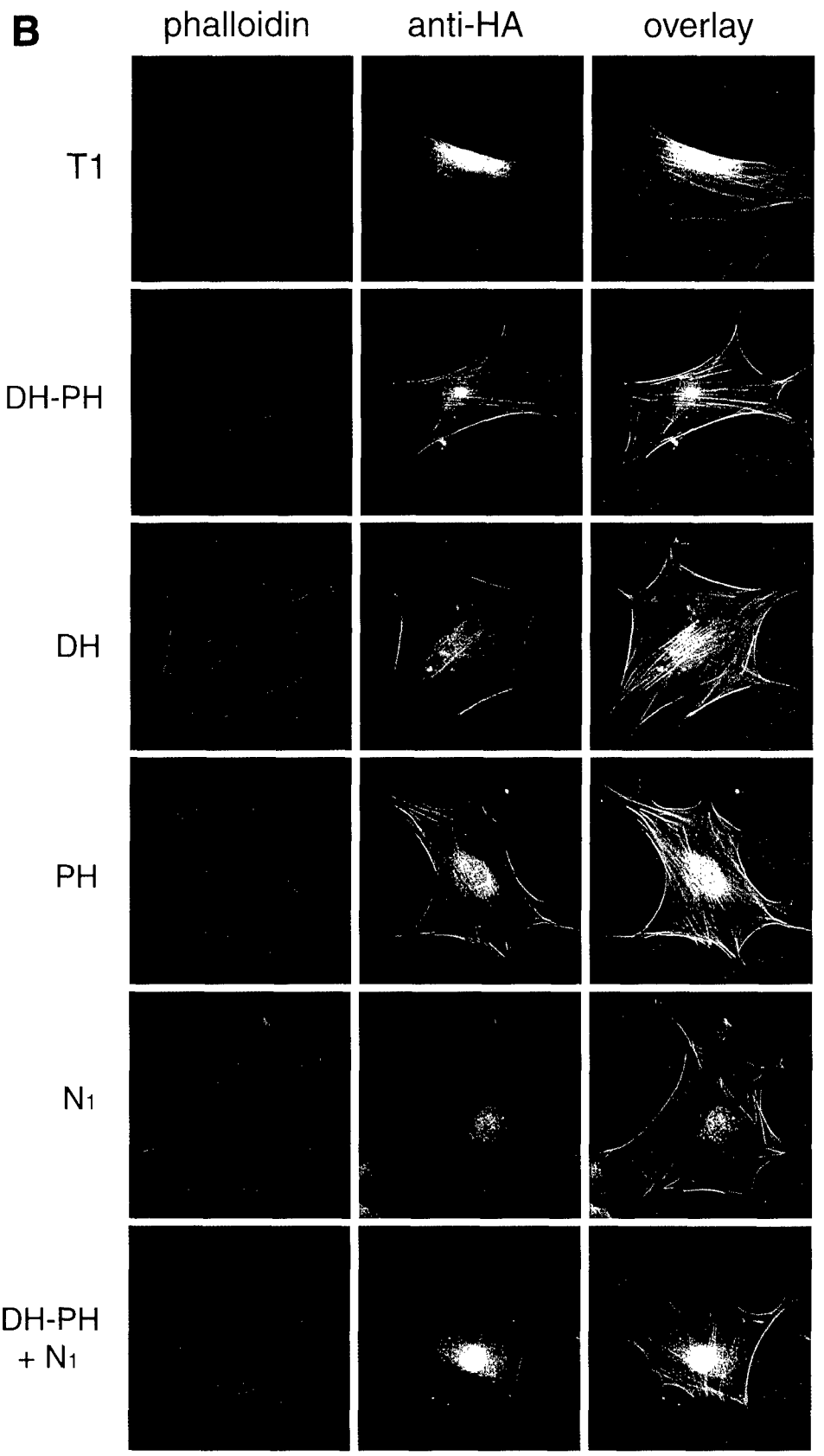

FIG. 5—*Continued.*

termines the localization pattern of onco-Dbl by the N-terminal sequences.

Isolated N-terminal fragment of proto-Dbl inhibits onco-Dbl transforming activity. The negative regulatory function of the N-terminal sequences raised the possibility that the isolated N terminus of proto-Dbl might interfere with the biological activity of oncogenic Dbl. To test this hypothesis, the cDNAs encoding the N1 (residues 1 to 482) and N2 (residues 286 to 482) polypeptides were cloned into the mammalian expression vector pCEFL and cotransfected with onco-Dbl into NIH 3T3 cells. Compared with the empty vector, N1 reduced onco-Dbl transforming activity by ~90% at a dose of 2 μg/100-mm dish, while N2 consistently caused ~25% inhibition under similar conditions (Fig. 6). At a lower dose (0.2 μg/100-mm dish), however, only N1 showed significant inhibition of onco-Dbl activity. Neither N1 nor N2 had a detectable effect on proto-Dbl transforming activity when the foci were induced by proto-Dbl overexpression (2 μg of cDNA/100-mm dish; data not shown). To confirm that the N-terminal sequence-caused inhibition was specific for onco-Dbl, we examined the ability of N1 and N2 to affect the transforming functions of a *dbl*-related oncogene, *lbc*, and oncogenic v-*ras*. Distinct from their effects on onco-Dbl, neither peptide showed any sign of inhibiting oncogene-induced focus formation at 2 μg of cDNA/dish (Fig. 6). These results indicate that the N terminus of proto-Dbl can specifically act on onco-Dbl or the onco-Dbl pathway and negatively influence its biological activity.

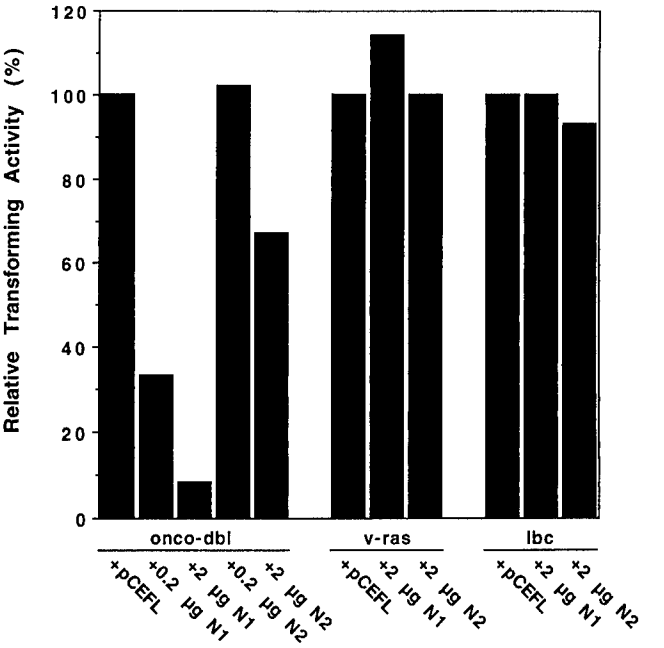

FIG. 6. N-terminal sequences of proto-Dbl specifically inhibit onco-Dbl transforming activity. NIH 3T3 cells were transfected with pZipneo-onco-Dbl (4 ng/100-mm dish) together with pCEFL vector or cDNAs encoding the N1 or N2 sequences in pCEFL vector at the indicated doses (micrograms per 100-mm dish). The *lbc* oncogene (0.1 μg/100-mm dish) together with the pCEFL vector or the N1 or N2 cDNA in the pCEFL vector (2 μg/dish) or oncogenic v-*ras* cDNA (0.1 μg/dish) together with vector or the N1 or N2 cDNA (2 μg/dish) in pCEFL were cotransfected in parallel. The focus-forming activity of each oncogene cotransfected with the empty pCEFL vector was set at 100%. The relative focus-forming activities represent results from four independent experiments.

Interaction of N-terminal sequences with the PH domain of proto-Dbl. The above-characterized negative regulatory function of the N terminus of proto-Dbl could be rationalized by an intramolecular interaction involving the N-terminal regulatory sequences and the C-terminal functional module, thereby affecting the GEF activity of the DH domain and the intracellular targeting function of the PH domain. To test this hypothesis, we first employed a glutathione-agarose pull-down assay using the insect cell-expressed GST-N1 peptide as a probe to detect possible interaction with the C-terminal functional motifs, i.e., the DH-PH module, DH domain, or PH domain. The DH-PH module, DH domain, and PH domain were transiently expressed in Cos-7 cells as HA-tagged proteins, and the cell lysates were incubated with immobilized GST or GST-N1. As shown in Fig. 7A, GST-N1 was able to stably associate with the DH-PH module and the PH domain but not with the DH domain, whereas the GST control did not bind to any of the three proteins. When the N1 polypeptide was expressed in Cos-7 cells and subjected to the pull-down assay with the immobilized GST-PH domain, we found that GST-PH was able to tightly bind to HA-N1 in the glutathione-agarose coprecipitates under conditions in which GST alone did not interact with N1 (Fig. 7B). Therefore, the N-terminal 482 residues of proto-Dbl can form a physical complex with the C-terminal DH-PH functional module via the PH domain.

To further delineate the region of amino acids in the N terminus that may contribute to direct interaction with the PH domain, the sequentially deleted N2, N3, and N4 polypeptides, encoding residues 286 to 482, 349 to 482, and 408 to 482, respectively, were employed as GST-tagged probes to detect possible binding to the PH domain. Figure 7C shows that while none of the three N-terminal peptides bound to the DH domain at a detectable level, N2, but not N3 or N4, was capable of binding directly to the PH domain. These results imply that the region between amino acids 286 and 348 contains an important element(s) that is involved in interaction with the PH domain.

To test whether stable association between the N terminus and the PH domain could occur in cells, a Myc-tagged N2 peptide was coexpressed with the HA-tagged DH-PH module, DH domain, or PH domain in Cos-7 cells, and the coimmunoprecipitation pattern of Myc-N2 with the HA-tagged proteins was determined. In contrast to the lack of detectable association by HA-DH, both HA-DH-PH and HA-PH formed a stable complex with Myc-N2, as revealed by the anti-Myc Western blot of the anti-HA immunoprecipitates (Fig. 7D). Thus, the N-terminal sequences of proto-Dbl can bind tightly to the C-terminal PH domain in cells and are likely to do so intramolecularly. Such an interaction may have a direct impact on both the GEF activity and intracellular localization of proto-Dbl, which are essential for its transforming activity, causing the observed autoinhibitory behaviors.

DISCUSSION

Although most Dbl family members contain diverse multifunctional motifs, they all have the structural array of a central DH domain in tandem at the carboxyl terminus with a PH

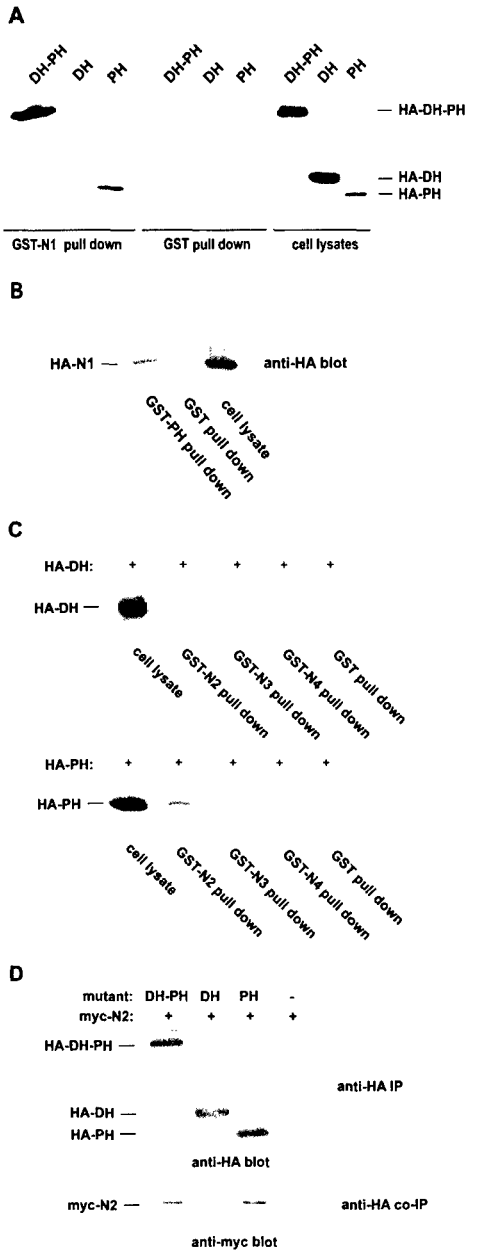

FIG. 7. N-terminal sequences of proto-Dbl interact directly with the PH domain. (A) GST-N1 polypeptide forms a stable complex with the DH-PH module or the PH domain of proto-Dbl. The DH-PH module, DH domain, or PH domain was transiently expressed in Cos-7 cells as an HA-tagged protein. About 2 μg of GST or GST-N1 immobilized on glutathione-agarose beads was incubated with the cell lysates for 1 h at 4°C. After three washes, the agarose bead coprecipitates were subjected to anti-HA Western blotting analysis. (B) PH domain complexes with N1 polypeptide of proto-Dbl in vitro. Immobilized GST or GST-PH (~2 μg/sample) was incubated with Cos-7 lysates expressing HA-N1, and the coprecipitates were detected by anti-HA immunoblotting. (C) Immobilized GST-N2 (residues 286 to 482), GST-N3 (349 to 482), or GST-N4 (408 to 482) was incubated with cell lysates expressing HA-DH or HA-PH. The association of the HA-tagged DH or PH domain with the GST fusion coprecipitates was detected by anti-HA Western blot. (D) DH-PH module and the PH domain but not the DH domain associate with the N2 polypeptide in cells. The Myc-tagged N2 polypeptide was coexpressed in Cos-7 cells with the HA-tagged DH-PH, DH, or PH construct. Cell lysates were subjected to anti-HA immunoprecipitation (IP) followed by anti-HA or anti-Myc Western blotting.

domain. Previous studies of onco-Dbl have established that the DH domain is primarily responsible for Rho GTPase binding and GEF activity, while the PH domain is involved in intracellular targeting and is necessary for the transforming activity of onco-Dbl (8, 50). Truncation of the N-terminal 497 residues of proto-Dbl results in oncogenic activation (42), suggesting that the N-terminal sequences contain negative regulatory elements imposing a constraint on the C-terminal DH-PH module. To date, the mechanism which the N terminus employs in the negative regulation of proto-Dbl activity and the regions of the molecule contributing to the regulation remain unclear. In this study, we provide direct evidence that proto-Dbl adopts an autoinhibitory mechanism for controlling its biochemical and biological activities. We identified the region between amino acids 275 and 349 as a critical inhibitory motif that impairs GEF catalytic activity and the intracellular targeting activity of the DH-PH module. The autoinhibitory effects are likely to arise through direct intramolecular interaction of this region with the PH domain, limiting the access of Rho GTPases to the DH domain and masking the intracellular targeting function of the PH domain. Such an autoinhibitory mode may be optimal for proto-Dbl regulation, since incoming upstream signals could exert their effects by modulation of either the N-terminal motif or the C-terminal PH domain.

Inhibitory effects of N-terminal sequences of proto-Dbl on the DH-PH module. Our previous structural mapping studies indicate that the DH-PH module of Dbl represents the minimum constitutively active structural unit that confers Rho GTPase exchange activity and cell-transforming potential (20). We show here that the presence or absence of the C-terminal 100 amino acids just outside the PH domain did not cause any change in transforming activity for either proto-Dbl or onco-Dbl, indicating that these sequences are not involved in regulation of the DH-PH module. A series of deletion mutations into the N terminus resulted in an apparent two-step activation of the proto-Dbl transforming activity: removal of the N-terminal 100 or 274 residues caused minor but significant enhancement, while further truncation to residue 348 led to full-blown activation of the focus-forming activity that is similar to the capacity of the DH-PH module (Fig. 1). These results prompted us to speculate that the N-terminal sequences impose a two-layer regulatory mechanism on the DH-PH module. The N-terminal 100 residues and sequences between residues 275 and 349 either act independently in negatively controlling the DH-PH activity or act coordinately so that the N-terminal 100 residues may further reinforce the negative constraint imposed by the following sequences. This is analogous to the situation of the *vav* proto-oncogene product, in which removal of the N-terminal 66 or 127 residues led to only partial activation of the transforming activity, while full activation was achieved by truncation of the N-terminal 186 residues (1).

The cellular transforming activity of Dbl is intimately dependent upon its catalytic GEF activity on Rho GTPases (54). The inhibitory effects of deletions of proto-Dbl on transformation indeed reflect their relative GEF activities on Cdc42 and RhoA when the purified mutants were tested in vitro (Fig. 2). The N terminus appears to potently inhibit the GEF ability of the DH-PH module, implying that an intramolecular interaction is at work in the regulatory mechanism. Residues 275 to

349, in particular, seem to contain the critical inhibitory element(s) for GEF activity, reminiscent of the major inhibitory region involved in the regulation of transforming activity (Fig. 1B). We show that the significantly reduced GEF activity of proto-Dbl and the deletion mutants that were generated at the N terminus of residue 274 was due to their reduced ability to interact with Rho GTPase, further establishing that the N-terminal sequences limit the access of the DH catalytic site for Rho proteins. The fact that the in vitro GEF activities of the proto-Dbl mutants closely correlate with their Cdc42- and RhoA-activating potential in vivo and with their cellular transforming activity strongly suggests that proto-Dbl maintains a low basal transforming capability, at least in part by downregulation of its ability to activate Rho GTPases through the N-terminal sequences.

By comparing the distinct intracellular distribution patterns of proto-Dbl and the DH-PH module, we come to the conclusion that the N-terminal sequences also dictate the intracellular location of proto-Dbl. Consistent with previous subcellullar fractionation results (53), our confocal microscopy data clearly demonstrate that the PH domain of Dbl colocalizes with the actin structure of cells, and this property of the PH domain is responsible for bringing the DH-PH module to a similar location. However, the presence of the N-terminal sequences in proto-Dbl appeared to overrule the PH function, leading the molecule to a perinuclear location. In cells in which the polypeptide encoding the N-terminal sequences was overexpressed together with the DH-PH module, the DH-PH protein was found to translocate from the actin-associated locations to the perinucleus, further confirming that the N-terminal sequences are involved in regulation of the cellular localization pattern of proto-Dbl. These observations raise the possibility that the N-terminal sequences may block ligand binding to the PH domain, resulting in loss of the targeting function of PH.

Autoinhibition of proto-Dbl by intramolecular interaction. Although the mechanism of intramolecular interaction was considered in the regulation of many Dbl family members, including Vav, Tiam1, Ect2, Ost, Net1, and proto-Dbl (1, 4, 21, 33, 42), and in the case of the Ras-specific GEF Sos1 (11, 40), there has been little biochemical evidence available to directly support such a mode of regulation for the GEFs until recently. A nuclear magnetic resonance spectroscopic study on an extended DH domain of proto-Vav most recently has revealed that the immediate N-terminal sequences, including the critical Tyr174 residue, could interact directly with the catalytic core region of the DH domain, achieving an autoinhibition conformation (3). Similar to but distinct from the proto-Vav protein, proto-Dbl was found in the current study to maintain a basal inactive state by specific binding of the N-terminal sequences to the PH domain, providing a biochemical rationale for another autoinhibitory mechanism in the negative regulation of a Dbl family member.

The structural arrangement of the N-terminal sequences of proto-Dbl is not known but appears to be different from those of proto-Vav protein and other Dbl family GEFs. Limited sequences homologies between a >300-residue span of the N terminus and the intermediate filament protein vimentin suggest that the N-terminal region may contain an extended α-helical coiled-coil structure (41). In agreement with the functional analysis, i.e., transformation capacity, GEF activity, and Rho GTPase binding activity, our sequential N-terminal deletion mutants point to the region between amino acids 275 and 349 as critical in interaction with the PH domain. The observed direct binding interaction between the N terminus and the PH domain allows us to present a model to rationalize the previous (20, 42, 53) and above-described functional data: by interacting with the PH domain, the N terminus of proto-Dbl maintains the molecule at an autoinhibited basal state. This intramolecular interaction would mask the PH-ligand binding site, resulting in an inactive PH domain and allowing the N terminus to dictate the cellular location of the molecule. Although the DH domain may not be directly inhibited by the N terminus, as proto-Vav is (3), since no binding interaction was detected between them, the allosteric hindrance brought by the N-terminal interaction with PH domain could effectively limit the access of the Rho GTPase substrates to the DH catalytic sites, indirectly affecting the Rho protein-activating potential. This model could also explain the observations that proto-Dbl (T1) remains weakly active as a GEF and can bind to Cdc42 with reduced affinity (Fig. 2 and 4).

Such a mode of autoinhibition is interesting from another angle. It provides a physiologically relevant peptide ligand, i.e., the coiled-coiled N-terminal motif, for a PH domain. Although the significance of various phosphoinositol phosphates as PH domain binding partners is well established (10, 39), physiologically important protein ligands for the PH domain remain rare. Consistent with our previous cell fractionation studies, which implicated the PH domain of Dbl in association with the Triton X-100-insoluble component of the cytoskeleton (53), we demonstrate in this study by immunofluorescence that Dbl PH extensively colocalizes with actin stress fibers in cells, suggesting that the PH domain is involved in interaction with a protein factor. Thus, it is possible that the N terminus binding to the PH domain may function as a switch in proto-Dbl regulation so that the basal, autoinhibited state can be relieved of the N-terminal constraint when a cytoskeletal protein factor binds to the PH domain by competing with the N-terminal sequences. It will be of great interest to obtain the molecular details of the N terminus-PH domain complex by structural biology means.

Mechanism of proto-Dbl activation. Understanding the autoinhibitory mechanism of proto-Dbl is an important step toward elucidating the mechanism of its activation. Recent progress in studies of the mechanism of Rho GTPase activation, in particular, the Dbl-like GEF activation, has provided quite a few possibilities on how the autoinhibited state of proto-Dbl could become activated. First, a phosphorylation event that modifies either the N-terminal constraining sequences or the PH domain may result in the desired relief of the structural constraint of the N terminus-PH domain interaction. However, serine/threonine rather than tyrosine phosphorylation is more likely to play a role in proto-Dbl activation, since proto-Dbl was found to be phosphosphorylated mainly on serine and threonine residues (15). Second, interaction with heterotrimeric G-protein α or βγ subunits may lead to effective translocation and activation of proto-Dbl. The analogy here includes p115RhoGEF, which utilizes its N terminus to couple directly to Gα12/Gα13, resulting in enhanced GEF catalytic activity and membrane translocation (5, 19). Moreover, a recent study also found that Gβγ can bind directly to the N-terminal 100 amino acids of proto-Dbl (35). Third, various

phosphoinositol lipids may be involved in proto-Dbl activation, given our finding that the PH domain of Dbl can bind to PIP2 (4, 5) and PIP3 (3, 4, 5) selectively. The conformational change of the PH domain induced by such an interaction could therefore lead to reduced binding to the N terminus of proto-Dbl, resulting in an open, active conformation. Finally, similar to the Cdc42-specific exchange factor in budding yeast Cdc24, proto-Dbl may need to be recruited to the targeting site via interaction with a Far1-like scaffolding protein, which recognizes a conserved motif found in the N termini of both Cdc24 and proto-Dbl (7). If Cdc24 is a good analogue for proto-Dbl, it is likely that a combination of the above events will be required for the production of a fully activated proto-Dbl molecule. These possible proto-Dbl-activating events are currently under investigation.

Autoinhibition and activation—a common theme in small-G-protein pathways. The autoinhibitory mode of regulation utilized by proto-Dbl falls into an emerging theme that appears to govern many aspects of small-G-protein signaling. Sos1, one of the best-understood Ras GEFs, is known to involve both N-terminal and C-terminal sequences to achieve autoinhibitory control of its Ras GEF activity (11). In addition to proto-Dbl, p115RhoGEF, Ost, Tiam1, Ect2, Net1, and Asef of the Dbl family all seem to employ some degree of autoinhibition to maintain themselves in a basal state (16, 19, 21, 22, 33, 41), although the molecular basis for their negative regulation remains unclear. In the context of the present results on proto-Dbl regulation, the recently illustrated tertiary structure of the autoinhibitory mode of Vav regulation, which involves an intramolecular interaction between the N-terminal Tyr174 containing an α-helix and the Rho GTPase binding site of the DH domain (3), suggests that the biochemical role of the N-terminal sequences in the Dbl family GEFs may be diverse, so that direct modulation of either the DH or the PH domain could be involved in controlling the activity of the DH-PH module. The activation scheme for the GEFs, by the same token, would reflect a similar divergence which could involve an array of distinct mechanisms in absorbing different incoming signals to provide signal transduction divergence.

The recent characterization of the autoinhibitory mechanisms of the Rho GTPase effectors PAK1 and WASP also provides interesting parallels to the Dbl family Rho GEFs (25, 27). In both cases, the N-terminal CRIB motif of the molecules interacts specifically with the C-terminal functional module, the kinase domain for PAK1, or the VCA domain for WASP to achieve an autoinhibition state by masking the access of the immediate downstream target, the PAK1 substrates, or the Arp2/3 complex (25, 27). Activation of such an autoinhibition state occurs when activated Cdc42/Rac recognizes the CRIB motif, leading to allosteric relief of the target-interactive sites. Therefore, from Rho GEFs to effectors, the autoinhibition mechanism seems to be a common feature that the small-G-protein cascades utilize to mediate signal flows in a highly regulated manner.

ACKNOWLEDGMENTS

This work was supported by National Institutes of Health grant GM 53943 and U.S. Army grant BC990290 to Y.Z.F.B. is an American Heart Association Southern Consortium postdoctoral fellow.

We acknowledge the technical assistance of Catherine Ottaviano.

REFERENCES

1. **Abe, K., I. P. Whitehead, J. P. O'Bryan, and C. J. Der.** 1999. Involvement of NH_2-terminal sequences in the negative regulation of Vav signaling and transforming activity. J. Biol. Chem. **274:**30410–30418.
2. **Aghazadeh, B., K. Zhu, T. J. Kubiseski, G. A. Liu, T. Pawson, Y. Zheng, and M. K. Rosen.** 1998. Structure and mutagenesis of the Dbl homology domain. Nat. Struct. Biol. **12:**1098–1107.
3. **Aghazadeh, B., W. E. Lowry, X.-Y. Huang, and M. K. Rosen.** 2000. Structural basis for relief of autoinhibition of the Dbl homology domain of proto-oncogene Vav by tyrosine phosphorylation. Cell **102:**625–633.
4. **Alberts, A. S., and R. Treisman.** 1998. Activation of RhoA and SAPK/JNK signaling pathways by the RhoA-specific exchange factor mNET1. EMBO J. **17:**4075–4085.
5. **Bhattacharyya, R., and P. B. Wedegaertner.** 2000. Gα13 requires palmitoylation for plasma membrane localization, Rho-dependent signaling, and promotion of p115-RhoGEF membrane binding. J. Biol. Chem. **275:**14992–14999.
6. **Boriack-Sjodin, P. A., S. M. Margarit, D. Bar-Sagi, and J. Kuriyan.** 1998. The structural basis of the activation of Ras by Sos. Nature **394:**337–343.
7. **Butty, A.-C., P. M. Pryciak, L. S. Huang, I. Herskowitz, and M. Peter.** 1998. The role of Far1p in linking the heterotrimeric G protein to polarity estblishment proteins during yeast mating. Science **282:**1511–1516.
8. **Cerione, R. A., and Y. Zheng.** 1996. The Dbl family of oncogenes. Curr. Opin. Cell Biol. **8:**216–222.
9. **Cherfils, J., and P. Chardin.** 1999. GEFs: structural basis for their activation of small GTP-binding proteins. Trends Biochem. Sci. **24:**306–311.
10. **Cohen, G. B., R. Ren, and D. Baltimore.** 1995. Modular binding domains in signal transduction proteins. Cell **80:**237–247.
11. **Corbalan-Garcia, S., S. M. Margarit, D. Galron, S.-S. Yang, and D. Bar-Sagi.** 1998. Regulation of SOS activity by intramolecular interactions. Mol. Cell. Biol. **18:**880–886.
12. **Crespo, P., K. E. Schuebel, A. A. Ostrom, J. S. Gutkind, and X. R. Bustelo.** 1997. Phosphotyrosine dependent activation of Rac1 GDP/GTP exchange by the vav proto-oncogene product. Nature **385:**169–172.
13. **Fleming, I. N., C. M. Elliott, F. G. Buchanan, C. P. Downes, and J. H. Exton.** 1999. Ca^{2+}/calmodulin-dependent protein kinase II regulates Tiam1 by reversible protein phosphorylation. J. Biol. Chem. **274:**12753–12758.
14. **Goldberg, J.** 1998. Structural basis for activation of ARF GTPase: mechanism of guanine nucleotide exchange and GTP-myristoyl switch. Cell **95:**237–248.
15. **Graziani, G., D. Ron, A. Eva, and S. K. Srivastava** 1989. The human dbl proto-oncogene product is a cytoplasmic phosphoprotein which is associated with the cytoskeletal matrix. Oncogene **4:**823–829.
16. **Habets, G. G. M., E. H. M. Scholtes, D. Zuydgeest, R. van der Kammen, J. C. Stam, A. Berns, and J. G. Collard.** 1994. Identification of an invasion-inducing gene, Tiam-1, that encodes a protein with homology to GDP-GTP exchangers for rho-like proteins. Cell **77:**573–549.
17. **Hall, A.** 1998. Rho GTPases and the actin cytoskeleton. Science **279:**509–514.
18. **Han, J., K. Luby-Phelps, B. Das, X. Shu, Y. Xia, R. Mosteller, K. Murali, J. R. Falck, M. A. White, and D. Broek.** 1998. Role of substrates and products of PI 3-kinase in regulating activation of Rac-related guanosine triphosphatases by Vav. Science **279:**558–560.
19. **Hart, M. J., X. Jiang, T. Kozasa, W. Roscoe, W. D. Singer, A. G. Gilman, P. C., Sterweis, and G. Bollag.** 1998. Direct stimulation of the guanine nucleotide exchange activity of p115RhoGEF by Gα13. Science **280:**2112–2114.
20. **Hart, M., A. Eva, D. Zangrilli, S. Aaronson, T. Evans, R. A. Cerione, and Y. Zheng.** 1994. Cellular transformation and guanine nucleotide exchange activity are catalyzed by a common domain on the *dbl* oncogene product. J. Biol. Chem. **269:**62–65.
21. **Horii, Y., J. F. Beeler, K. Sakaguchi, M. Tachibana, and T. Miki.** 1994. A novel oncogene, ost, encodes a guanine nucleotide exchange factor that potentially links Rho and Rac signaling pathways. EMBO J. **13:**4776–4786.
22. **Kawasaki, Y., T. Senda, T. Ishidate, R. Koyama, T. Morishita, Y. Iwayama, O. Higuchi, and T. Akiyama.** 2000. Asef, a link between the tumor suppressor APC and G-protein signaling. Science **289:**1194–1197.
23. **Khosravi-Far, R., M. Chrzanowska-Wodnicka, P. A. Solski, A. Eva, K. Burridge, and C. J. Der.** 1994. Dbl and Vav mediated transformation via mitogen-activated protein kinase pathways that are distinct from those activated by oncogenic Ras. Mol. Cell. Biol. **14:**6848–6857.
24. **Khosravi-Far, R., P. A. Solski, M. S. Kinch, K. Burridge, and C. J. Der.** 1995. Activation of Rac and Rho and mitogen-activated protein kinases are required for Ras transformation. Mol. Cell. Biol. **15:**6443–6453.
25. **Kim, A. S., L. T. Kakalis, N. Abdul-Manan, G. A. Liu, and M. K. Rosen.** 2000. Autoinhibition and activation mechanism of the Wiskott-Aldrich syndrome protein. Nature **404:**151–158.
26. **Kiyono, M., Y. Kaziro, and T. Satoh.** 2000. Induction of Rac-guanine nucleotide exchange activity of RasGRF1/Cdc25Mm following phosphorylation by the nonreceptor tyrosine kinase Src. J. Biol. Chem. **275:**5441–5446.
27. **Lei, M., W. Lu, W. Meng, M.-C. Parrini, M. J. Eck, B. J. Mayer, and S. C. Harrison.** 2000. Structure of PAK1 in an autoinhibited conformation reveals

a multistage activation switch. Cell **102:**387–397.
28. **Li, R., and Y. Zheng.** 1997. Residues of the Rho family GTPases Rho and Cdc42Hs that specify sensitivity to Dbl-like guanine nucleotide exchange factors. J. Biol. Chem. **272:**4671–4681.
29. **Li, R., B. Debreceni, B. Jia, Y. Gao, G. Tigyi, and Y. Zheng.** 1999. Localization of the PAK1-, WASP-, and IQGAP1-specifying regions of the small GTPase Cdc42. J. Biol. Chem. **274:**29648–29654.
30. **Lin, R., R. A. Cerione, and D. Manor.** 1999. Specific contributions of the small GTPases Rho, Rac, and Cdc42 to Dbl transformation. J. Biol. Chem. **274:**23633–23641.
31. **Liu, X., H. Wang, M. Eberstadt, A. Schnuchel, E. T. Olejniczak, R. P. Meadows, J. M. Schkeryantz, D. A. Janowick, J. E. Harlan, E. A. S. Harris, D. E. Staunton, and S. W. Fesik.** 1998. NMR structure and mutagenesis of the N-terminal Dbl homology domain of the nucleotide exchange factor Trio. Cell **95:**269–277.
32. **Michiels, F., G. G. M. Habets, J. C. Stam, R. A. van der Kammen, and J. G. Collard.** 1995. A role for Rac in Tiam1-induced membrane ruffling and invasion. Nature **375:**338–340.
33. **Miki, T., C. L. Smith, J. E. Long, A. Eva, and T. P. Fleming.** 1993. Oncogene ect2 is related to regulators of small GTP-binding proteins. Nature **362:**462–465.
34. **Nern, A., and R. A. Arkowitz.** 1999. A Cdc24p-Far1p-Gbg protein complex required for yeast orientation during mating. J. Cell Biol. **144:**1187–1202.
35. **Nishida, K., Y. Kaziro, and T. Satoh.** 1999. Association of the proto-oncogene product Dbl with G protein βγ subunits. FEBS Lett. **459:**186–190.
36. **Olivo, C., C. Vanni, P. Mancini, L. Silengo, M. R. Torris, G. Tarone, P. Defilippi, and A. Eva.** 2000. Distinct involvment of Cdc42 and RhoA GTPases in actin organization and cell shape in untransformed and Dbl oncogene transformed NIH 3T3 cells. Oncogene **19:**1428–1436.
37. **Olson, M. F., N. G. Pasteris, J. L. Gorski, and A. Hall.** 1996. Faciogenital dysplasia protein (FGD1) and Vav, two related proteins required for normal embryonic development, are upstream regulators of Rho GTPases. Curr. Biol. **6:**1628–1633.
38. **Olson, M. F., P. Sterpetti, K. Nagata, D. Toksoz, and A. Hall.** 1997. Distinct roles for the DH and PH domains in the Lbc oncogene. Oncogene **15:**2827–2831.
39. **Pawson, T.** 1995. Protein modules and signaling networks. Nature **373:**573–580.
40. **Qian, X., W. C. Vass, A. G. Papageorge, P. H. Anborgh, and D. R. Lowy.** 1998. N terminus of Sos1 Ras exchange factor: critical roles for the Dbl and pleckstrin homology domains. Mol. Cell. Biol. **18:**771–778.
41. **Ron, D., S. R. Tronick, S. A. Aaronson, and A. Eva.** 1988. Molecular cloning and characterization of the human dbl proto-oncogene: evidence that its overexpression is sufficient to transform NIH3T3 cells. EMBO J. **7:**2465–2473.
42. **Ron, D., G. Graziani, S. A. Aaronson, and A. Eva.** 1989. The N-terminal region of proto-dbl down regulates its transforming activity. Oncogene **4:** 1067–1072.
43. **Ron, D., M. Zannini, M. Lewis, R. B. Wickner, L. T. Hunt, G. Graziani, S. R. Trinick, S. A. Aaronson, and A. Eva.** 1991. A region of proto-Dbl essential for its transforming activity shows sequence similarity to a yeast cell-cycle gene, Cdc24, and the human break point cluster gene, bcr. New Biol. **3:**372–379.
44. **Soisson, S. M., A. S. Nimnual, M. Uy, D. Bar-Sagi, and J. Kuriyan.** 1998. Crystal structure of the Dbl and Pleckstrin homology domains from the human son of sevenless protein. Cell **95:**259–268.
45. **Stam, J. C., E. E. Sander, F. Michiels, F. N. van Leeuwen, H. E. T. Kain, R A. van der Kammen, and J. G. Collard.** 1997. Targeting of Tiam1 to the plasma membrane requires the cooperative function of the N-terminal pleckstrin homology domain and an adjacent protein interaction domain. J. Biol. Chem. **272:**28447–28454.
46. **Tatsumoto, T., X. Xie, R. Blumenthal, I. Okamoto, and T. Miki.** 1999. Human Ect2 is an exchange factor for Rho GTPases, phosphorylated in G2/M phases, and involved in cytokinesis. J. Cell Biol. **147:**921–927.
47. **Van Aelst, L., and C. D'Souza-Schorey.** 1997. Rho GTPases and signaling networks. Genes Dev. **11:**2295–2322.
48. **Whitehead, I. P., Q. T. Lambert, J. A. Glaven, K. Abe, K. L. Rossman, G. M. Mahon, J. M. Trzaskos, R. Kay, S. L. Campbell, and C. J. Der.** 1999. Dependence of Dbl and Dbs transformation on MEK and NF-κB activation. *Mol. Cell. Biol.* **19:**7759–7770.
49. **Whitehead, I., H. Kirk, C. Tognon, G. Trigo-Gonzalez, and R. Kay.** 1995. Expression cloning of Lfc, a novel oncogene with structural similarities to guanine nucleotide exchange factors and to the regulatory region of protein kinase C. J. Biol. Chem. **270:**18388–18395.
50. **Whitehead, I. P., S. Campbell, K. L. Rossman, and C. J. Der.** 1997. Dbl family proteins. Biochim. Biophys. Acta **1332:**F1–F23.
51. **Zheng, Y., M. Hart, and R. A. Cerione.** 1995. Guanine nucleotide exchange catalyzed by *dbl* oncogene product. Methods Enzymol. **256:**77–84.
52. **Zheng, Y., M. Olson, A. Hall, R. A. Cerione, and D. Toksoz.** 1995. Direct involvement of the small GTP-binding protein Rho in *lbc* oncogene function. J. Biol. Chem. **270:**9031–9034.
53. **Zheng, Y., D. Zangrilli, R. A. Cerione, and A. Eva.** 1996. The pleckstrin homology domain mediates transformation by oncogenic Dbl through specific intracellular targeting. J. Biol. Chem. **271:**19017–19020.
54. **Zhu, K., B. Debreceni, R. Li, and Y. Zheng.** 2000. Identification of Rho GTPase-dependent sites in the DH domain of oncogenic Dbl that are required for transformation. J. Biol. Chem. **275:**25993–26001.
55. **Zhu, K., B. Debreceni, F. Bi, and Y. Zheng.** 2001. Oligomerization of DH domain is essential for Dbl-induced transformation. Mol. Cell. Biol. **21:**425–437.

Dbl family guanine nucleotide exchange factors

Yi Zheng

Department of Molecular Sciences, University of Tennessee Health Science Center, Memphis, TN 38163, U.S.A.

Address for correspondence: Yi Zheng, Department of Molecular Sciences, University of Tennessee, 858 Madison Avenue, Memphis, TN 38163, U.S.A. Phone: 901-448-5138; fax: 901-448-7360; e-mail: yzheng@utmem.edu

Summary

The Dbl family guanine nucleotide exchange factors are multifunctional molecules that transduce diverse intracellular signals leading to the activation of Rho GTPases. The tandem Dbl homology and Pleckstrin-homology domains shared by all members of this family represent the structural module responsible for catalyzing the GDP/GTP exchange reaction of Rho proteins. Recent progresses in genomic, genetic, structural, and biochemical studies have implicated Dbl family members in diverse biological processes including organism growth and development, skeletal muscle formation, neuronal axon guidance and tissue organization. The detailed pictures of their auto-regulation, agonist controlled activation, and mechanism of interaction with Rho GTPase substrates have begun to emerge.

Introduction

The *dbl* oncogene product was originally isolated from a diffuse B-cell lymphoma. Subsequent amino acid sequence analysis found that a region in the central portion of Dbl protein, now known as Dbl homology (DH) domain, shares significant similarity with the yeast cell division cycle molecule Cdc24 and the human break point cluster region protein Bcr. Suspicion that Cdc24 might act upstream of Cdc42 in yeast led to the biochemical finding that both Dbl and Cdc24 function as guanine nucleotide exchange factors (GEFs) that stimulate the replacement of bound GDP by GTP of specific Rho family GTPases[1,2]. Over the past decade, a large group of proteins have joined the Dbl family by virtue of their structural similarities with Dbl in containing the DH domain and a tandem Pleckstrin homology (PH) domain which is invariably located at the immediate carboxyl terminus of DH domain. Many of them, including Vav, Tiam1, Ect2, Ost, Dbs, Lbc, Lfc, and Net, possess transformation or invasion capability like oncogenic Dbl. Others include proteins identified as gene products of sequences that are rearranged in human diseases (Bcr or FGD1) or as proteins with other catalytic functions, such as Sos or RasGRF that are Ras specific GEFs. Dbl family quickly became one of the largest families of growth regulatory molecules.

Current biochemical model depicts that Dbl family GEFs function immediately upstream of Rho GTPases in transmitting intracellular signals (Fig. 1). Stimulation of growth factor receptors, cytokine receptors, cell-to-cell or extracellular matrix-to-cell adhesion receptors, or the G-protein coupled serpentine receptors may all initiate intracellular signals that lead to Rho GTPase activation, a process which very likely involves one or multiple Dbl family members. The abilities to stimulate GDP dissociation from inactive Rho-GDP and to facilitate GTP loading to generate the active Rho-GTP species in cells are the hallmarks of the biochemical activities of the GEFs. Upon

activation by the GEFs, Rho GTPases interact in turn with a large array of effector targets that further relay the incoming signals to downstream signaling components resulting in diverse cell biological responses including actin cytoskeleton reorganization, transcriptional activation of genes, stimulation of DNA synthesis, endocytic or exocytic membrane trafficking, and regulation of translation (reviewed in ref. 3, 4).

This review focuses on recent progresses made in understanding the biological functions and the molecular mechanisms underlying the biochemical activities of Dbl family GEFs. The mode of regulation of Dbl family members and the mechanistic interactions between the GEFs and Rho GTPase substrates are discussed in depth.

Evolution and genetics

DH domain does not share significant sequence homology with other subtypes of small G-protein GEFs such the Cdc25 domain and Sec7 domain that are specific to Ras or ARF family small GTPases, indicating that the Dbl family proteins are evolutionarily unique. Recently completed genome sequencing projects have revealed that there are at least 3 Dbl family GEFs in *S. cerevisiae*, 18 in *C. elegans*, 23 in *Drosophila*, and 46 in *Homo sapien*[5]. The number of Dbl family may increase further when detailed annotations of the genomic sequences become available, since there are additional ~30 partial sequences in human genomes that appear to encode DH domain containing proteins. The number of GEF substrates, Rho family GTPases, also increases with evolution, from 5 in *S. cerevisiae* to 16 in human, but is significantly less than the number of their positive regulators in higher eukaryotes, suggesting that the function of individual GEFs is more specialized in mammals. Indeed, many mammalian Dbl family members are tissue and cell type specific, and their biochemical GEF activities range from highly seletive toward one Rho GTPase substrate to more promiscuous toward multiple Rho proteins (Table 1).

The first genetic evidence of Dbl family function came from Cdc24, a bud site assembly molecule in *S. cerevisiae* whose function was known to be closely associated with Cdc42[3]. Various Cdc24 mutant phenotypes implicate it as an essential component regulating vegetative growth, cell mating, polarity establishment, and cell orientation[6]. Rom2, a multiple copy suppressor of rho1 mutations, appears to act in the Tor2-Rho1/Rho2 pathway controlling cell shape and growth[7]. The functional link between Dbl family GEFs and Rho GTPases was further strengthened when UNC-73, a large multifunctional molecule in *C. elegans* containing two separate DH-PH motifs, was found to regulate cell actin structure and movement and the loss of its function resulted in multiple defects in axon guidance and neuronal cell migration[8]. In *Drosophila*, the Dbl family member SIF protein was suggested to be involved in regulation of synaptic differentiation since it is found to be associated with plasma membrane of synaptic terminals and mutations in SIF led to defects in neuronal morphology[9]. Recently a set of genetic studies presented evidence that Trio, a homolog of UNC-73, mediates the effects of axon guidance factors on actin dynamics[10]. The genetic phenotypes of Trio mutations suggest a biochemical pathway linking the transmembrane tyrosine phosphatase Dlar and the Abl tyrosine kinase to the Trio-Rac-Pak signaling complex. In mice, Trio deficiency causes skeletal muscle deformation and neuronal disorder[11], and elimination of the vav gene which encodes a hematopoietic cell specific GEF results in impaired lymphoid development, lymphopedia, and defective immune responses of B- and T-lymphocytes[12], suggesting more complex roles of the GEFs in mammals. Interestingly, Dbl knock-out mice do not display any apparent abnormalities (A. Eva, personal communication), raising the possibility that multiple Dbl family genes could play redundant roles.

So far, the only compelling evidence that Dbl family GEFs are involved in human genetic disorder came from the studies of FGD1[13]. Mutation of FGD1 in DH domain is found to cosegregate with faciogenital dysplasia. Whether the DH domain in Bcr which is absent in Bcr-Abl fusion in chronic myelogenous and acute lymphocytic leukemias[2] or the GEF activity of LARG which is retained in MLL-LARG fusion in acute myeloid leukemia[14] plays a role in these diseases remains to be seen.

Biochemical functions

Dbl family GEFs are multifunctional molecules containing diverse structural motifs in addition to the conserved DH-PH domains (Fig. 2). Early biochemical studies using oncogenic Dbl as a model system have established that while DH domain is responsible for the GEF catalytic activity, the adjacent PH domain is involved in intracellular targeting of DH domain. Furthermore, the DH-PH module constitutes the minimum structural unit bearing transforming function[1,2]. This appears to be a generalized principle among Dbl family GEFs as similar conclusions have been drawn in the cases of Lbc, Lfc, Dbs, and other GEFs. Demonstration of substrate binding and catalytic activities in reconstituted GEF reactions using purified GEFs and examination of Rho GTPase activation states induced by over-expression of the putative GEFs in fibroblasts or other types of cells have provided the bulk of the data on the biochemical functions of Dbl members (Table 1). Some of them, like Cdc24, FGD1, Tiam1, and Lbc, are highly specific toward a single Rho protein, while others, including Dbl, Ost, Ect2, and Bcr, behave quite promiscuously by working on multiple Rho GTPases. The early view that certain members of Dbl family may function by binding to Rho GTPases without GEF activity (e.g. Ect2)[1] does not seem to hold up, since recent studies have revealed that a variety of regulatory signals (e.g. phosphorylation)[15] may be required for

the activation of GEF activity. Furthermore, mutants generated in the DH domain that retain substrate binding activity but are catalytically compromised acted as dominant-negatives in cells[16], suggesting that a threshold of GEF catalytic activity, in addition to the Rho binding activity, is required for the function.

The combination of a few additional lines of evidence also help establish that Dbl family GEFs function by activation of Rho GTPases in cells. The evidence include that the Dbl family oncoprotein induced foci are morphologically similar to those transformed by constitutively active Rho GTPases, but distinct from that seen when cells are transformed by other types of oncogenes such as Ras, Raf, or Src[2]; coexpression of Dbl family members with dominant negative mutants of Rho family GTPases blocks their transforming activity[3]; mutants of the GEFs that are no longer able to interact or activate Rho protein substrates behave dominant negatively in cells[15,16]; and many cellular activities induced by Dbl family proteins, such as actin cytoskeleton reorganization, cytokinesis, stimulation of G1 to S phase transition, Jun N-terminal kinase activation, cyclin D1 induction, and SRF and NF-kB activations, are associated with the activation of signaling pathways known to be mediated by active Rho GTPases or by Rho GTPase effector targets[2,3,17].

It is therefore not surprising that many Dbl family members display transforming activity in fibroblast transfection assays, and some, through activation of Rac1 or related pathway, regulate cell migration and tumor metastasis. The important issues currently attracting much attention are which pathways among the many regulated by the GEFs are essential for cell transformation or metastasis and whether interference with selected pathways can be explored for anti-cancer drug design. One needs to caution that given the multifunctional nature of these proteins (Fig. 2), it is certainly possible that many of the GEF molecules bear GEF-independent functions. Determining what these other functions might be and how they effect on the GEF-elicited pathways by Dbl family

members should also provide leads to a more comprehensive understanding of the GEF functions.

Mechanisms of regulation

Many members of the Dbl family seem to exist in an inactive or partially active state prior to stimulation. Current literature suggests that their basal states may be maintained by one of three possible regulatory modes involving intra- or inter-molecular interactions (Fig. 3). The first is through the intramolecular interaction between DH and PH domains. Examples of such an interaction include Vav and Sos1 in which cases binding to PIP3 by the PH domain seems to alleviate an inhibitory effect on the DH domain[18,19]. The second possible mode of regulation is through the intramolecular interaction of a regulatory domain with the DH or PH domain of the GEF protein. Such interactions are expected to impose a constraint on the normal DH and/or PH domain function by masking the access of Rho GTPase substrate and/or altering the PH domain intracellular targeting. The examples of such regulation include Vav and Dbl[20,21], and may also include Asef, Lbc, and p115RhoGEF. The third possible mode involves oligomerization through an intermolecular interaction between DH domains. This mode of regulation has been suggested recently in the cases of RasGRF1, RasGRF2 and onco-Dbl[22,23], and is postulated to play a role in efficient execution of the GEF function. The incoming upstream signals, via the heterotrimeric G-protein Gα or Gβγ subunits, protein tyrosine or serine/threonine kinases, and/or phosphoinositol lipids, may contribute by varying degrees to the alteration of these auto-regulatory modes, resulting in intracellular translocation of GEF and stimulation of GEF catalytic activity. A few representative cases of GEF regulations are illustrated in Fig. 4.

Activation by GTP-binding proteins - Bradykinin, LPA, bombesin and other G-protein coupled receptors have been known to activate Rho GTPase pathways[3,4]. Both Gα and Gβγ subunits have been suggested to have roles in inducing Rho mediated actin stress fiber formation and/or focal adhesion assembly. Gβγ in *S. cerevisiae* was the first to be found to directly interact with a RhoGEF, Cdc24, in response to pheromone-receptor activation[2,3]. Rsr1, a Ras-related GTPase, also directly interacts with Cdc24 to target it to the budding site of the cell[1,2]. Subsequent biochemical studies identify p115RhoGEF, LARG, and GTRAP48/PDZ-RhoGEF as a subset of GEFs containing RGS-like domain that binds to and is activated by Gα13[14,24,25]. Dbl protein was also suggested to be able to bind to Gβγ and Gα13 through its N-terminal regulatory sequences[26,27], although it remains to be seen if such interactions are physiologically relevant. Early experiments carried out in Swiss 3T3 fibroblast cells suggested that Cdc42, Rac1, and RhoA act in a linear cascade fashion in mediating signal flows causing cytoskeleton changes[4], and that they all are involved in Ras-induced transformation in NIH 3T3 cells[3,4]. The GEFs between these small G-protein hierarchy chains remain to be identified. One possible scenario is that the link is a single GEF molecule such as Tiam1, which is recently found to contain a Ras-binding domain and therefore may activate Rac1 promptly in response to Ras. Alternatively, a class of GEFs containing both DH domain and Ras-activating Cdc25 domain like Sos and RasGRF could serve to activate Ras and Rac1 simultaneously or sequentially in response to stimuli, since both of these catalytic functional motifs have been recently found to confer respective GEF activity toward Rac1 and Ras, respectively[19,28]. However, activation of the DH domain in these two-headed GEFs may require additional modulators like E3b1 and Eps8 in the case for Sos1[29], where a macromolecular complex seems to be needed to unmask the GEF activity for Rac1.

Activation by protein kinases – In response to extracellular stimuli, many Dbl family GEFs become phosphorylated by protein kinases which may contribute to their activation. The best understood case is Vav, which is phosphorylated by Src family tyrosine kinases after cytokine or adhesion receptor activation[12]. In the basal state, a stretch of N-terminal sequences folds into an α-helical structure and binds to the active site of DH domain, masking the access of Rac1[20]. Upon phosphorylation at residue Tyr174, these amino acid sequences become unstructured and the constraint on DH domain is relieved. Another example of activation by phosphorylation is Ect2, a regulator of cytokinesis whose GEF activity toward Rho is induced by Cdk-related kinases during cell cycle progression[15]. It remains a challenge to sort out the physiologically meaningful phosphorylation events that regulate many GEF functions.

Regulation by phosphoinositol kinases – The PI3 kinase homolog TOR2 was shown to be involved in activation of the GEF ROM2 and the GTPase Rho1 cascade in yeast[7], suggesting that the lipid product of the kinase, PIP3, may play a role in GEF activation. In mammalian cells, early studies have shown that treatment with the PI3K inhibitor wortmannin inhibited Rac effect activated by growth factor receptors[3,4], and the invariable presence of a PH domain in Dbl family GEFs makes it a valid hypothesis that PIPs may affect GEF activity and/or location by binding to the PH domain. Indeed, many PH domains derived from Dbl family were shown to be capable of interaction with PIPs. The more convincing evidence that such interaction may contribute to the modulation of GEF function came from studies of Vav and Sos1, both of which displayed enhanced GEF activity toward Rac1 upon PIP3 binding to the PH domain[18,19]. Interestingly, PIP2, the substrate of PI3K, was found to inhibit substrate binding and

GEF activity of the DH domain of Vav and Sos1[30], suggesting that PIPs regulate the intramolecular interaction between DH and PH domains. The GEF activity of Dbl toward Cdc42, on the other hand, was found to be inhibited by either PIP2 or PIP3 binding to the PH domain[31]. Although lipid binding is important for plasma membrane targeting, but apparently it is not essential for cytoskeleton localization of Dbl, nor cell transformation.

Regulation by other intermolecular interactions – In *S. cerevisiae*, the GEF activity of Cdc24 is subjected to regulation by two adapter/scaffolding molecules, Bem1 and Far1. The formation of a Cdc24-Far1-Gβγ complex functions as a landmark for orientation of the cytoskeleton during growth[32]. In mammalian cells, discovery of Far1-like large scaffolding molecules still awaits. Filamin, an actin crosslinker, was shown to be a potential target of the PH domain of Trio[33], while Frabin, a FGD1-related GEF, was found to contain actin cross-linking activity itself[34]. The membrane associated molecule radixin interacts with Dbl and may also recruit the Rho GDP-dissociation inhibitor (GDI) to the complex[35]. Other regulatory interactions of GEFs reported recently include Asef interaction with the tumor suppressor APC which results in its activation[36], p115RhoGEF interaction with HIV gp41 which leads to a negative effect on the GEF function[37], Tiam1 binding to the hyaluronic acid-binding receptor CD44 and to the cytoskeletal protein ankyrin, both of which positively regulate the Rac1-specific GEF activity[38,39], and Tiam1 interaction with tumor metastasis suppressor nm23H1 that results in a decrease in GEF activity toward Rac1[40]. Most recently, two novel Dbl family GEFs ephexin and GTRAP48 have been shown to form a signaling complex at the receptor level with EphA and EAAT4, respectively[25,41], mediating neuronal growth cone dynamics or glutamate transporter functions. It is foreseeable that future studies of GEFs converging from

diverse biological areas may uncover more unique, physiological meaningful interactions that have regulatory effect on GEF functions.

Overall, the biochemical mechanisms of the spatial and temporal regulation of GEFs remain poorly understood. In addition to GEF activation, concomitant upstream signals are likely required to suppress the negative regulations imposed upon Rho GTPase substrates by the GTPase-activating proteins (GAPs) and GDIs[3,4]. To this end, the regulatory networks employed by PIX[42] and Cdc24[32] (Fig. 4) provide some clues that large signaling complex could be involved to enhance the counter-reactive ability of a GEF for negative regulations and to ensure signaling specificity.

Mechanism of guanine nucleotide exchange on Rho GTPases

In analogy with GEF activation of Ras and heterotrimeric Gα, the Dbl family GEFs are thought to involve sequential GDP-dissociation and GTP-binding steps to facilitate GDP/GTP exchange onto Rho GTPase substrates[43]. The exchange reactions are initiated when GEFs recognize the GDP-bound Rho proteins, followed by stimulation of GDP-dissociation to achieve a binary GEF-Rho complex in which the small G-protein exists in a nucleotide-free state. This transient reaction intermediate is then dissociated by GTP-binding to the Rho protein and the final product, GTP-bound Rho, is released. The highlights of the biochemical function of Dbl family GEFs in such a scheme are that they serve dual roles in the reaction: to destabilize GDP interaction with Rho proteins and to stabilize the nucleotide-depleted, transition state of the substrate. The strongest evidence supporting the GEF reaction mechanism came from the observation that the nucleotide-free form of Rho proteins bind to GEFs with much higher affinity than the GDP- or GTP-bound form, enabling such an intermediate complex to be obtained easily *in vitro*. A few recent observations, however, suggest that the reaction mechanism may

be more complex: the exchange reaction of Rho GTPases catalyzed by Dbl family GEFs depends on the concentration and nature of incoming free nucleotides, and the GEFs appear to affect both GDP dissociation and GTP binding kinetics (our unpublished results). It is therefore likely that the biochemical activities of GEFs may be further extended to influencing the GTP-binding step. More detailed studies are required to differentiate whether the dynamic process of GEF reactions is through sequential GDP dissociation-nucleotide free state-GTP association or direct GTP displacement of bound GDP.

The evidence that isolated, purified DH domains are active in stimulating nucleotide exchange showed that DH domain constitutes the necessary and sufficient structural unit catalyzing GEF reactions. The three dimensional structures of three distinct members of Dbl family, TrioN, Sos1, and βPIX, depict that these DH domains fold into highly homologous α-helical bundles and are unrelated to other proteins that interact with Rho family GTPases and other GEF families[44,45,46]. Systematic mutagenesis of DH domains of Dbl and TrioN mapped CR1, CR3, a part of α6, and the DH-PH junction site that are exposed near the center of one side of the molecule as the important sites involved in the formation of a Rho GTPase interactive pocket[16,44]. Recent determination of the structure of the DH-PH module of Tiam1 bound to Rac1 provides a framework for interpreting these and other biochemical studies aimed at delineating the structural determinants of the Rho proteins involved in GEF coupling[47] (Fig. 5a). Firstly, Rac1 makes direct contact with the CR1, CR3, and the C-terminus of α9 close to the PH junctional site, confirming that residues of these regions of DH are involved in GEF interaction. Secondly, the interaction with Tiam1 has altered the conformation of the sequences in and immediately flanking switch 1 and switch 2 regions of Rac1, and not

unlike the cases of other GEF-G complexes, disturbed the native coordination for Mg^{2+} cofactor. In particular, Ala59 has moved within 2Å of the Mg^{2+} binding site to disrupt effective Mg^{2+} chelation. This in part explains the previously observed lowered Mg^{2+}-binding affinity to Rho proteins when a GEF is present[48]. Thirdly, a large portion of β2/β3 and switch 2 regions of Rac1 engages in extensive surface contact with Tiam1 residues, providing docking sites for GEF recognition and stabilizing the complex formation. One or more residues in the β2/β3 region, S41, N43, N52, and W56 in particular, appear to be the key structural elements dictating the specificity by interacting with the α7 region of Tiam1 that represents the most variable part of the molecule in this "lock and fit" model (Fig. 5b). A unique feature for Tiam1-Rac1 interaction is that the GEF may not be involved in direct interference with the binding of either α- or β-phosphate of the guanine nucleotide, raising the possibility that Dbl family GEF reaction mechanism might be different from that of Cdc25 or Sec7 domains in GEFs for Ras or ARF GTPases.

Interestingly, the Tiam1-Rac1 complex dimerizes through a largely hydrophobic surface area of DH domain including the CR2 region (Fig. 5a). This provides an explanation of previous findings that RasGRF1 and Dbl could form functional oligomers through DH domain to mediate their cellular functions[22,23] and further supports a self-regulatory role of DH domain in a subset of Dbl family proteins. Moreover, conformationally different from the isolated Sos1 DH-PH module[45], the PH domain of Tiam1 does not seem to contribute to Rac1 binding in the complex. It is likely that the PH domain plays mostly a structural role in maintaining the integrity of the adjacent DH domain, or alternatively, the snap shot of the crystals may have failed to capture a more dynamic interaction between the PH domain and the DH domain or the small G-protein.

More work is needed to clarify the involvement of the neighboring PH domain in DH domain function.

It should be noted that although Dbl family GEFs appear to be the major class of molecules that positively regulate Rho GTPase activities, exceptional cases involving non-DH domain motifs or phosphoinositol lipids have been reported to stimulate guanine nucleotide exchange or GDP dissociation of Rho GTPases. For example, Salmonella SopE protein can effectively activate Rac1 and Cdc42 to facilitate bacteria entry into the host cells[49], and the Rap1 specific GEF, C3G, is found to be an active GEF toward the Rho protein TC10 in insulin-stimulated GLUT4 translocation[50]. The biochemical and structural basis of these GEF reactions requires further investigation.

Conclusions

Recent genetic, cell biological, structural, as well as biochemical studies have implicated Dbl family GEFs as the major positive regulators of Rho GTPases in diverse biological settings. *In vitro* biochemical studies have established the role of the conserved DH domain in Rho GTPase interaction and activation and the role of the tandem PH domain in intracellular targeting and/or regulation of DH domain function. The near completion of genomic sequencing and the rapid progress in gene annotation of human and many other organisms symbolize that the initial identification stage of Dbl family members is close to an end. More systematic characterizations of their biochemical function, mode of regulation and signaling mechanisms in various physiologically relevant systems will likely to assign each to specific intracellular pathways and logically represents the next important step towards understanding the mechanism of control of signal flows through these GEFs and their specific Rho GTPase substrates. With increasing appreciation of a close relationship between the activation

status of Dbl family members and human pathological conditions such as cancer, drug discovery efforts aimed at interfering the GEF functions of Dbl proteins may prove to be worthy endeavors.

Acknowledgements

The number of papers cited have been limited by space constraints. I thank Yuan Gao for data base searches and Feng Bi and Yuan Gao for help with graphics. I am grateful to David Worthylake for Tiam1-Rac1 coordinates. Work in my laboratory is supported by National Institutes of Health, American Cancer Society, and Department of Defense Breast Cancer Program.

References

1. Whitehead, I. P., et al. (1997) Dbl family proteins. *Biochim. Biophys. ACTA* 1332, F1-F23.

2. Cerione, R. A. and Zheng, Y. (1996) The Dbl family of oncogenes. *Curr. Opin. Cell Biol.* 8, 216-222.

3. Van Aelst, L., and D'Souza-Schorey, C. (1997) Rho GTPases and signaling networks. *Gene & Dev.* 11, 2295-2322.

4. Hall, A. (1998) Rho GTPases and the actin cytoskeleton. *Science* 279, 509-514.

5. Venter, J. C.., et al. (2001) The sequence of the human genome. *Science* 291, 1304-1351.

6. Butty, A.-C., Pryciak, P. M., Huang, L. S., Herskowitz, I., and Peter, M. (1998) The role of Far1p in linking the heterotrimeric G protein to polarity estblishment proteins during yeast mating. *Science* 282, 1511-1516.

7. Schmidt, A., et al. (1997) The yeast phosphatodylinositol kinase homolog TOR2 activates RHO1 and RHO2 via the exchange factor ROM2. *Cell* 88, 531-542.

8. Steven, R., et al. (1998). Unc-73 activates the Rac GTPase and is required for cell and growth cone migrations in C. elegans. *Cell* 92, 785-795.

9. Sone, M., et al., (1997) Still life, a protein in synaptic terminals of drosophila homologous to GDP-GTP exchangers. *Science* 275, 543-547.

10. Newsome, T. P., et al. (2000). Trio combines with Dock to regulate Pak activity during photoreceptor axon pathfinding in Drosophila. *Cell* 101, 283-294.

11. O'Brien, S. P., et al. (2000) Skeletal muscle deformity and neuronal disorder in Trio exchange factor-deficient mouse embryos. *Proc. Natl. Acad. Sci. U.S.A.* 97, 12074-12078.

12. Bustelo, X. R. (2000) Regulatory and signaling properties of the Vav family. *Mol. Cell Biol.* 20, 1461-1477.

13. Pasteris, N. G., et al. (1994) Isolation and characterization of the faciogenital dysplasia (Arskog-Scott syndrome) gene: A putative Rho/Rac guanine nucleotide exchange factor. *Cell* 79, 669-678.

14. Kourlas, P. J., et al. (2000) Identification of a gene at 11q23 encoding a guanine nucleotide exchange factor: evodence for its fusion with MLL in acute myeloid leukemia. *Proc. Natl. Acad. Sci. USA* 97, 2145-2150.

15. Tatsumoto, T., et al (1999). Human Ect2 is an exchange factor for Rho GTPases, phosphorylated in G2/M phases, and involved in cytokinesis. *J. Cell Biol.* 921-927.

16. Zhu, K., et al. (2000) Identification of Rho GTPase-dependent sites in the DH domain of oncogenic Dbl that are required for transformation. *J. Biol. Chem.* 275, 25993-26001.

17. Whitehead, I. P., et al. (1999) Dependence of Dbl and Dbs transformation on MEK and NF-kB activation. *Mol. Cell. Biol.* 19, 7759-7770.

18. Han, J., et al. (1998) Role of substrates and products of PI 3-kinase in regulating activation of Rac-related guanosine triphosphatases by Vav. *Science* 279, 558-560.

19. Nimnual, A. S., et al. (1998) Coupling of Ras and Rac guanosine triphosphatases through the Ras exchanger Sos. *Science* 279, 560-563.

20. Aghazadeh, B., et al. (2000) Structural basis for relief of autoinhibition of the Dbl homology domain of proto-oncogene Vav by tyrosine phosphorylation. *Cell* 102, 625-633.

21. Bi, F., et al. (2001) Autoinhibition mechanism of proto-Dbl. *Mol. Cell. Biol.* 21, 1463-1474.

22. Anborgh, P. H., et al. (1999) Ras-specific exchange factor GRF: oligomerizarion through its Dbl homology domain and calcium-dependent activation of Raf. *Mol. Cell. Biol.* 19, 4611-4622.

23. Zhu, K., et al. (2001) Oligomerization of DH domain is essential for Dbl-induced transformation. *Mol. Cell. Biol.* 21, 425-437.

24. Hart, M. J., et al. (1998) Direct stimulation of the guanine nucleotide exchange activity of p115RhoGEF by Gα13. *Science* 280, 2112-2114.

25. Jackson, M., et al., (2001) Modulation of the neuronal glutamate transporter EAAT4 by two interacting proteins. *Nature* 410, 89-93.

26. Nishida, K., et al. (1999). Association of the proto-oncogene product Dbl with G protein βγ subunits. *FEBS Letters* 459, 186-190.

27. Jin, S., and Exton, J. H. (2000) Activation of RhoA by association of Galpha(13) with Dbl. *Biochem. Biophys. Res. Commun.* 277, 718-721.

28. Fan, W.-T., et al. (1998) The exchange factor Ras-GRF2 activates Ras-dependent and Rac-dependent mitogen-activated protein kinase pathways. *Curr. Biol.* 8, 935-938.

29. Scita, G., et al. (1999) EPS8 and E3B1 transduce signals from Ras to Rac. *Nature* 401, 290-293.

30. Das, B., et al. (2000) Control of intramolecular interactions between the pleckstrin homology and Dbl homology domains of Vav and Sos1 regulates Rac binding. *J. Biol. Chem.* 275, 15074-15081.

31. Russo, C., et al. (2001) Modulation of oncogenic Dbl activity by phosphoinositol phosphate binding to PH domain. *J. Biol. Chem.* in press.

32. Gulli, M.-P., et al. (2000) Phosphorylation of the Cdc42 exchange factor Cdc24 by the PAK-like kinase Cla4 may regulate polarized growth in yeast. *Mol. Cell* 6, 1155-1167.

33. Bellanger, J.-M., et al. (2000) The Rac1- and RhoG-specific GEF domain of Trio targets filamin to remodel cytoskeletal actin. *Nature Cell Biol.* 2, 888-892.

34. Obaishi, H., et al. (1998) Frabin, a novel FGD1-related actin filament-binding protein capable of changing cell shape and activating c-Jun N-terminal kinase. *J. Biol. Chem.* 273, 18697-18700.

35. Takahashi, K., et al. (1998) Interaction of radixin with Rho small G protein GDP/GTP exchange protein Dbl. *Oncogene* 16, 3279-3284.

36. Kawasaki, Y., et al. (2000) Asef, a link between the tumor suppressor APC and G-protein signaling. *Science* 289, 1194-1197.

37. Zhang, H., et al. (1999) Functional interaction between the cytoplasmic leucine-zpper domain of HIV-1 gp41 and p115RhoGEF. *Curr. Biol.* 9, 1271-1274.

38. Bourguignon, L. Y., et al. (2000) CD44 interaction with Tiam1 promotes Rac1 signaling and hyaluronic acid-mediated breast tumor cell migration. *J. Biol. Chem.* 275, 1829-1838.

39. Bourguignon, L. Y., et al. (2000) Ankyrin-Tiam1 interaction promotes Rac1 signaling and metastatic breast tumor cell invasion and migration. *J. Cell Biol.* 150, 177-191.

40. Otsuki, Y., et al. (2001) Tumor metastasis suppressor nm23H1 regulates Rac1 GTPase by interaction with Tiam1. *Proc. Natl. Acad. Sci. U. S. A.* 98, 4385-4390.

41. Shamah, S., et al., (2001) EphA receptors regulate growth cone dynamics through the novel guanine nucleotide exchange factor ephexin. *Cell* 105, 233-244.

42. Manser, E., et al. (1998) PAK kinases are directly coupled to the PIX family of nucleotide exchange factors. *Mol. Cell* 1, 183-192.

43. Cherfils, J. and Chardin, P. (1999) GEFs: structural basis for their activation of small GTP-binding proteins. *Trends Biochem. Sci.* 24, 306-311.

44. Liu, X., et al. (1998) NMR structure and mutagenesis of the N-terminal Dbl homology domain of the nucleotide exchange factor Trio. *Cell* 95, 269-277.

45. Soisson, S. M., et al. (1998) Crystal structure of the Dbl and Pleckstrin homology domains from the human son of sevenless protein. *Cell* 95, 259-268.

46. Aghazadeh, B., et al. (1998) Structure and mutagenesis of the Dbl homology domain. *Nature Struct. Biol.* 12, 1098-1107.

47. Worthylake, D. K., et al. (2000) Crystal structure of Rac1 in complex with the guanine nucleotide exchange region of Tiam1. *Nature* 408, 682-688.

48. Zhang, B., et al. (2000) The role of Mg^{+2} cofactor in guanine nucleotide exchange and GTP hydrolysis reactions of Rho family GTPases. *J. Biol. Chem.* 275, 25299-25307.

49. Hardt, W.-D., et al. (1998) S. typhimurium encodes an activator of Rho GTPases that induces membrane ruffling and nuclear responses in host cells. *Cell* 93, 815-826.

50. Chiang, S.-H., et al. (2001) Insulin-stimulated GLUT4 translocation requires the CAP-dependent activation of TC10. *Nature* 410, 944-948.

Table 1. Biochemical and biological functions of mammalian Dbl family members

Dbl family member	Biochemical activities	Biological properties/activities	Accession
Dbl	GEF for most Rho GTPses including Cdc42, Rac and Rho	proto-oncogene product brain, gonads and adrenal glands specific	X12556
Bcr	GEF for Cdc42, Rac and Rho	implicated in leukemia predominantly brain	Y00661
Abr	GEF for Cdc42, Rac and Rho	predominantly brain	U01147
Ect2	GEF for Cdc42, Rac and Rho	proto-oncogene product regulator of mitosis	NM007900
FGD1	GEF for Cdc42	implicated in faciogenital dysplasia and mammalian skeletal development	NM004463
FGD2	to be determined	embryonic development	NM013710
Lbc/Brx	GEF for Rho	proto-oncogene product; binds to nuclear hormone receptor	NM006738
Lfc	GEF for Rho, binds to Rac	proto-oncogene product	U28495
p115RhoGEF/Lsc	GEF for Rho	proto-oncogene product; binds to Gα13	U64105
Net1	GEF for Rho	proto-oncogene product	U02081
Ost/Dbs	GEF for Cdc42 and Rho binds to Rac	proto-oncogene product at least three isoforms	Z35654
p190RhoGEF	GEF for Rho	inhibits neurite outgrowth binds to microtubules	U73199
RasGRF1	GEF for Rac and Ras	dual Rac and Ras activator; activates Ras through a separate Cdc25 domain	X67241
RasGRF2	GEF for Rac and Ras	dual Rac and Ras activator; activates Ras through a separate Cdc25 domain	U67326
Kalirin/Duo	GEF for Rac and Rho	two DH-PH modules; multiple isoforms due to alternative splicing	AF232669
Trio	GEF for Rac and Rho Target of Rho	two DH-PH modules with distinct substrate specificity; at least two isoforms; implicated in skeletal muscle and neuronal development	U42390
Asef	GEF for Rac	enriched in brain; binding to tumor suppressor APC leads to activation	AB042199
Pix/Cool	GEF for Rac	at least two isoforms; binds to Rac effector PAK	AF044673
Frabin	GEF for Cdc42	binds to actin	AF038388

Table 1. Continue

Vav	GEF for Rac1	proto-oncogene product; hematopoietic cell -specific; implicated in lymphopenia	X64361
Vav2	GEF for Rho, Rac, and Cdc42	proto-oncogene product;	NM009500
Vav3	GEF for Rho and Rac	proto-oncogene product;	NM020505
hPEM-2	GEF for Cdc42	predominantly brain	AB007884
GEF-H1	GEF for Rac and Rho	associates with microtubule	U72206
GTRAP48 /KIAA0380 /PDZ-RhoGEF	GEF for Rho	predominantly brain cerebellum; associates with neuronal glutamate transporter; binds to Gα13	AF225961
LARG	GEF for RhoA	fuses to MLL gene in acute myeloid leukemia; interacts with Gα12 and Gα13	AF180681
Tiam1	GEF for Rac	proto-oncogene product; mediate T-lymphoma invasionand metastasis	NM009384
Tiam2	GEF for Rac	two isoforms; cerebellum and testis specific	NM012454
Tim	to be determined	proto-oncogene product	U02082
Sos1	GEF for Rac and Ras	activates Rac and Ras through distinct DH and Cdc25 domains	Z11574
Sos2	GEF for Rac and Ras	activates Rac and Ras through distinct DH and Cdc25 domains	Z11664
GEF337	GEF for RhoA	to be determined	AB002335
Stef	GEF for Rac1	to be determined	AB022915
p114RhoGEF	GEF for RhoA	to be determined	AB011093
Ngef/ephexin	GEF for RhoA, Rac1, Cdc42	proto-oncogene product; predominantly in brain mediates Eph regulation of growth cone	NM019867
Collybistin	to be determined	two splice variants; predominantly in brain	AJ250425
Intersectin	GEF for Cdc42	two splice variants; brain-specific	NM003024

Figure Legends

Figure 1. Signaling role of Dbl family GEFs in the regulation of Rho GTPase functions. In mammalian cells, stimulation of a variety of cell surface receptors, including growth factor receptors, cytokine receptors, cell-cell or cell-extracellular matrix adhesion receptors and G-protein-coupled serpentine receptors, may all lead to the activation of specific Dbl family GEFs. The activated GEFs in turn catalyze the exchange of bound GDP for GTP on specific Rho GTPases resulting in their activation. The GTP-bound Rho proteins may further interact with multiple effector targets leading to diverse cellular responses such as actin cytoskeleton reorganization, endocytosis and exocytosis, transcription activation, stimulation of DNA synthesis, and/or translational regulation.

Figure 2. Schematic depiction of the domain structures of representative Dbl family members. Abbreviations: Ac, acidic amino acid rich motif; C2, calcium-dependent lipid binding; Cdc25, RasGEF motif; CC, coiled coil; CR, cysteine rich zinc butterfly motif; CH, calponin homology; DH, Dbl homology; EF, EF hand calcium binding motif; Ig, immunoglobulin-like; IQ, calmodulin binding motif; kinase, serine/threonine kinase motif; P, proline rich SH3 binding motif; PDZ, DHR or GLGF domain; PEST, amino acids P, E, S, and T rich, degradation motif; PH, Pleckstrin homology; RBD, Ras binding domain; REM, Ras exchanger motif; RhoGAP, RGS, regulator of G-protein signaling motif; Rho GTPase activating protein motif; Sec14, sec14-like; SH2, Src homology 2; SH3, Src homology 3; TR, Tat/RAG8-related.

Figure 3. Intra- and inter-molecular interactions implicated in auto-regulation of Dbl family GEFs. (a) Potential DH/PH interaction within a DH-PH functional module may block the access of Rho GTPase substrates. (b) Interaction between an intramolecular regulatory domain and the DH or PH domain may mask the DH domain and/or affect the targeting function of the PH domain. (c) Oligomerization through DH domain may allow the recruitment of multiple Rho substrates into one signaling complex.

Figure 4. Regulation of a few Dbl family GEFs in intracellular signaling networks. (a) Phosphorylation by Ca^{2+}/Calmodulin-dependent kinase II or related kinases, interaction with PI-3 kinase product PIP3, binding to cell surface molecule CD44 or cytoskeleton protein ankyrin, as well as direct coupling to activated Ras, may be involved in the translocation and/or activation of Tiam1 GEF activity. Interaction with the tumor metastasis supressor nm23H1, on the other hand, negatively regulates Tiam1 GEF activity. (b) Heterotimeric G-protein Gα13 coupled with a tyrosine kinase may regulate intracellular localization and GEF activity of p115RhoGEF. (c) βPIX may serve as a scaffold in activation of Rac1-PAK pathway. βPIX effectively forms a stable complex with Rac, PAK and other molecules such as Cat1/Git-1 and may exert both GEF-dependent and GEF-independent functions in the complex signaling. (d) Heterotrimeric G-protein βγ subunits, small G-protein Rsr1, multiple adaptor molecules (Far1 and Bem1), Cdc42-effector Cla4 kinase, and cell cycle-dependent kinase together contribute to the effective onset and offset of the GEF activity toward Cdc42 and the intracellular localization of Cdc24.

Figure 5. Mechanism of Rac1 activation by the DH-PH module of Tiam1. (a) The three-dimensional view of Tiam1-Rac1 tetramer complex. Two identical units of Tiam1-Rac1 complex are in a back-to-back dimer configuration through interaction of extensive hydrophobic surface areas in DH domains. Switch regions of Rac1 are shown in red, and the rest of Rac1 are shown in green. One set of DH-PH module is in light yellow and light blue, and the other unit is in darker colors. (b) Expanded view of the regions of Tiam1-Rac1 complex that specify GEF-Rac interaction. The β2/β3 residues S41, N43, N52, and W56 of Rac1 form both hydrogen bonds and van der Waal's contacts with the α7/α7b residues Q1177, S1179, H1178, E1183, S1184, and I1187 of Tiam1.

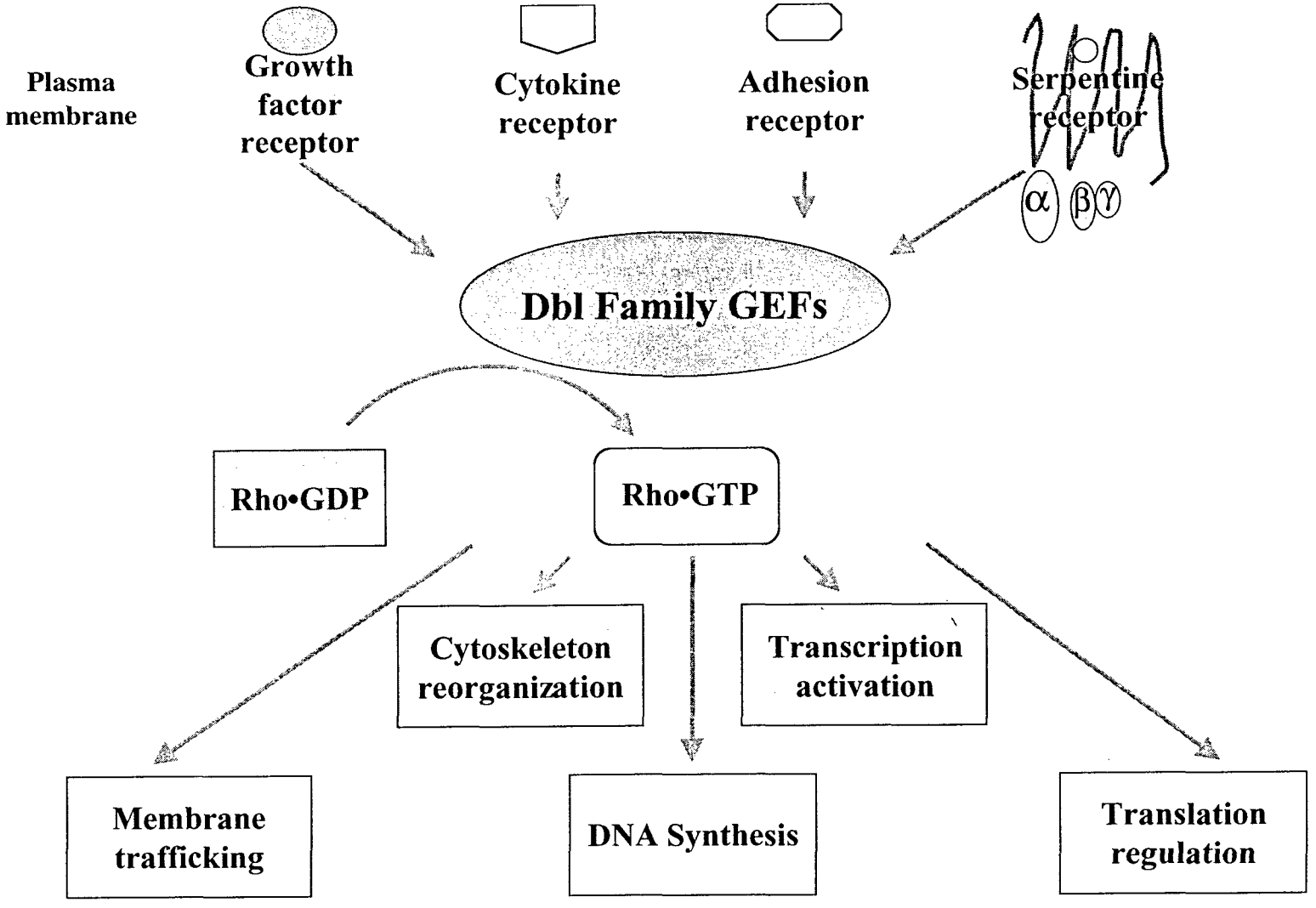
Plasma membrane
Growth factor receptor
Cytokine receptor
Adhesion receptor
Serpentine receptor
α
βγ
Dbl Family GEFs
Rho•GDP
Rho•GTP
Cytoskeleton reorganization
Transcription activation
Membrane trafficking
DNA Synthesis
Translation regulation

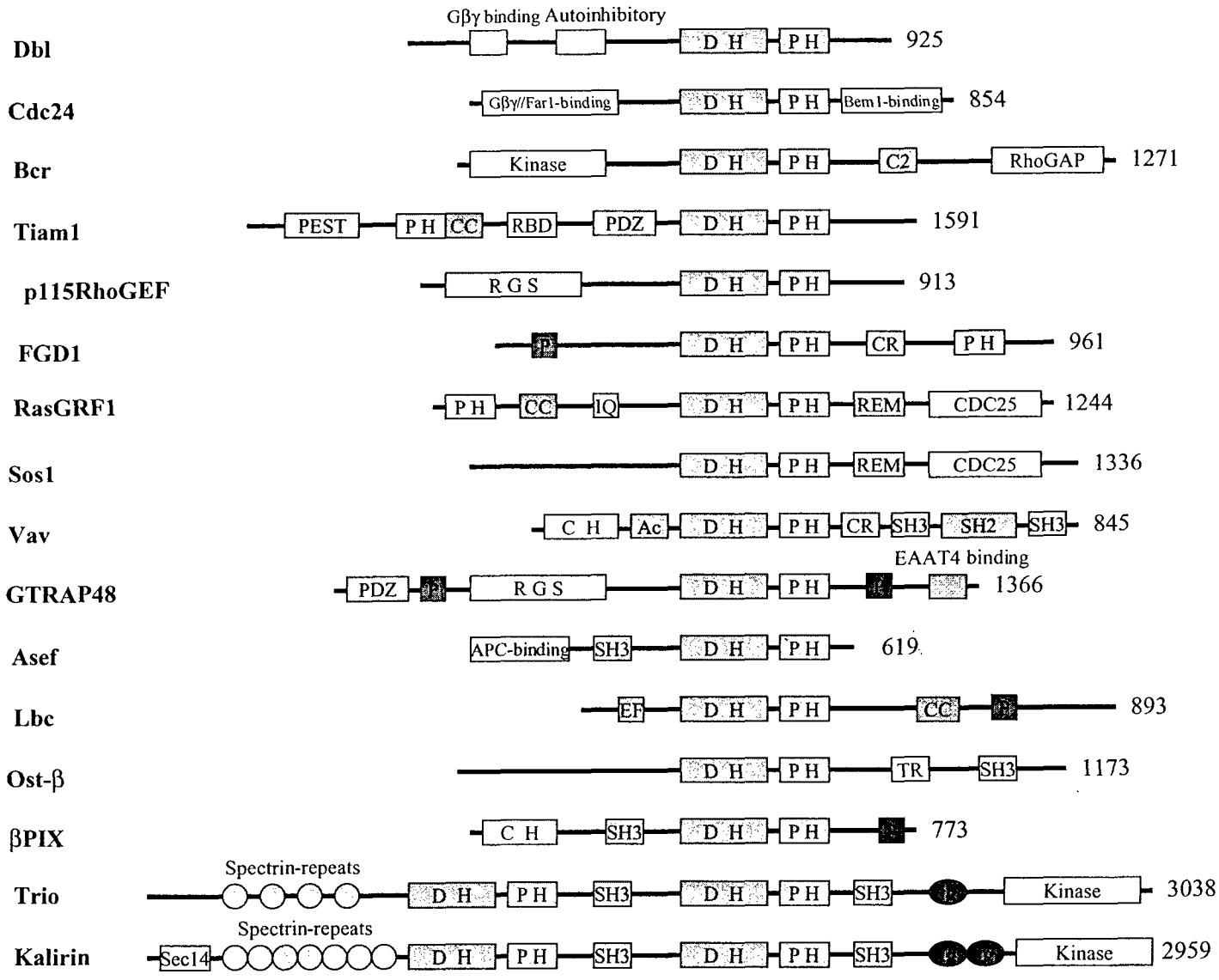
Gβγ binding Autoinhibitory
Dbl
D H
P H
925
Cdc24
Gβγ//Far1-binding
Bem1-binding
854
Bcr
Kinase
C2
RhoGAP
1271
Tiam1
PEST
CC
RBD
PDZ
1591
p115RhoGEF
R G S
913
FGD1
CR
961
RasGRF1
IQ
REM
CDC25
1244
Sos1
1336
Vav
C H
Ac
SH3
SH2
845
EAAT4 binding
GTRAP48
PDZ
1366
Asef
APC-binding
619
Lbc
EF
893
Ost-β
TR
1173
βPIX
773
Spectrin-repeats
Trio
3038
Kalirin
Sec14
2959

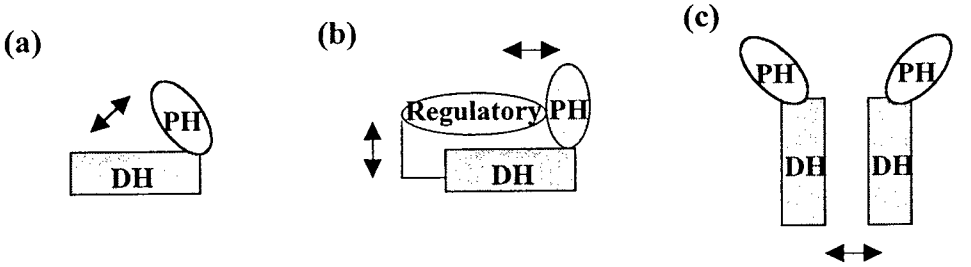
(a)
PH
DH
(b)
Regulatory
PH
DH
(c)
PH
PH
DH
DH

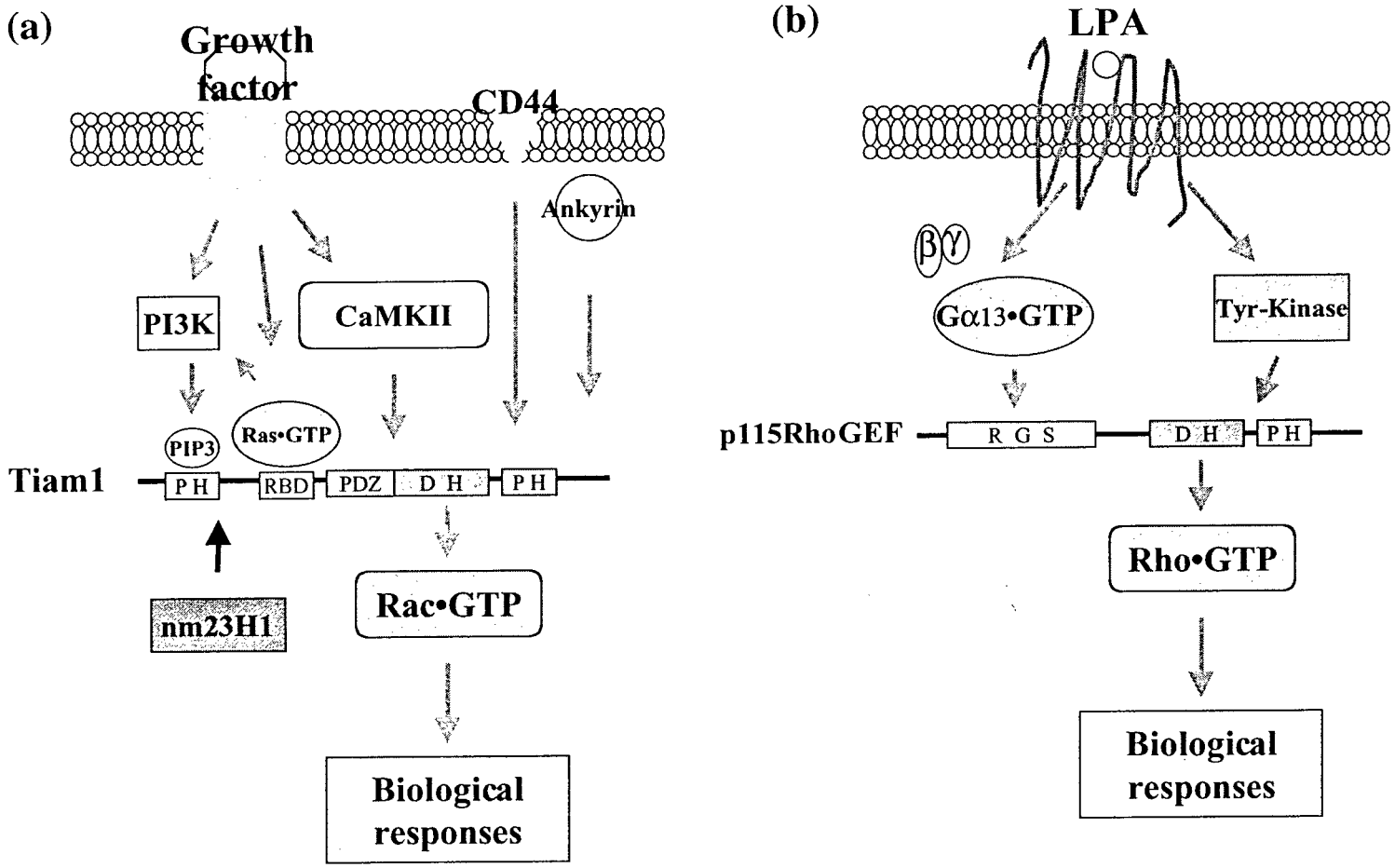
(a)
Growth factor
CD44
Ankyrin
PI3K
CaMKII
PIP3
Ras•GTP
Tiam1
PH
RBD
PDZ
DH
PH
nm23H1
Rac•GTP
Biological responses
(b)
LPA
βγ
Gα13•GTP
Tyr-Kinase
p115RhoGEF
RGS
DH
PH
Rho•GTP
Biological responses

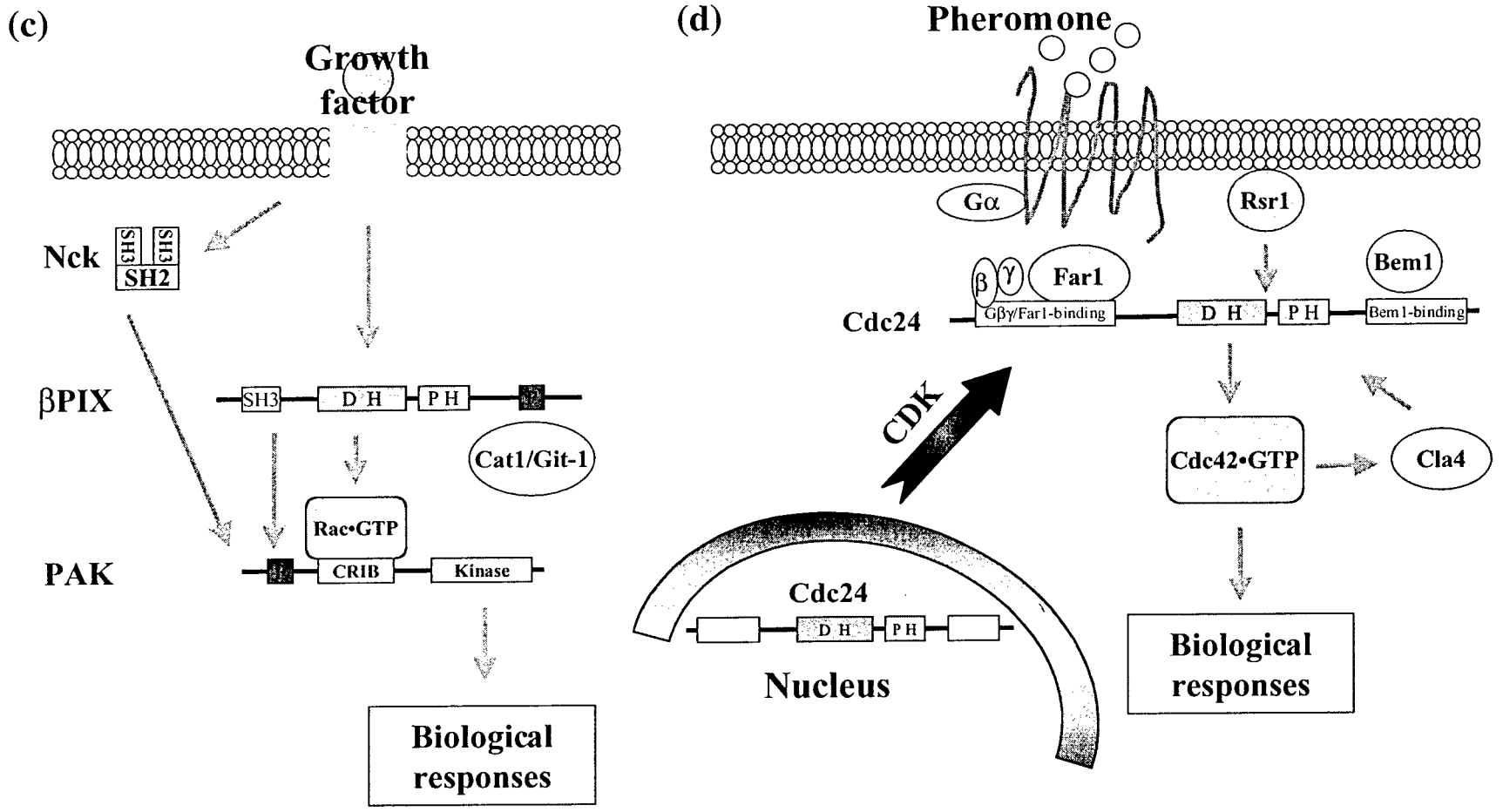
(c)
Growth factor
Nck
SH3
SH3
SH2
βPIX
SH3
D H
P H
Cat1/Git-1
Rac•GTP
PAK
CRIB
Kinase
Biological responses
(d)
Pheromone
Gα
Rsr1
β
γ
Far1
Bem1
Cdc24
Gβγ/Far1-binding
D H
P H
Bem1-binding
CDK
Cdc42•GTP
Cla4
Cdc24
D H
P H
Nucleus
Biological responses

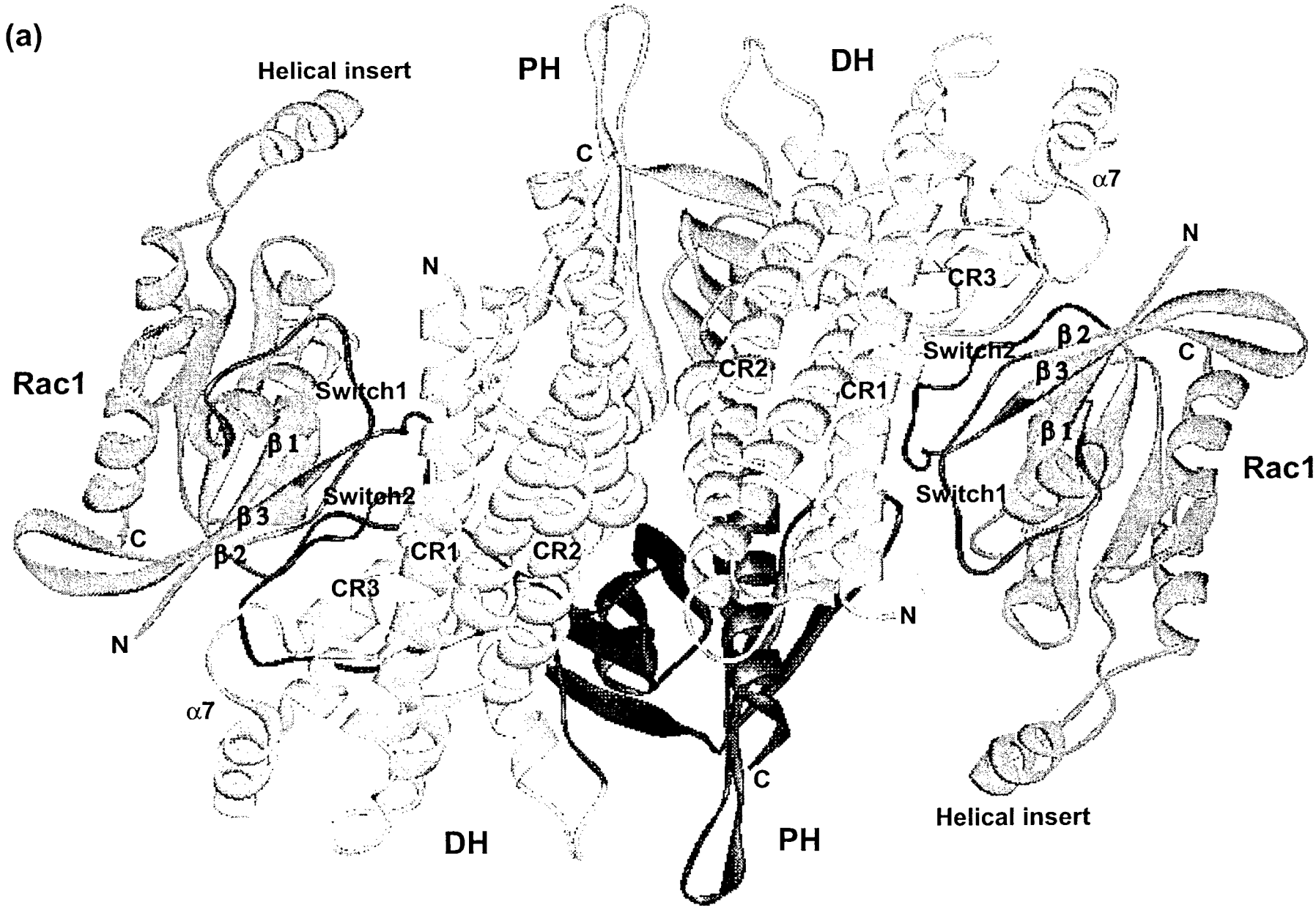
(a)
Helical insert
PH
DH
C
α7
N
CR3
Rac1
Switch1
β 1
β 2
β 3
Switch2
CR2
CR1
C
N
Rac1
Switch2
β 2
β 3
β 1
C
Switch1
CR1
CR2
CR3
N
N
α7
C
DH
PH
Helical insert

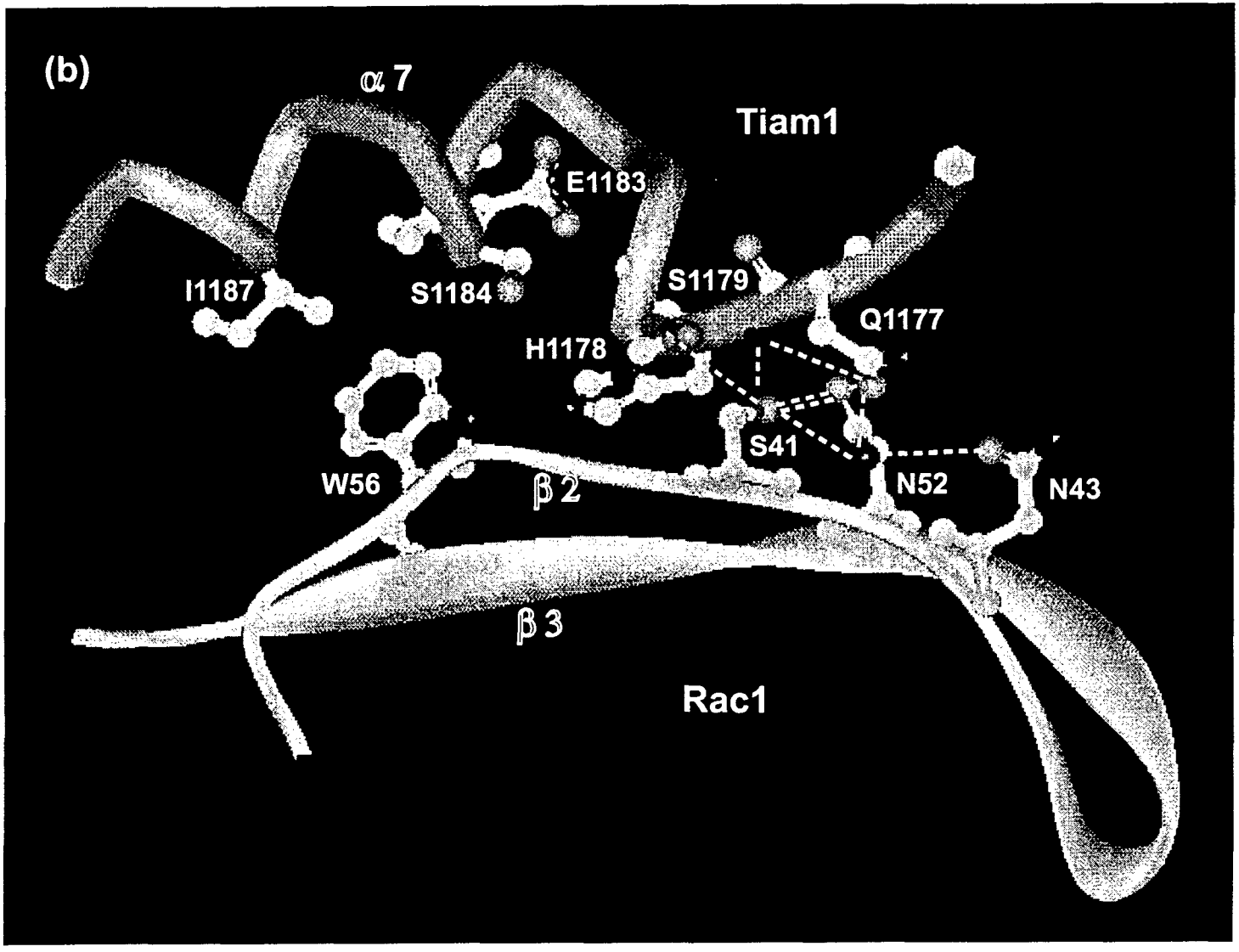
(b)
α 7
Tiam1
E1183
I1187
S1184
S1179
Q1177
H1178
S41
W56
β 2
N52
N43
β 3
Rac1

Na,K-ATPase regulates the formation of tight junctions and desmosomes through RhoA GTPase

Sigrid A Rajasekaran[*Ψ], Lawrence G Palmer[*], Sun Y Moon[#], Alejandro Peralta Soler[+], Gerard L Apodaca[¶], Jeffrey F Harper[‡], Yi Zheng[#], and Ayyappan K Rajasekaran[Ψ]

[Ψ]Department of Pathology and Laboratory Medicine, University of California, Los Angeles, Los Angeles, California 90095, [*]Department of Physiology, Weill Medical College of Cornell University, New York, New York 10021, [#] Department of Biochemistry, University of Tennessee, Memphis, Tennessee 38163, [+]Lankenau Medical Research Center, Wynnewood, Pennsylvania 19096. [‡] Department of Cell Biology, The Scripps Research Institute, La Jolla, CA 92037, [¶] Department of Cell Biology and Physiology, University of Pittsburgh, Pittsburgh, Pennsylvania, 15261.

Author for correspondence
Ayyappan K. Rajasekaran
Department of Pathology and Laboratory Medicine
Room 13-344 CHS
University of California, Los Angeles
Los Angeles, CA 90095
Phone (310) 825-1199
Fax (310) 267-2410
Email: arajasekaran@mednet.ucla.edu

Abstract

The mechanisms by which the formation of tight junctions and desmosomes are regulated in polarized epithelial cells are not well understood. Here we demonstrate that an increased intracellular sodium level caused by the inhibition of Na,K-ATPase prevents the formation of tight junctions and desmosomes, and negatively regulates the activity of RhoA GTPase. Our results indicate that the intracellular sodium level maintained by the Na,K-ATPase is an upstream regulator of RhoA GTPase function in epithelial cells and might play a crucial role in the biogenesis of polarized epithelia. These results demonstrate that the Na,K-ATPase activity not only regulates a variety of transport functions but is also crucial to maintain the structure of polarized epithelial cells.

Introduction

Junctional complexes such as tight junctions, adherens junctions, and desmosomes play a fundamental role in maintaining the polarized phenotype and vectorial transport functions of epithelial cells. The tight junction *(zonula occludens)* forms a continuous belt at the boundary between the apical and lateral plasma membrane domains of neighboring epithelial cells[1]. Structurally characterized by the fusion of the exoplasmic leaflets of contiguous plasma membranes, tight junctions selectively regulate the passage of molecules across the paracellular pathway *(gate function)* and passively separate molecules into the apical and basolateral plasma membrane domains *(fence function)*. A functional tight junction is crucial to maintain the polarized phenotype of epithelial cells[2,3,4]. The adherens junction (*zonula adherens*) is localized below the tight junction and consists of cell adhesion and signaling molecules and may regulate events that mediate adhesion between epithelial cells[5]. Desmosomes are focal points of intercellular contact at which neighboring cells are tightly bound to one another and provide resilience and tensile strength to the epithelial monolayer[6]. The mechanisms that regulate the formation and maintenance of these junctions in epithelial cells are not well understood.

The Na,K-ATPase is an oligomeric transmembrane protein consisting of two non-covalently linked α- and β-subunits. It catalyses an ATP-dependent transport of three sodium ions out and two potassium ions into the cell per pump cycle, thereby generating a transmembrane sodium gradient across the plasma membrane. The sodium gradient generated by the enzyme provides the primary energy for uptake and extrusion of a wide variety of solutes by epithelial cells and is crucial for efficient functioning of other Na^+-coupled transport systems[7,8]. The Na,K-ATPase is localized to the basolateral plasma membrane in most epithelial cells and

has been widely used as a marker for epithelial polarity[9]. However, a role for the Na,K-ATPase itself in the induction of epithelial polarity has not been shown.

Earlier studies have implicated E-cadherin function in the formation and maintenance of junctional complexes and the polarized phenotype of epithelial cells[10,11,12]. E-cadherin is a transmembrane protein localized to the basolateral plasma membrane in polarized epithelial cells and mediates cell-cell contact between epithelial cells by homophilic interaction[13]. Recent studies using a negative dominant mutant of E-cadherin in MDCK cells did not affect tight junctions or desmosomes[14] indicating that other factors are involved in the maintenance of these junctions in MDCK cells. Recently, we have shown that in Moloney-sarcoma virus transformed MDCK (MSV-MDCK) cells expression of E-cadherin alone was not sufficient to induce tight junctions and desmosomes and that it required co-expression of Na,K-ATPase β-subunit and E-cadherin to induce these junctions and a polarized phenotype in MSV-MDCK cells[15]. We also found that MSV-MDCK cells contain about three-fold more intracellular sodium levels ($[Na^+]_i$) compared to wild type MDCK cells. Forced expression of both the Na,K-ATPase β-subunit and E-cadherin but not E-cadherin alone significantly reduced the $[Na^+]_i$ and induced a polarized phenotype with the formation of tight junctions and desmosomes in MSV-MDCK cells[15]. These studies indicated that the $[Na^+]_i$ regulated by the Na,K-ATPase may play a role in the formation of epithelial tight junctions and desmosomes and the induction of a polarized phenotype of epithelial cells.

RhoA GTPase, a Ras-related small GTP binding protein, is involved in the formation of stress fibers in Swiss 3T3 cells[16,17,18]. Recent studies have indicated a role for RhoA GTPase in the assembly and function of tight junctions in MDCK cells[19,20,21]. However, mechanisms that regulate RhoA function in polarized epithelial cells are not known. In this study, we demonstrate that the $[Na^+]_i$ regulated by Na,K-ATPase is crucial for the formation of tight junctions and

desmosomes and that inhibition of Na,K-ATPase negatively regulates RhoA GTPase activity in epithelial cells. These results for the first time provide evidence that the structure and function of polarized epithelial cells are linked and that the Na,K-ATPase plays a crucial role in the regulation of the structure-function relationship in polarized epithelial cells.

Results

To understand the role of Na,K-ATPase in the formation of tight junctions and desmosomes we utilized a Ca^{2+}-switch assay which is commonly used to monitor the development of junctional complexes in MDCK cells. In the Ca^{2+}-switch assay[22], MDCK monolayers formed in the presence of low calcium (<5μM) medium, are transferred to medium containing normal calcium levels (1.8mM), which increases cell-cell contact and initiates the assembly of junctional complexes. To test whether Na,K-ATPase enzymatic activity is necessary for the development of junctions, we pretreated MDCK monolayers maintained in low calcium medium with ouabain (50μM), a specific inhibitor of Na,K-ATPase, for one hour prior to transfer to normal calcium containing medium. At selected times, the cells were fixed and the presence of tight junctions was monitored by immunofluorescence localization of tight junction proteins, transmission electron microscopy (TEM), and by measuring the transepithelial electrical resistance (TER). Desmosomes were visualized by immunofluorescence of desmosomal proteins and TEM.

Prior to the Ca^{2+}-switch (zero hour), the tight junction protein ZO-1 was localized intracellular in both control and ouabain-treated cells (Fig. 1A and C). At one and two hours after the Ca^{2+}-switch, ZO-1 was localized to the plasma membrane with a discontinuous staining pattern. A visible difference in the ZO-1 staining pattern between control and ouabain-treated cells was not detected at these time points (data not shown). At three hours, the ZO-1 staining in control cells showed a continuous staining pattern (Fig. 1B) indicating that the tight junctions were established. By contrast, in ouabain-treated cells, the ZO-1 staining remained discontinuous with a beaded appearance and with regions clearly lacking ZO-1 (Fig. 1D, arrows). Prolonged incubation did not change the discontinuous staining pattern of ZO-1. Instead, ZO-1 became

even more intracellular. Other tight junction proteins such as occludin showed a similar staining pattern (data not shown). Ouabain treatment did not affect the protein levels of ZO-1 as revealed by immunoblot analysis (data not shown). These results showed that in the presence of ouabain tight junction proteins translocate to the plasma membrane but fail to form a complete ring-like pattern like in control cells.

A functional tight junction is required to maintain the polarized distribution of distinct apical and basolateral markers. In MDCK cells the transepithelial electrical resistance (TER) measurement during the Ca^{2+}-switch assay has been utilized to monitor the formation of functional tight junctions[21,22]. Cells grown on Transwell filters were subjected to a Ca^{2+}-switch assay and the development of TER was measured as described in Materials and Methods. The TER in control cells gradually increased after the Ca^{2+}-switch and within three hours reached ~ $200\Omega \cdot cm^2$, a value reported for MDCK clone II[21,22] (Fig. 1E). In contrast, the TER in ouabain-treated cells reached only ~ $50\Omega \cdot cm^2$ and this value did not increase over four hours of ouabain treatment. Moreover, confocal microscope vertical (X-Z) sections revealed a polarized distribution of β-catenin (a basolateral marker) [23] (Fig.1L) and GP135 (an apical marker)[24] (Fig.1N) in control cells, whereas, in ouabain-treated cells these markers were distributed in a non-polarized fashion (Fig. 1 M, O). These results indicate that ouabain-mediated inhibition of Na,K-ATPase activity prevents the formation of functional tight junctions and epithelial polarization in MDCK cells.

To follow the assembly of desmosomes we utilized antibodies against desmoplakin, a peripheral membrane protein and desmocollin, a transmembrane protein localized to desmosomes[6]. Both markers showed identical patterns. The results obtained from the anti-desmocollin antibody staining are shown (Fig. 1F-I). In control and ouabain-treated cells, at zero

hour of the Ca^{2+}-switch, desmocollin was distinctly localized intracellular with barely detectable levels on the plasma membrane (Fig. 1F and H). After three hours of Ca^{2+} switch the desmocollin staining in control cells revealed a distinct dot like pattern circumventing the cells, typical of the desmosome staining pattern in MDCK cells (Fig. 1G). By contrast, in ouabain-treated cells, after three hours of Ca^{2+}-switch, desmocollin was predominantly intracellular with barely detectable staining at the cell-cell contacts (Fig. 1I). This pattern was maintained after prolonged incubation with ouabain. The immunofluorescence staining patterns of desmocollin and desmoplakin were predominantly intracellular at one and two hours after the Ca^{2+}-switch (data not shown). Immunoblot analysis of desmoglein (a membrane component of the desmosome) and desmoplakin did not show significant changes in the levels of these proteins in ouabain-treated cells (data not shown). These results demonstrate that inhibition of Na,K-ATPase activity prevents the translocation of desmosomal proteins to the plasma membrane while it does not affect the translocation of tight junction proteins to the plasma membrane.

To further confirm the effect of ouabain on the assembly of tight junctions and desmosomes we performed TEM of control and ouabain-treated cells after three hours of Ca^{2+}-switch. TEM revealed the presence of typical tight junctions, adherens junctions, and desmosomes in cell-cell contact sites in control cells (Fig. 1J). In contrast, in ouabain-treated cells tight junctions and desmosomes were rarely detected, although adherens junction like structures were clearly seen (Fig. 1K). Quantitative analysis of the TEM data was performed by scoring the number of tight junctions and desmosomes in approximately 50 cell-cell contact sites. Control cells revealed tight junctions and desmosomes in 96% and 100% of cell-cell contacts, respectively. In contrast, ouabain-treated cells showed putative tight junctions in only 14%, and desmosome-like structures in 15% of the cell-cell contacts. Ouabain-treated cells

showed typical adherens junctions in 54% of the cell-cell contacts. Taken together, these results demonstrate that inhibition of Na,K-ATPase by ouabain prevents the formation of tight junctions and desmosomes and the polarized phenotype in MDCK cells.

Next, we utilized K^+ depletion to inhibit Na,K-ATPase[25,26,27] and to confirm the effect of ouabain-mediated inhibition of Na,K-ATPase activity on the formation of tight junctions and desmosomes. In this assay, the pump function can be restored by the addition of K^+ and thus the reversibility of the effect of Na,K-ATPase inhibition can be tested. MDCK cells maintained in low calcium medium were pre-incubated in K^+- and Ca^{2+}-free buffer for one hour to inactivate the Na,K-ATPase and the Ca^{2+}-switch assay was performed in K^+-free medium. Immunofluorescence staining of ZO-1 after three hours of switch to K^+-free medium containing Ca^{2+} showed ZO-1 localized to the plasma membrane although without forming a continuous ring like structure (Fig. 2A). This pattern was similar to that of ouabain-treated cells (Fig. 1D). Subsequent incubation of these cells for five hours in K^+-containing medium resulted in a complete ZO-1 ring circumventing the cells (Fig. 2B). The TER of MDCK cells in K^+-free buffer did not increase up to three hours after the Ca^{2+}-switch (Fig. 2E). However, upon transfer of the cells from K^+-free to K^+-containing culture medium, the resistance increased dramatically and reached a value of $\sim 400\ \Omega \cdot cm^2$ (Fig. 2E) within only two hours indicating the formation of functional tight junctions. Confocal microscope vertical (X-Z) sections of cells maintained in K^+-free medium revealed a non-polarized distribution of β-catenin (Fig. 2H) and GP135 (Fig. 2J). Subsequent transfer of these cells to K^+-containing culture medium resulted in the polarized distribution of these markers (Fig. 2 I, K). The assembly of desmosomes in K^+-free buffer was similar to ouabain-treated cells. In K^+-free buffer the translocation of desmocollin to the plasma membrane was inhibited and the staining was predominantly intracellular (Fig. 2C). Subsequent

incubation of these cells in K^+-containing culture medium for five hours resulted in a dot-like desmocollin staining at the sites of cell-cell contact (Fig. 2D), indicating the formation of desmosomes. Electron microscopy studies confirmed the absence of tight junctions and desmosomes in MDCK cells maintained in K^+-free buffer (Fig. 2F) while a subsequent transfer to K^+-containing culture medium resulted in the formation of tight junctions and desmosomes (Fig. 2G). Quantitative TEM analysis of cells maintained in K^+ -free buffer showed the presence of tight junctions and desmosomes in only 2% and 3% of cell-cell contacts, respectively. After K^+ restoration there was a dramatic increase in tight junctions and desmosomes. Tight junctions were detected in 90%, and desmosomes in 85% of cell-cell contacts. These results further demonstrate that Na,K-ATPase enzymatic activity is necessary for the formation of tight junctions and desmosomes in MDCK cells.

Inhibition of Na,K-ATPase results in an increased intracellular sodium concentration[27,28,29,15] and sodium measurements using atomic emission spectrometry revealed that the intracellular sodium levels $[Na^+]_i$ of MDCK cells (~12 mM) [15] increased more than 10-fold upon ouabain treatment or 7-fold by K^+ depletion. To test whether the inhibition of tight junction and desmosome formation was due to increased intracellular sodium we first treated MDCK cells with ouabain in Na^+-free medium to prevent the increase of $[Na^+]_i$ after ouabain treatment. Cells maintained in low calcium medium were subjected to a Ca^{2+}-switch in a Na^+-free medium with or without ouabain as described in Materials and Methods. After three hours of Ca^{2+}-switch, the cells were fixed and stained for tight junction and desmosomal proteins. As shown in Figure 3, both control (Fig. 3A) and ouabain-treated cells (Fig. 3B) clearly showed a complete ZO-1 ring on the plasma membrane indicating that tight junctions are formed in these cells. Immunofluorescence of desmocollin (Fig.3 C, D) and desmoplakin (not shown) revealed a

distinct dot like staining pattern circumventing the cells in both control (Fig. 3C) and ouabain-treated cells (Fig. 3D). Both control and ouabain-treated cells showed high TER values within four hours of Ca^{2+}-switch in Na^+-free medium (Fig. 3E). Under Na^+-free conditions the control cells had a higher TER resistance compared to cells maintained in normal medium (compare Fig. 1E and 3E), possibly due to decreased tight junction permeability. Confocal microscope vertical (X-Z) sections confirmed the polarized distribution of β-catenin and GP135 in both control and ouabain- treated cells (Fig. 3H-K). In contrast to the effect of ouabain on junction formation in Na^+-containing medium ouabain treatment in Na^+-free medium did not decrease the number of tight junctions or desmosomes in both control (Fig. 3F) and ouabain-treated cells (Fig. 3G). Cell-cell contacts of cells in Na^+-free medium showed tight junctions and desmosomes similar to control cells in Na^+-containing medium. These results indicate that the observed effect of ouabain on the formation of junctions is not due to a toxic side effect. These results also suggest that the low intracellular sodium concentration maintained by Na,K-ATPase is involved in the regulation of the formation of tight junctions and desmosomes in MDCK cells.

To further confirm that increased intracellular sodium might affect the formation of tight junctions and desmosomes we treated MDCK cells with the sodium ionophore gramicidin and a potassium ionophore, valinomycin. Gramicidin A is an ion-channel forming antibiotic that greatly facilitates Na^+ entry into cells[30], and specifically increases the intracellular Na^+ concentration. Valinomycin is a cyclic dodecadepeptide that transports K^+ through the plasma membrane, inducing a potassium leak[31]. Intracellular sodium measurements revealed a more than 12-fold increase in $[Na^+]_i$ in gramicidin treated cells while valinomycin treated cells did not reveal a significant change in the intracellular sodium levels compared to untreated MDCK cells. Treatment of MDCK cells with gramicidin during the Ca^{2+}-switch showed an effect similar to

that of ouabain. While at zero hour ZO-1 was localized intracellular (data not shown), three hours after the Ca^{2+}-switch, ZO-1 was clearly localized on the plasma membrane although without a continuous ring pattern (Fig. 4A). The immunofluorescence staining of occludin showed identical results (data not shown). In the presence of gramicidin, three hours after the Ca^{2+}-switch, the immunofluorescence of desmocollin (Fig. 4B), and desmoplakin (data not shown) showed a predominantly intracellular staining pattern similar to ouabain-treated cells (compare Figs. 4B and 1I). In contrast to gramicidin-treated cells, valinomycin-treated cells behaved more like control cells. While at zero hour ZO-1 was localized intracellular (data not shown), three hours after the Ca^{2+}-switch ZO-1 formed a continuous ring at the plasma membrane (Fig. 4C). Occludin showed a similar staining pattern (data not shown). Both, desmocollin (Fig. 4D) and desmoplakin (data not shown) showed a punctate staining pattern at cell-cell contact sites. Consistent with the localization of tight junction proteins, valinomycin-treated cells had TER values of about $250\Omega \cdot cm^2$ within four hours. In contrast, gramicidin-treated cells did not develop TER with time (Fig. 4E). Confocal microscope vertical (X-Z) sections of gramicidin treated cells revealed non-polarized distribution of β-catenin (Fig. 4F) and GP135 (Fig. 4H) while in valinomycin treated cells these markers were distributed in polarized fashion (Fig. 4G, I). Furthermore, TEM revealed tight junctions and desmosomes in valinomycin-treated cells, but showed a significant decrease in junctions in gramicidin-treated cells. Quantitative analysis of the TEM data revealed tight junctions and desmosomes in 100% of the cell-cell contacts in valinomycin-treated cells. In contrast, gramicidin treated cells showed putative tight junctions in only 23 %, and desmosome-like structures in 14 % of the cell-cell contacts. Taken together, these results demonstrate that an increased intracellular sodium level

prevents the assembly of functional tight junctions and desmosomes and the induction of polarity in MDCK cells.

Recent studies have implicated a role for filamentous actin in the regulation of tight junctions[19,21] and desmosomes[32]. Therefore, we tested whether Na,K-ATPase plays a role in the organization of the actin cytoskeleton during the formation of tight junctions and desmosomes in MDCK cells. Organization of the actin cytoskeleton was monitored by FITC-phalloidin labeling and epifluorescence microscopy. In control cells, at zero hour stress fibers were not detected at the bottom of the cells (Fig. 5A). After one hour of Ca^{2+}-switch stress fibers began to appear at the bottom of the cells (data not shown) and after three hours bundles of stress fibers were noticed (Fig. 5B). These bundles of stress fibers gradually disappeared and were not detected after 48 hours of Ca^{2+}-switch (data not shown). In contrast, in ouabain-treated cells the bundled stress fibers did not form (Fig. 5C and D). However, these cells showed a distinct cortical actin cytoskeleton at the bottom of the cells (Fig. 5D). Like in ouabain-treated cells, K^+ depletion also inhibited the formation of bundles of stress fibers and induced a distinct cortical actin at the base of the cells (Fig. 5E). Adding K^+ to the cells maintained in low K^+ resulted in bundles of stress fibers as seen in control cells (compare Fig. 5B and F). The formation of bundled stress fibers was markedly inhibited by gramicidin but not by valinomycin (data not shown). These results strongly suggest that the transient formation of bundled stress fibers may play a role in the assembly of tight junctions and desmosomes and that inhibition of Na,K-ATPase prevents the formation of bundled stress fibers.

The RhoA GTPase has been implicated in the regulation of actin stress fiber formation in fibroblasts and in epithelial cells[16,17,33,21]. Moreover, both RhoA and Rac1, a closely related family member, have been shown to be essential for the assembly and the function of tight

junctions in MDCK cells[21]. Therefore, we tested the possible involvement of these GTPases in the Na,K-ATPase mediated formation of junctional complexes. For this purpose, we determined the endogenous levels of active RhoA in control cells and ouabain-treated cells using an *in vitro* biochemical assay[34,35]. In this assay, GST-Rhotekin, a GST-fusion protein containing the Rho binding domain (which binds active RhoA bound to GTP) is incubated with cell lysate and the bound, active RhoA is detected by immunoblot analysis. The specificity of this assay is demonstrated by loading the cell lysate with a non-hydrolyzable analog of GTP, GTPγS (total RhoA) and by replacing GTPγS with GDP that inactivates Rho and therefore does not bind to GST-Rhotekin (Fig. 5G, compare lanes 9 and 10). Consistent with the formation of stress fibers, control cells showed high levels of active RhoA (Fig. 5G, lanes 5-8 and Fig. 5G') compared to ouabain-treated cells in which the level of active RhoA gradually decreased and became undetectable after two hours treatment (Fig. 5G, lanes 1-4 and Fig. 5G'). The protein levels of RhoA remained unchanged in both control and ouabain-treated cells (Fig. 5G, labeled as total, lanes 1-10). Like in ouabain-treated cells, depletion of K^+ resulted in the inhibition of RhoA activity (Fig. 5H, lanes 1-3 and Fig. 5H'). and addition of K^+ resulted in the reappearance of the RhoA activity (Fig. 5H, lanes 4 and 5 and Fig. 5H'). These results indicate that the Na,K-ATPase activity has a direct impact on the activation state of RhoA. Gramicidin-treated cells showed reduced RhoA activity compared to valinomycin treated cells (Fig. 5I, compare lanes 2-4 to 5-7, and Fig. 5I') indicating that increased intracellular sodium inhibits the function of RhoA. We also measured the endogenous Rac1 activity in response to the modulation of Na,K-ATPase activity and found that neither the expression level nor the activation state of Rac1 was affected by ouabain or K^+-depletion (data not shown). Thus, Na,K-ATPase appears to be a specific upstream regulator of RhoA GTPase.

To further validate the specific role of RhoA in the formation of tight junctions and desmosomes we utilized MDCK cells expressing wild type RhoA GTPase (MDCK-RhoA $_{wt}$) under the control of the tetracycline repressible transactivator. In MDCK-RhoA $_{wt}$ cells, the levels of RhoA increased several fold after withdrawal of the transcription repressor doxicycline (DC) (Fig. 6A)[36]. In induced cells (-DC) the level of active RhoA was 2.7- fold more than that of control cells maintained in the presence of doxicycline (+DC). Three hours after ouabain treatment, induced cells showed 2.1-fold more active RhoA GTPase than uninduced cells (Fig. 6B). Consistent with the presence of active RhoA in induced cells, bundled stress fibers were distinctly seen after three hours of ouabain treatment, whereas these fibers were scarcely present in uninduced cells (Fig. 6C and D). Upon ouabain treatment RhoA induced cells revealed an uninterrupted ZO-1 staining pattern, whereas uninduced cells showed a disrupted staining pattern (Fig. 6E and F). The TER of ouabain treated induced cells was significantly higher than that of uninduced cells ($P<0.01$) (Fig. 6I). Furthermore, confocal microscope vertical sections revealed a polarized distribution of β-catenin and GP135 in induced ouabain treated cells (Fig. 6J and L). In contrast, in noninduced cells these markers were distributed in a non-polarized fashion (Fig. 6K and M). These results demonstrate that functional tight junctions are formed even in the presence of ouabain in RhoA over-expressing cells. Desmocollin revealed a distinct plasma membrane localization in induced ouabain treated cells (Fig. 6G), whereas uninduced cells showed an intracellular staining pattern (Fig. 6H). TEM revealed tight junctions and desmosomes in 88% of the cell-cell contacts in induced ouabain treated cells, whereas uninduced cells showed putative tight junctions in only 12 % and desmosome-like structures in 18 % of the cell-cell contacts (Fig. 6N and O). These results further demonstrate that Na,K-ATPase mediates its action through

RhoA and that RhoA function is essential for the formation of tight junctions and desmosomes and to maintain the polarized phenotype of MDCK cells.

The cell adhesion molecule E-cadherin has been implicated in the formation and maintenance of tight junctions and desmosomes[11,12]. Therefore, we tested whether ouabain treatment of MDCK cells affects the expression or localization of E-cadherin in these cells. In control cells, at zero hour E-cadherin showed a predominant intracellular staining. At this time point the plasma membrane localization of E-cadherin was barely detectable (Fig. 7A). After three hours of Ca^{2+}-switch the intracellular staining of E-cadherin decreased dramatically while the plasma membrane staining increased (Fig. 7B). In ouabain-treated cells at zero hour E-cadherin was localized intracellularly similar to that of control cells (Fig. 7C). At three hours after Ca^{2+}-switch, like in control cells, the intracellular E-cadherin staining decreased and the plasma membrane staining increased at cell-cell contact sites (Fig. 7D). Immunoblot analysis of total cell lysates of control and ouabain-treated cells showed no differences in the levels of E-cadherin, α-, β-, and γ-catenin (Fig. 7E). Co-immunoprecipitation showed no detectable differences in the levels of α-, β-, and γ-catenin associated with E-cadherin in control and ouabain-treated cells (data not shown). In addition, ouabain-treated cells revealed adherens junctions (Fig.1K), the formation of which requires functional E-cadherin[11,12,5]. These results indicate that E-cadherin is functional in ouabain treated cells and that inhibition of Na,K-ATPase function did not affect the expression or localization of E-cadherin and catenins in MDCK cells.

Discussion

We utilized two independent methods, ouabain treatment and K^+ depletion to show that inhibition of Na,K-ATPase increases $[Na^+]_i$ and prevents the formation of functional tight junctions, desmosomes and the induction of polarity in MDCK cells. A role for $[Na^+]_i$ in the formation of these junctions is further demonstrated by using the sodium ionophore gramicidin. The presence of these junctions in cells treated with ouabain in Na^+-free media rule out that the observed effects of ouabain are not due to a toxic side effect. Rapid restoration of tight junctions, desmosomes and epithelial polarity upon K^+-repletion further demonstrated that the effects of Na,K-ATPase inhibition were neither toxic nor a dead end in the assembly of functional tight junctions, desmosomes and the induction of polarity. By biochemical quantification of active RhoA we demonstrated that the $[Na^+]_i$ maintained by the Na,K-ATPase is crucial for the normal functioning of RhoA GTPase and that inhibition of Na,K-ATPase negatively regulates RhoA function in MDCK cells.

ZO-1 was clearly localized on the plasma membrane in Na,K-ATPase inhibited MDCK cells. Nevertheless, lack of TER indicates that Na,K-ATPase function is essential for the formation of functional tight junctions. E-cadherin dependent signaling events have been suggested to mediate the translocation of tight junction proteins from the cytoplasm to the plasma membrane[38,23]. Since ouabain-treated MDCK cells express functional E-cadherin, the localization of tight junction proteins at the plasma membrane suggests that E-cadherin mediated signaling events might not have been affected in these cells. It has been suggested that tight junctions and desmosomes are formed in a co-ordinate manner following E-cadherin mediated cell-cell contact in epithelial cells [11,12]. Our results strongly suggest that the formation of tight junctions and desmosomes are regulated by independent mechanisms. While the tight junction

proteins were clearly localized to the plasma membrane after the calcium switch in the presence of ouabain, and K^+ -depletion the localization of desmosomal proteins to the plasma membrane was highly reduced and desmosomes were poorly assembled under these conditions. These results demonstrate that signaling events that mediate the translocation of desmosomal proteins to the plasma membrane and the formation of desmosomes requires the function of Na,K-ATPase and might be regulated in part by E-cadherin-independent mechanisms.

Although studies using inhibitors and mutant forms of RhoA GTPase have implicated a role for RhoA GTPase in the assembly of tight junctions[19-21] , we now demonstrate by biochemical quantification that active RhoA GTPase is essential for the assembly of functional tight junctions, desmosomes and induction of polarity in MDCK cells. Ouabain treatment consistently reduced the activity of endogenous active RhoA in wild type MDCK cells and of exogenously expressed RhoA in the MDCK T23 clone indicating that inhibition of Na,K-ATPase specifically inhibits RhoA activity. Despite the plasma membrane localization of tight junction proteins, TER measurements revealed that the formation of functional tight junctions is inhibited when active RhoA GTPase levels were drastically reduced upon inhibition of Na,K-ATPase. These results are consistent with studies in which expression of a dominant negative form of RhoA in MDCK cells resulted in the localization of tight junction proteins on the plasma membrane yet these cells failed to form functional tight junctions [21]. Moreover, when sufficient levels of active RhoA is maintained by over expression of wild type RhoA, functional tight junctions were formed even in the presence of ouabain indicating that RhoA function is crucial for the formation of functional tight junctions in MDCK cells[21]. Our biochemical analysis revealed that the levels of active Rac 1 remained the same in control and ouabain treated cells (data not shown) indicating that Na,K-ATPase mediates its action specifically through RhoA

GTPase. We suggest that after the tight junction proteins are targeted to the tight junction region, actin polymerization mediated by RhoA GTPase might be necessary for the molecular reorganization and association of tight junction proteins such as ZO-1 to the actin cytoskeleton for the final assembly of functional tight junctions. Plasma membrane localization of desmosomal proteins and the formation of desmosomes in ouabain treated cells over expressing wild type RhoA demonstrates that Na,K-ATPase regulated RhoA function is essential for both the translocation of desmosomal proteins to the plasma membrane and the formation of desmosomes in MDCK cells. These events may require active actin polymerization mediated active RhoA GTPase. In fact, a recent study clearly demonstrated a role for stress fibers in the assembly of desmosomes in keratinocytes[32]. Polarized distribution of apical and basolateral markers in RhoA induced MDCK-RhoA $_{wt}$ cells treated with ouabain indicate that Na,K-ATPase regulated RhoA GTPase function is essential to maintain the polarity in MDCK cells.

Increased $[Na^+]_i$ due to either inhibition of Na,K-ATPase or by gramicidin treatment significantly reduced the RhoA activity. Restoration of RhoA activity upon K^+ repletion strongly suggests that increased $[Na^+]_i$ negatively and reversibly regulates RhoA function. The mechanism by which increased $[Na^+]_i$ affects RhoA function is currently not known. It is possible that Na^+ might directly bind to specific regulators of RhoA to modulate its function or the consequent changes induced by disruption of Na^+ gradient, such as, changes in intracellular pH, calcium, and membrane depolarization may affect RhoA function. RhoA activity is modulated by a set of regulatory proteins. Rho is activated through GDP-GTP exchange, which is promoted by guanine nucleotide exchange factors (GEFs), whereas inactivation is stimulated by GTPase activating proteins (GAPs)[17,39,18]. Stabilization of the inactive GDP-bound form of Rho appears to be mediated by Rho guanine nucleotide dissociation inhibitors (Rho-GDIs)[17,39,18].

whether this modulation of RhoA activity is through direct or indirect effect by Na,K-ATPase on the regulators of Rho is not clear at this stage.

Our biochemical assay directly detects the GTP bound form of RhoA. Therefore, reduced RhoA activity upon inhibition of Na,K-ATPase activity suggests that increased $[Na^+]_i$ may either inhibit the function of GEFs resulting in the accumulation of the inactive form of Rho (Rho-GDP) or may promote the functions of GAPs or Rho-GDIs affecting the activation of Rho. We recognize that increased $[Na^+]_i$ may induce multiple biochemical changes in cells. However, rapid reversibility of effects induced by Na,K-ATPase inhibition such as formation of tight junctions, desmosomes, bundled actin stress fibers, restoration of RhoA activity and induction of polarity by K^+-repletion strongly suggests that normal $[Na^+]_i$ maintained by Na,K-ATPase plays a crucial role in the assembly of junctions and induction of polarity in epithelial cells.

Despite functional E-cadherin expression in ouabain-treated cells, absence of functional tight junctions and desmosomes and lack of polarity indicates that E-cadherin function is not sufficient for the formation of these junctions and the induction of polarity in MDCK cells. Supporting our data, Troxell et al[14] have shown that expression of a dominant negative mutant of E-cadherin in MDCK cells did not affect tight junctions or desmosomes. In fact, the number of tight junction strands increased in cells expressing the dominant negative mutant of E-cadherin. Potempa and Ridley[37] have shown that hepatocyte growth factor stimulation in MDCK cells did not affect tight junctions and desmosomes but specifically affected adherens junctions the formation of which requires functional E-cadherin. Furthermore, we have shown that ectopic expression of E-cadherin alone in MSV-MDCK cells is not sufficient to induce tight junctions and desmosomes and that only when Na,K-ATPase function was sufficiently restored by co-expression of both E-cadherin and β-subunit of Na,K-ATPase tight junctions and desmosomes were formed in these cells[15]. In view of these recent results, we suggest that E-cadherin mediated cell-cell contacts have a role in the signaling events that mediate translocation of tight junction

proteins to the plasma membrane, an essential event required for the assembly of tight junctions in epithelial cells. Thus, E-cadherin function is essential but may not be sufficient for the formation of functional tight junctions and the induction of polarity in MDCK cells. Formation of functional tight junctions and desmosomes might be mediated by E-cadherin independent mechanisms that require normal functioning of Na,K-ATPase.

Based on our results we propose a model for the formation of tight junctions and desmosomes in epithelial cells. According to this model tight junctions and desmosomes are formed in parallel by two independent pathways (Fig. 8) yet linked by RhoA GTPase. E-cadherin mediated signaling events translocate tight junction proteins from the cytoplasm to the plasma membrane. Formation of functional tight junctions requires active polymerization of actin mediated by RhoA. The desmosomal assembly might be mediated by signaling events regulated by Na,K-ATPase. These signaling events might be directly involved in the translocation of desmosomal proteins to the plasma membrane. Alternatively, RhoA mediated actin polymerization could be involved in the translocation of desmosomal proteins to the plasma membrane and the final assembly of desmosomes. Thus, Na,K-ATPase mediated RhoA function may play a central role in the formation of tight junctions and desmosomes and thus in the biogenesis of polarized epithelia.

Materials and Methods

Ca^{2+}switch assay

Confluent MDCK monolayers (clone II passage 4 kindly provided by Dr. Enrique Rodriguez-Boulan) were subjected to calcium switch assay as described earlier[23]. Briefly, the cells were trypsinized until single cell suspensions were obtained and plated onto Costar Transwells with 0.4 μm pore size (Corning Inc., Corning, NY) ($3x10^6$ cells/24 mm) or glass coverslips in a 12-well tissue culture plate ($4x10^5$ cells/well). The cells were allowed to attach in normal Ca^{2+}-containing DMEM (1.8 mM Ca^{2+}). Thereafter, the cells were rinsed gently in SMEM (Life Technologies, Inc. Rockville, MD) containing <5 μM Ca^{2+} (low Ca^{2+} medium) and 5% dialyzed fetal bovine serum (FBS) and incubated for about 16 h at 37°C. Prior to transfer of the cells to medium containing normal Ca^{2+}-levels (1.8 mM) the MDCK monolayers were pretreated with either Ouabain (50 μM, Sigma Chemical Co. St.Louis MO), Gramicidin (1 μM, Molecular Probes, Eugene, OR), or Valinomycin (50 μM, Molecular Probes) for one hour in low Ca^{2+} medium at 37°C. DMSO, used as a solvent for these drugs, was added to control cells. For the switch, the low Ca^{2+}-medium was replaced by normal culture medium containing the corresponding drugs and the cells were incubated at 37°C for indicated times. Sodium free conditions were obtained as described in Fernandez and Malnic[40]. For this purpose single cell suspension of MDCK cells were plated onto Transwells, allowed to attach, and incubated in low Ca^{2+} medium as described above. The switch was performed using NMDG buffer in which NaCl was substituted with N-methyl-D-glucamine (NMDG, Sigma Chemical Co.) (5 mM KCl, 1.8 mM $CaCl_2$, 1 mM $MgCl_2$, 30 mM Hepes, 147 mM N-methyl-D-glucamine, 10 mM Glucose, pH 7.4). Prior to the experiment the cells were rinsed twice with Ca^{2+}-free NMDG buffer (NMDG buffer lacking $CaCl_2$ and FBS) and then incubated in Ca^{2+}-free NMDG buffer containing 5%

dialyzed FBS and either DMSO or ouabain as described above. For the switch the Ca^{2+}-free NMDG-buffer was replaced with NMDG-buffer containing DMSO or ouabain, respectively, and the cells were incubated at 37°C for up to 4 hours. Potassium free conditions were obtained as described in Le *et al*[41]. For this purpose, the Ca^{2+} switch was performed using a K^+-free buffer (140 mM NaCl, 1.8 mM $CaCl_2$, 1 mM $MgCl_2$, 20 mM Hepes, 10 mM Glucose, pH 7.4) which contained 5% FBS dialyzed against the K^+-free buffer. Prior to the experiment the cells were rinsed twice with Ca^{2+}– and K^+-free buffer (K^+-free buffer lacking $CaCl_2$) and pre-incubated in Ca^{2+}-/K^+-free buffer/5% FBS for one hour. For the K^+ repletion the cells were incubated in normal medium at 37°C for 3-5 hours. The Ca^{2+}-switch assays for MDCK-RhoA $_{wt}$ cells were performed as described earlier[36].

Immunofluorescence and confocal microscopy

Immunofluorescence was performed on cells fixed with methanol as described previously[23]. Antibodies against ZO-1 and occludin (Zymed Laboratories Inc., S. San Francisco, CA), desmocollin (DC7G6, gift from Dr. Wheelock), desmoplakin (gift from Dr. Manijeh Pasdar), and E-cadherin (DECMA, Sigma Chemical Co) were used. To detect filamentous actin the cells were fixed in paraformaldehyde and labeled with FITC-phalloidin (Sigma Chemical Co). Epifluorescence analysis was performed using an Olympus AX 70 (Provis) microscope. Confocal microscopy to monitor polarized distribution of domain specific markers was performed as described earlier[23] using as a Fluoview laser scanning confocal microscope (Olympus America Inc, Melville, NY). To detect FITC- labeled antigens, samples were excited at 488 nm with an Argon laser and the light emitted between 525-540 nm was recorded. Images were generated and analyzed using the Fluoview image analysis software (version 2.1.39).

Immunoblot analysis

For immunoblot analysis, monolayers were lysed in a lysis buffer (95 mM NaCl, 25 mM Tris pH 7.4, 0.5 mM EDTA, 2 % SDS, 1 mM phenylmethylsulfonyl fluoride (PMSF), and 5 μg/ml each of antipain, leupeptin, and pepstatin). The lysates were briefly sonicated and centrifuged at 14,000 rpm in a microfuge for 10 min. The supernatants were used for further analysis. Protein concentrations of the cell lysates were determined using the BioRad DC reagent (BioRad Laboratories, Hercules, CA) according to manufacturer's instructions. Equal amounts of protein (100 μg) were separated by SDS-PAGE and transferred to nitrocellulose membrane (Schleicher & Schuell Inc., Keene, NH). The blots were blocked with 10 % non-fat dry milk in PBS and then incubated for 2 hrs at RT with primary antibody diluted in 10 % milk/PBS. After incubation the blots were washed three times with PBS/0.3 % Tween-20 and then incubated for 1 hr at RT with HRP-conjugated secondary antibody (1:4000 in 10 % milk). Bound antibody was detected by peroxidase-catalyzed enhanced chemiluminescence (ECL) (NEN Life Science Products, Boston, MA). Densitometric analysis and quantification of the intensity of the individual bands was carried out with an ImageQuant software package (Molecular Dynamics, Sunnyvale, CA).

Transepithelial electrical resistance (TER) measurements

To measure the transepithelial electrical resistance, the cells on Transwell filters were subjected to the Ca^{2+}-switch assay as described above and at the indicated time points the resistance of the monolayers was determined using an EVOM Epithelial Voltohmeter (World Precision Instruments, Inc., Sarasota, FL). The values were normalized for the area of the filter after subtracting the background resistance of a filter without cells.

Electron microscopy

Confluent monolayers grown on Transwells (see above) were fixed in 2.5% glutaraldehyde in 0.1M sodium cacodylate buffer, pH 7.4, for 2-4 hours at room temperature and processed for transmission electron microscopy as described earlier[23]. Ultrathin sections were contrasted with uranyl acetate and lead citrate and examined with a Joel (1200EX) electron microscope. The presence of tight junctions and desmosomes was quantified in approximately 50 randomly selected cell-cell contact sites in each experiment. In MDCK cells adherens junctions were not easily discernable when tight junctions were present and therefore they were not quantified. However, when tight junctions were absent, like in ouabain treated cells, adherens junctions were clearly observed and quantified. Representative results are shown.

Endogenous RhoA/Rac1 activity assay

The glutathione agarose-immobilized GST-PAK1, which contains the Rac1 interactive domain of human PAK1 (residues 51-135) and GST-Rhotekin which contains the Rho binding domain of Rhotekin (residues 1-89) were expressed and purified in E. coli by using the pGEX-2T vector as described earlier[34,35]. The cells were washed with ice-cold PBS buffer once before lysis on the dish in a buffer containing 50 mM TrisHCl, pH 7.4, 100 mM NaCl, 10 mM $MgCl_2$, 1% Triton X-100, 1 mM DTT, 10 μg/ml each of leupeptin and aprotinin, and 1 mM PMSF at 4°C. Cell lysates were clarified by centrifugation at 13,000 g at 4°C for 10 min. To load the endogenous small G-proteins with GDP or GTPγS, aliquots of lysates were incubated for 10 min at ambient temperature in the presence of 10 mM EDTA and 0.5 mM GDP or GTPγS. The loading reactions were stopped by the addition of 20 mM $MgCl_2$ and switching the temperature to 4°C. Equal volumes of lysates were incubated with GST-PAK1 or GST-Rhotekin (10 μg per lysate sample) immediately for 40 min at 4°C under constant agitation. The lysate-incubated

beads were washed three times with the lysis buffer, and the bound RhoA and Rac1, were detected by anti-RhoA and anti-Rac1 antibodies (Santa Cruz Biotech., Inc. Santa Cruz, CA Upstate Biotechnology, Inc. Lake Placid, NY) and visualized by enhanced chemiluminescence (ECL) (NEN Life Science Products, Boston, MA). Quantification of the immunoblots was performed using AlphaImager system (Alpha Innotech, SanLeandro, CA). For comparison of the level of the active RhoA and Rac1, the amount of GST-Rhotekin or PAK-bound small GTP-binding protein was normalized to the total amount of RhoA and Rac1 in cell lysates in each sample.

Atomic emission spectrometry

Subconfluent monolayers of MDCK cells treated without or with 50 μM ouabain, 1 μM Gramicidin, or 50 μM Valinomycin for 2 hours or cells incubated in K^+-free buffer for 2 hours were rinsed three times with 10 ml of 0.25 M sucrose. The cells of five 100 mm dishes each were pooled in 0.25 M sucrose, digested with HNO_3 (Ultrex II, J.T. Baker, Phillipsburg, NJ) at a final concentration of 40% at 65°C for 15 hours and diluted 1:2 with Millipore Milli-Q UF plus filtered water. The ion concentrations were measured using an Inductively Coupled Plasma Atomic Emission Spectrometer (Vista Axial 730, Varian, Walnut Creek, CA). The concentrations for Na^+(588.995 nm), K^+(766.941 nm), and Mg^{2+}(285.213 nm) were determined and the Na^+ and K^+ concentrations were normalized to the total Mg^{2+} content (internal control).

Acknowledgements: We thank Drs. Ernest Wright and Gregory Payne for critical reading of the manuscript. We thank Dr. Joel Pardee for encouragement and support. We are very grateful to Dr. Elliot Landaw for statistical analysis of the TER data. This work is primarily supported by a Grant-in-Aid award 1162-Gl1 from the American Heart Association (Western States Affiliate) (to A. K. R) and in part by Department of Defense grants PC991140 and PC970546 (to A. K. R), a Department of Defense Breast Cancer Program grant BC990290 (to Y. Z) and NIH CA67113 grant (to A. P. S). Metal analysis was supported by a NSF grant DBI-0077378 to J.F.H. SAR is supported by a Fellowship from Toohey Foundation. AKR is a member of the Jonsson Comprehensive Cancer Center.

References

1. Farquhar, M.G. & Palade, G.E. Junctional complexes in various epithelia. *J. Cell Biol.* **17**, 375-412 (1963).

2. Rodriguez-Boulan, E. & Nelson, W.J. Morphogenesis of the polarized epithelial cell phenotype. *Science* **245**, 718-725 (1989).

3. Mitic, L.L. & J. Anderson, J.M. Molecular architecture of tight junctions. *Ann. Rev. Physiol.* **60**, 121-142 (1998).

4. Stevenson, B.R. & Keon, B.H. The tight junction: morphology to molecules. *Ann. Rev. Cell Dev. Biol.* **14**, 89-109 (1998).

5. Yap, A.S., Brieher, W.M. & Gumbiner, B.M. Molecular and functional analysis of cadherin-based adherens junctions. *Ann. Rev. Cell Dev. Biol.* **13**, 119-146 (1997).

6. Garrod, D., Chidgey, M. & North, A. Desmosomes: differentiation, development, dynamics, & disease. *Curr. Opin. Cell Biol.* **5**, 670-678 (1996).

7. Lingrel, J.B. *et al.* Structure-function studies of the Na,K-ATPase. *Kidney Int.* **45**, Suppl. 44, S32-S39 (1994).

8. Katz, A.I. Role of Na-K-ATPase in kidney function in *The Na^+,K^+ Pump. Part B. Cellular Aspects* (ed. Skou, J.C., Norby, J.G., Maunsbach, A.B. & Esmann, M.) 207-232 (Alan R. Liss Inc., New York, 1988).

9. McNeil, H., Ozawa, M., Kemler, R. & Nelson, W.J. Novel function of the cell adhesion molecule uvomurulin as an inducer of cell surface polarity. *Cell* **62**, 309-316 (1990).

10. Imhof, B.A., Vollmers, H.P., Goodman, S.L. & Birchmeier, W. Cell-cell interaction and polarity of epithelial cells: specific perturbation using a monoclonal antibody. *Cell* **35**, 667-75 (1983).

11. Gumbiner, B., Stevenson, B. & Grimaldi, A. The role of the cell adhesion molecule uvomorulin in the formation and maintenance of the epithelial junctional complex. *J. Cell Biol.* **107**, 1575-1587 (1988).

12. Watabe, M., Nagafuchi, A., Tsukita, S. & Takeichi, M. Induction of polarized cell-cell association and retardation of growth by activation of the E-cadherin-catenin adhesion system in a dispersed carcinoma cell line. *J. Cell Biol.* **127**, 247-256 (1994).

13. Shapiro, L. *et al.* Structural basis of cell-cell adhesion by cadherins. *Nature* **374**, 327-337 (1995).

14. Troxell, M.L. *et al.* Inhibiting cadherin function by dominant mutant E-cadherin expression increases the extent of tight junction assembly. *J. Cell Sci.* **113,** 985-996 (2000).

15. Rajasekaran, S.A. *et al.* Na,K-ATPase β-subunit is required for epithelial polarization, suppression of invasion, and cell motility. *Mol. Biol. Cell* **12**, 279-295 (2001).

16. Ridley, A.J. & Hall. A. The small GTP-binding protein rho regulates the assembly of focal adhesions and actin stress fibers in response to growth factors. *Cell* **70**, 389-399 (1992).

17. Mackay, D.J.G. & Hall, A. Rho GTPases. *J. Biol. Chem.* **273**, 20685-20688 (1998).

18. Van Aelst, L. & D'Souza-Schorey, C. Rho GTPases and signaling networks. *Genes and Development* **11**, 2295-2322 (1997).

19. Nusrat, A. *et al.* Rho protein regulates tight junctions and perijunctional actin organization in polarized epithelia. *Proc. Natl. Acad. Sci.* **92**, 10629-10633 (1995).

20. Takaishi, K., Sasaki, T., Kotani, H., Nishioka, H. & Takai, Y. Regulation of cell-cell adhesion by Rac and Rho small G proteins in MDCK cells. *J. Cell. Biol.* **139**, 1047-1059 (1997).

21. Jou, T.-S., Schneeberger, E.E. & Nelson, W.J. Structural and functional regulation of tight junctions by RhoA and Rac1 small GTPases. *J. Cell Biol.* **142**, 101-115 (1998).

22. Gonzalez-Mariscal, L., Chavez de Ramirez, B. & Cereijido, M. Tight junction formation in cultured epithelial cells (MDCK). *J. Membrane Biol.* **86**, 113-125 (1985).

23. Rajasekaran, A.K., Hojo, M., Huima, T. & Rodriguez-Boulan, E. Catenins and Zonula Occludens-1 form a complex during early stages in the assembly of tight junctions. *J. Cell Biol.* **132**, 451-463 (1996).

24. Ojakian, G.K. & Schwimmer, R. The polarized distribution of an apical cell surface glycoprotein is maintained by interactions with the cytoskeleton of Madin-Darby canine kidney cells. *J. Cell Biol.* **107**, 2377-2387 (1988).

25. Buffin-Meyer, B. *et al.* Regulation of renal Na^+,$K(^+)$-ATPase in rat thick ascending limb during K^+-depletion: evidence for modulation of Na^+ affinity. *J. Physiology* **490**, 623-632 (1996).

26. Pressley, T.A. Ion concentration-dependent regulation of Na,K-pump abundance. *J. Membrane Biol.* **105**, 187-195 (1988).

27. Pollack, L.R., Tate, E.H. & Cook, J.S. Na^+,K^+-ATPase in HeLa cells after prolonged growth in low K^+ or ouabain. *J. Cell Physiol.* **106**, 85-97 (1981).

28. Yamamoto, K., Ikeda, U., Seino, Y., Tsuruya, Y., Oguchi, A., Okada, K., Ishikawa, S., Saito, T., Kawakami, K., Hara, Y. & Shimada, K. Regulation of Na,K-adenosine triphosphatase gene expression by sodium ions in cultured neonatal rat cardiocytes. *J. Clin. Invest.* **92**, 1889-1895 (1993).

29. Rayson, B.M. Rates of synthesis and degradation of Na+,K+-ATPase during chronic ouabain treatment. *Am. J. Physiol.* **256**, C75-C80 (1989).

30. Rothstein, A. & Mack, E. Volume-activated K^+ and Cl^- pathways of dissociated epithelial cells (MDCK): role of Ca^{2+}. *Am. J. Physiol.* **258**, C827-C834 (1990).

31. Vaaraniemi, J., Huotari, V., Lehto, V.P. & Eskelinen, S. Effect of PMA on the integrity of the membrane skeleton and morphology of epithelial MDCK cells is dependent on the activity of amiloride-sensitive ion transporters and membrane potential. *Eur. J. Cell Biol.* **74,** 262-272 (1997).

32. Vasioukhin, V., Bauer, C., Yin, M. & Fuchs, E. Directed actin polymerization is the driving force for epithelial cell-cell adhesion. *Cell* **100**, 209-219 (2000).

33. Jou, T.-S. & Nelson, W.J. Effects of regulated expression of mutant RhoA and Rac1 small GTPases on the development of epithelial (MDCK) cell polarity. *J. Cell Biol.* **142,** 85-100 (1998).

34. Zhu, K., Debrecini, B., Li, R. & Zheng, Y. Identification of Rho GTPase-dependent sites in the DH domain of oncogenic Dbl that are required for transformation. *J. Biol. Chem.* **275**, 25993-26001 (2000).

35. Ren, X., Kiosses, W. & Schwartz, M.A. Regulation of the small GTP-binding protein Rho by cell adhesion and the cytoskeleton. *EMBO J.* **18**, 578-585 (1999).

36. Leung, S.-M. *et al.* Modulation of endocytic traffic in polarized Madin-Darby canine kidney cells by the small GTPase RhoA. *Mol. Biol. Cell* **10**, 4369-4384 (1999).

37. Potempa, S. & Ridley, J.A. Activation of both MAP kinase and phosphatidylinositide 3-kinase by Ras is required for hepatocyte growth factor/scatter factor-induced adherens junction disassembly. *Mol. Biol. Cell* **9**, 2185-2200 (1998).

38. Balda, M.S. *et al.* Functional dissociation of paracellular permeability and transepithelial electrical resistance and disruption of the apical-basolateral intramembrane diffusion barrier by expression of a mutant tight junction membrane protein. *J. Cell Biol.* **134**, 1031-1049 (1996).

39. Hall, A. Rho GTPases and the actin cytoskeleton. *Science* **279**, 509-514 (1998).

40. Fernandez, R. & Malnic, G. H^+ ATPase and Cl^- interaction in regulation of MDCK cell pH. *J. Membrane Biol.* **163**, 137-145 (1998).

41. Le, T.L., Yap, A.S. & Stow, J.L. Recycling of E-cadherin: A potential mechanism for regulating cadherin dynamics. *J. Cell Biol.* **146**, 219-232 (1999).

Figure Legends:

Figure 1. Inhibition of Na,K-ATPase activity prevents the formation of tight junctions and desmosomes and the induction of polarity in MDCK cells. (A-D) Immunofluorescence localization of ZO-1. At zero hour in both control (A) and ouabain-treated cells (C) the ZO-1 staining is intracellular. At three hours ouabain-treated cells show incomplete ZO-1 rings (arrows in D) as compared to the complete ring-like staining revealed by control cells (B). (E) Transepithelial electrical resistance measurement. Ouabain-treated cells did not show an increase in the TER over time. (F-I) Immunofluorescence localization of desmocollin. Note that in ouabain-treated cells the desmocollin staining is predominantly intracellular (I) as compared to control cells (G). At zero hour in both control (F) and ouabain-treated cells (H) the desmocollin staining is intracellular. (J, K). Transmission electron microscopy. Tight junctions (arrows), adherens junctions (arrowheads), and desmosomes (asterisks) were formed in control cells (J), while ouabain-treated cells (K) had no tight junctions and desmosomes. Inserts are the higher magnification of the tight junction regions in J and K. (L-O). Confocal microscope X-Z sections. Note the basolateral localization of β-catenin (L) and GP135 (N) in control cells and non polarized distribution of these markers in ouabain treated cells (M and O). Scale bars in A-D and F-I = 10μ, J and K = 500nm and L-O 5μ.

Figure 2. Na,K-ATPase mediated inhibition of formation of tight junctions and desmosomes is reversible. Immunofluorescence localization of ZO-1 (A and B) and desmocollin (C and D). Cells incubated in K^+-free medium show an incomplete ZO-1 ring at the plasma membrane region (A) and intracellular localization of desmocollin (C). Replenishment of K^+ results in a complete ZO-1 ring (B) and plasma membrane localization of desmocollin (D).

(E). Measurement of TER. Note an increase in the TER as soon as the cells are shifted to K^+-containing medium. (F and G). Transmission electron microscopy shows junctional complexes. Note the absence of tight junctions and desmosomes under K^+-free medium (F) and their presence in K^+-containing medium (G). Inserts in F and G are the tight junction regions. (H-K) Confocal microscope X-Z sections. Note the non-polarized distribution of β-catenin (H) and GP135 (J) in under K^+-depleted condition and the polarized distribution of β-catenin (I) and GP135 (K) after K^+-repletion. Scale bars in A-D = 10μ, F and G = 500nm, and H-K=5μ.

Figure 3. Ouabain treatment under sodium free conditions does not affect the formation of tight junctions and desmosomes. (A and B) and (C and D) are the immunofluorescence localization of ZO-1 and desmocollin, respectively. Note the comparable staining pattern in control (A, C) and ouabain-treated (B, D) cells. (E). Measurement of TER. (F, G) Transmission electron micrographs of control (F) and ouabain-treated (G) cells show tight junctions and desmosomes. Inserts are the higher magnification of the tight junction region in F and G. (H-K) Confocal microscope X-Z sections. Note the polarized distribution of β-catenin and GP135 in control and ouabain treated cells. Scale bars in A-D = 10μ, F and G are 500nm and 1μ, respectively, and H-K 5μ.

Figure 4. Treatment of MDCK cells with the sodium ionophore gramicidin inhibits the formation of tight junctions. (A, C), immunofluorescence localization of ZO-1 and desmocollin, (B, D), respectively, of gramicidin (A, B) and valinomycin (C, D) treated cells. (E). TER measurement of gramicidin and valinomycin treated cells. (F-I) Confocal microscope X-Z sections. Scale bars in A-D = 10μ, F-I=5μ.

Figure 5. Inhibition of Na,K-ATPase prevents the formation of bundled stress fibers and inhibits RhoA GTPase activity. (A-F) FITC-phalloidin staining of filamentous actin. At 0 hours no stress fibers were detected in control cells (A) and cells treated with ouabain (C). Bundled stress fibers were present at 3 hours in control cells (B, arrows) but were not detected in ouabain-treated cells (D). In panels E and F phalloidin labeling of cells maintained under K^+-free condition (E) and cells transferred to K^+-containing medium (F) are shown. Note the presence of bundled stress fibers (arrows) after transfer to K^+-containing medium. Scale bars in A-F = 10μ. (G and G'). Effect of ouabain treatment on RhoA activity. (G) Immunoblot showing active and total RhoA in ouabain and control cells. The results shown are the representative data obtained from three independent experiments. (G') Quantification of the immunoblot data represents the average of three independent determinations done in duplicates. Bars indicate the standard error. For control the error bars are so small that they are not seen in the figure. (H and H'). Effect of K^+ depletion and repletion on the RhoA activity. Immunoblot of active and total RhoA (H) and quantification of the immunoblot data (H') representing the mean of two independent determinations done in duplicates. (I and I'). Effect of gramicidin and valinomycin on RhoA activity. Immunoblot of total and active RhoA (I) and quantification of the immunoblot data done in duplicates (I').

Figure 6. Formation of tight junctions, desmosomes and the induction of polarity in ouabain treated MDCK-RhoA $_{wt}$ cells over expressing RhoA. (A) Immunoblot showing induced Myc-tagged (*) RhoA after the withdrawal of the doxicycline. (B). Relative levels of active RhoA GTPase. (C,D). FITC-phalloidin staining of filamentous actin. (E,F). Immunofluorescence of ZO-1. (G,H). Immunofluorescence of desmocollin. (I). Measurement

TER (J-M). Confocal microscope X-Z sections. (N,O). Transmission electron microscopy. Inserts are the higher magnification of the tight junction region in N and O. Scale bars in J-M =5μ and N and O = 500nm.

Figure 7. E-cadherin and catenin expression in Ouabain-treated MDCK cells. (A-D) Immunofluorescence of E-cadherin. At 0 hour E-cadherin was localized intracellular in both control (A) and ouabain-treated (C) cells. At 3 hours E-cadherin was localized on the plasma membrane in control cells (B) and in ouabain-treated cells (D). (E) Immunoblot analysis of E-cadherin, α-catenin, β-catenin, and γ-catenin. Ouabain-treatment of MDCK cells during Ca^{2+}-switch did not significantly alter the expression levels of either E-cadherin, α-catenin, β-catenin, or γ-catenin. Scale bar = 10μ.

Figure 8. Schematic model of the formation of tight junctions and desmosomes in epithelial cells. (See text for details).

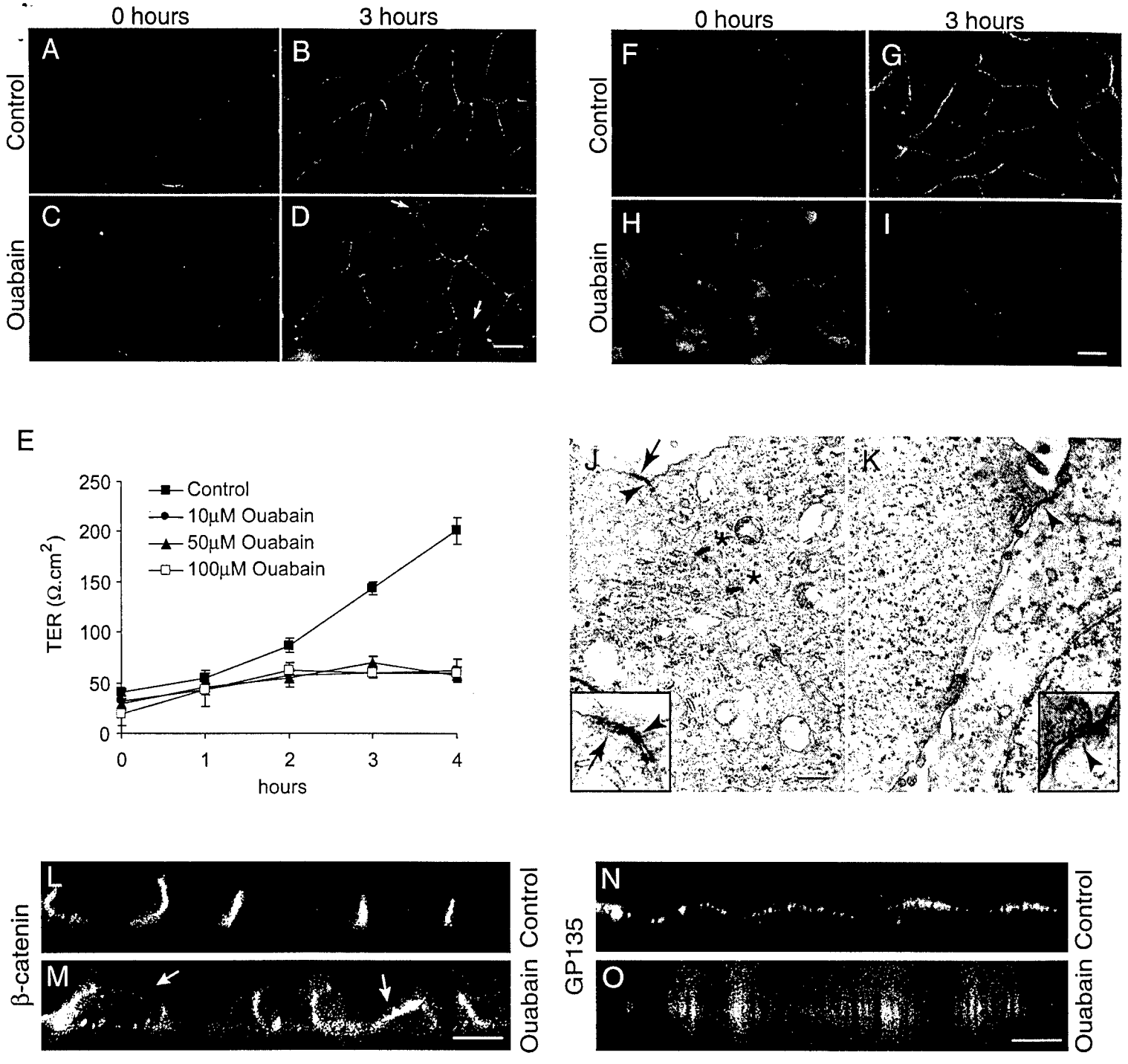
0 hours
3 hours
A
B
Control
C
D
Ouabain
0 hours
3 hours
F
G
Control
H
I
Ouabain
E
250
200
150
100
50
0
TER (Ω.cm²)
Control
10μM Ouabain
50μM Ouabain
100μM Ouabain
0
1
2
3
4
hours
J
K
β-catenin
L
M
Ouabain Control
GP135
N
O
Ouabain Control

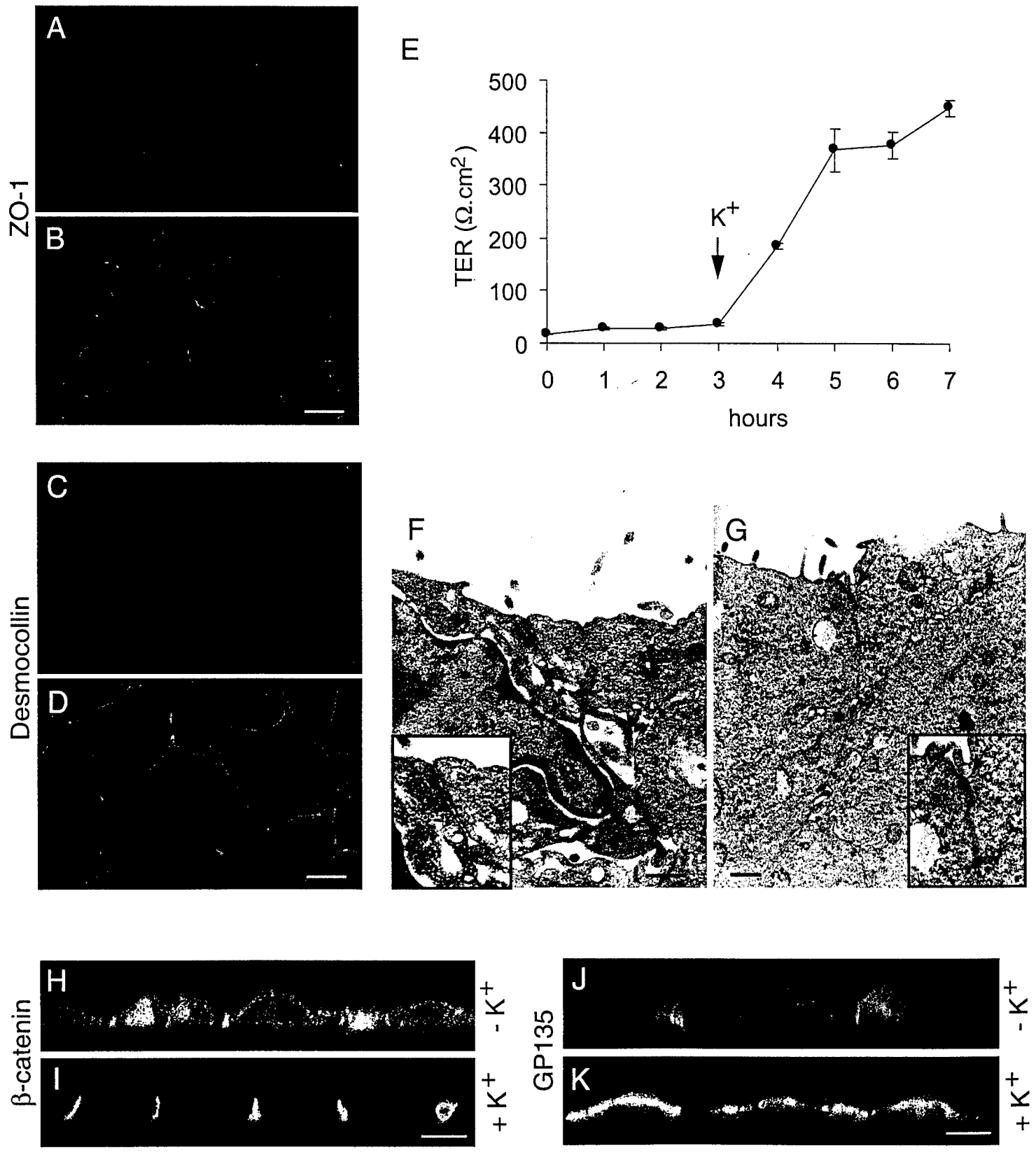
A
B
ZO-1
C
D
Desmocollin
E
500
400
300
200
100
0
TER (Ω.cm²)
K+
0 1 2 3 4 5 6 7
hours
F
G
H
I
β-catenin
- K+
+ K+
J
K
GP135
- K+
+ K+

A
B
ZO-1
Control
Ouabain
C
D
Desmocollin
Control
Ouabain
E
800
600
400
200
0
TER(Ω.cm2)
Control
Ouabain
0
1
2
3
4
hours
F
G
H
I
β-catenin
Ouab Con
J
K
GP135
Ouab Con

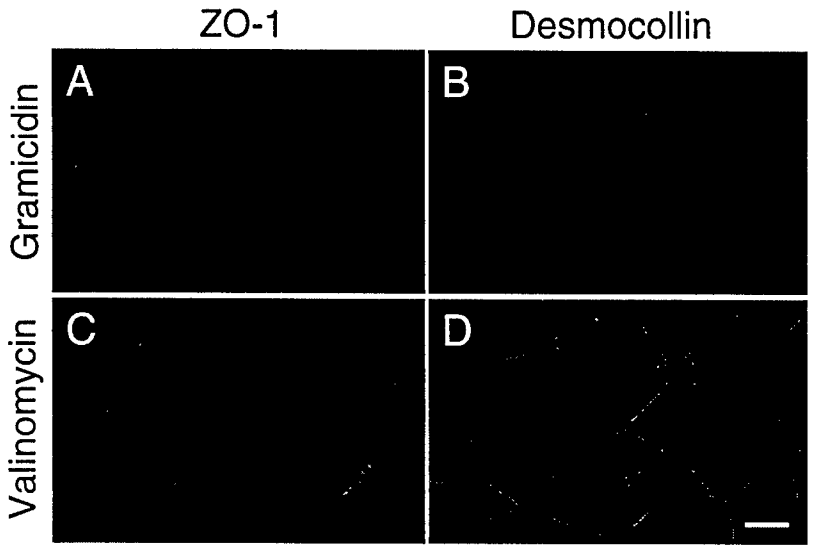
ZO-1
Desmocollin
A
B
C
D
Gramicidin
Valinomycin

E

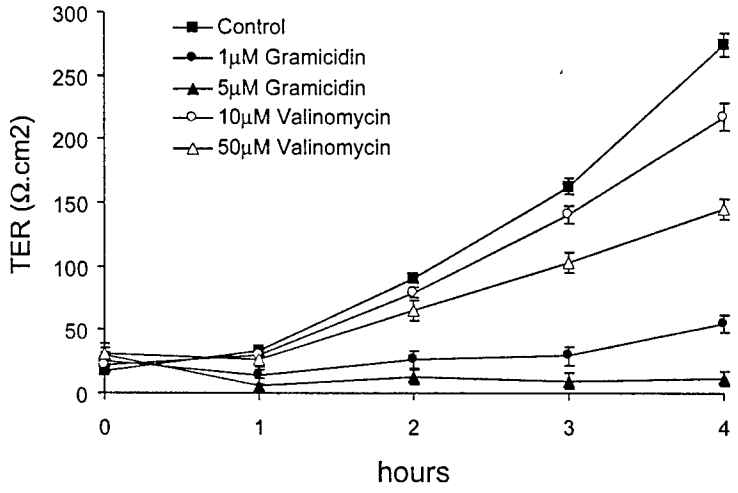
Control
1μM Gramicidin
5μM Gramicidin
10μM Valinomycin
50μM Valinomycin
TER (Ω.cm2)
300
250
200
150
100
50
0
0
1
2
3
4
hours

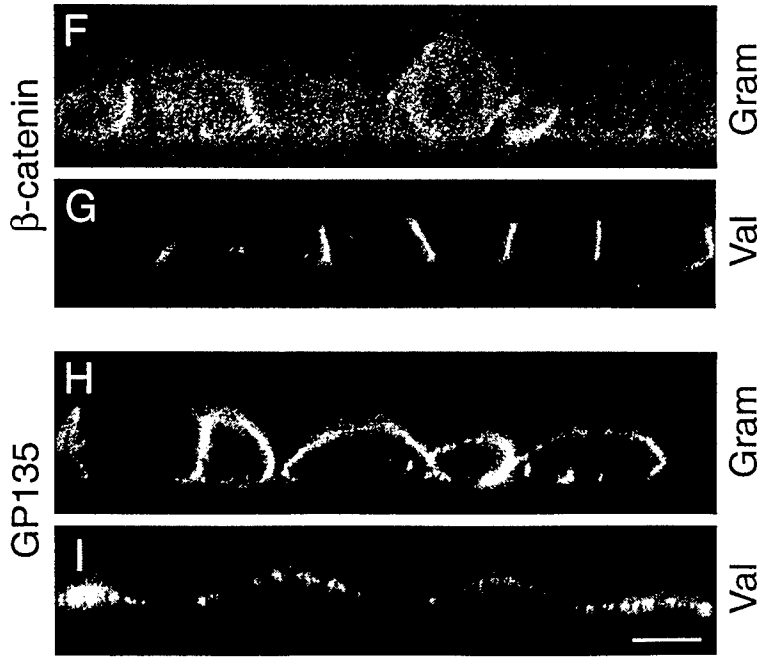
F
G
H
I
β-catenin
GP135
Gram
Val
Gram
Val

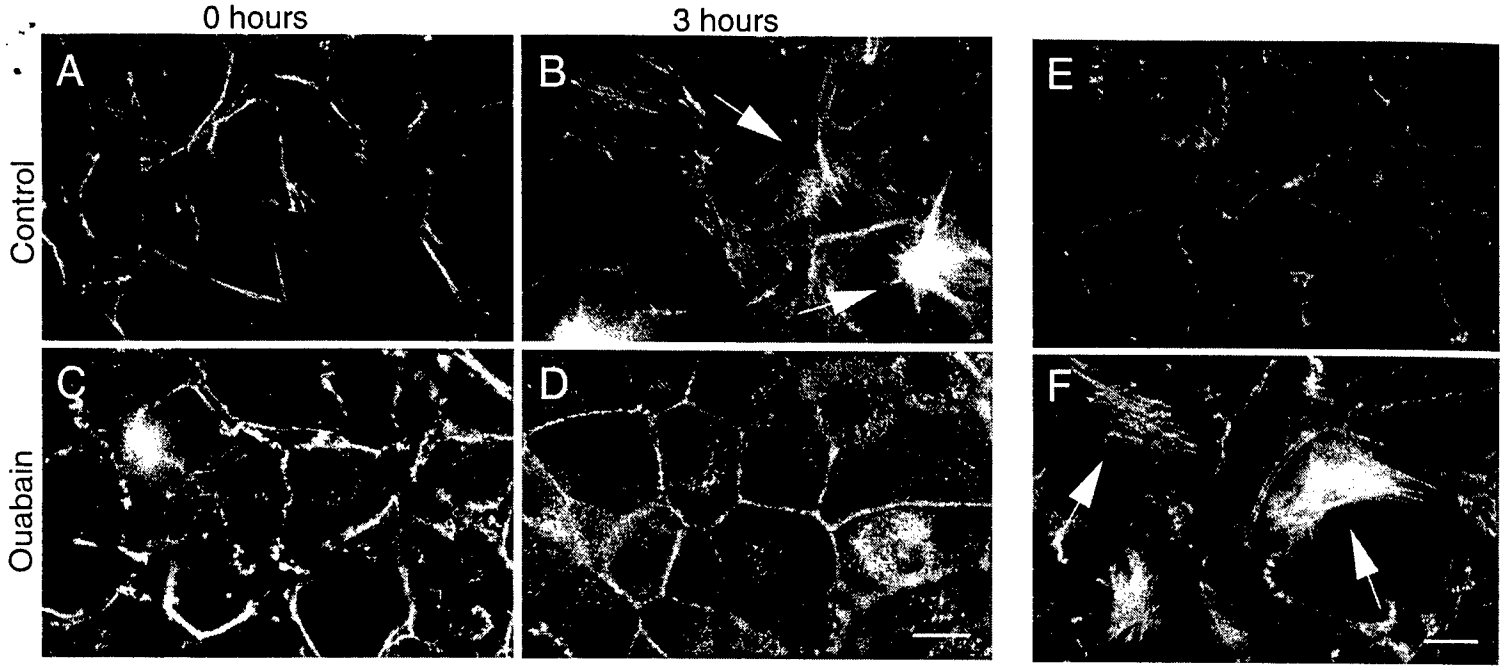
0 hours
3 hours
A
B
E
Control
C
D
F
Ouabain

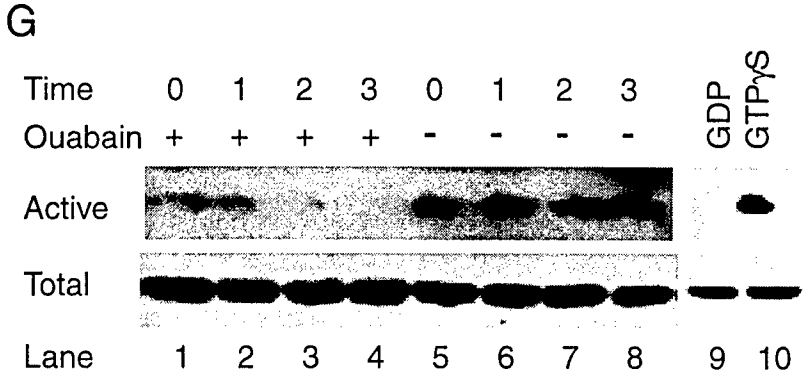
G
Time 0 1 2 3 0 1 2 3
Ouabain + + + + - - - -
GDP
GTPγS
Active
Total
Lane 1 2 3 4 5 6 7 8 9 10

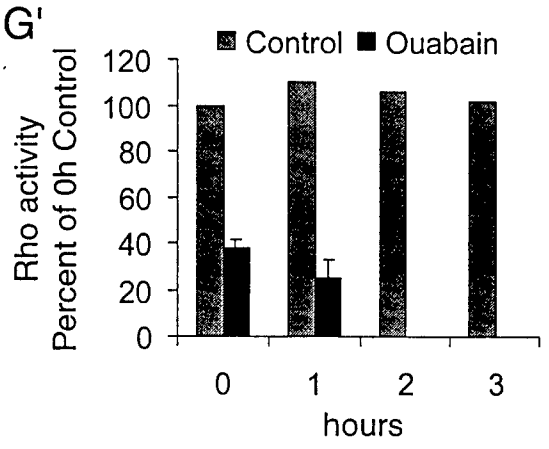
G'
Control
Ouabain
Rho activity
Percent of 0h Control
120
100
80
60
40
20
0
0 1 2 3
hours

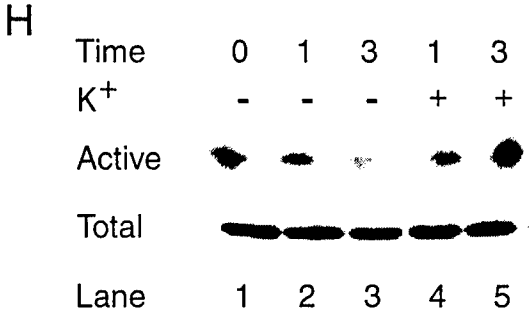
H
Time 0 1 3 1 3
K+ - - - + +
Active
Total
Lane 1 2 3 4 5

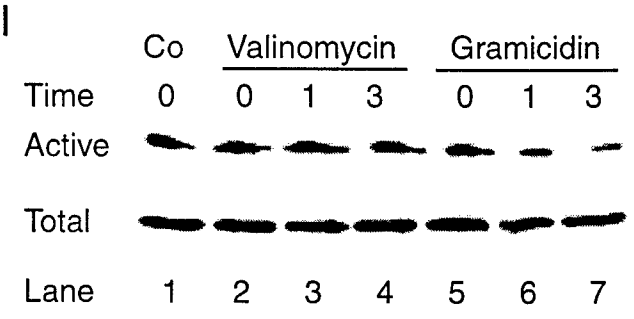
I
Co
Valinomycin
Gramicidin
Time 0 0 1 3 0 1 3
Active
Total
Lane 1 2 3 4 5 6 7

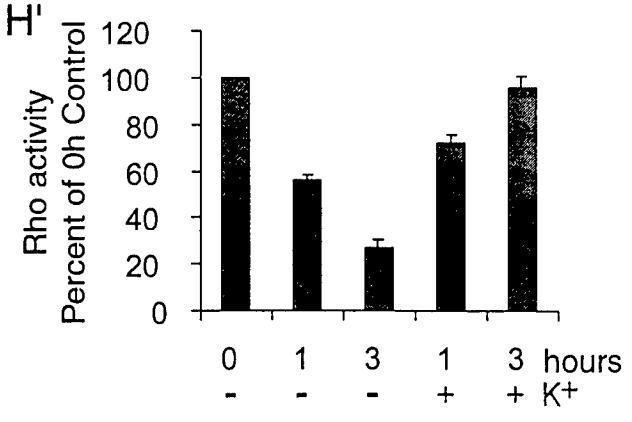
H'
Rho activity
Percent of 0h Control
120
100
80
60
40
20
0
0 1 3 1 3 hours
- - - + + K+

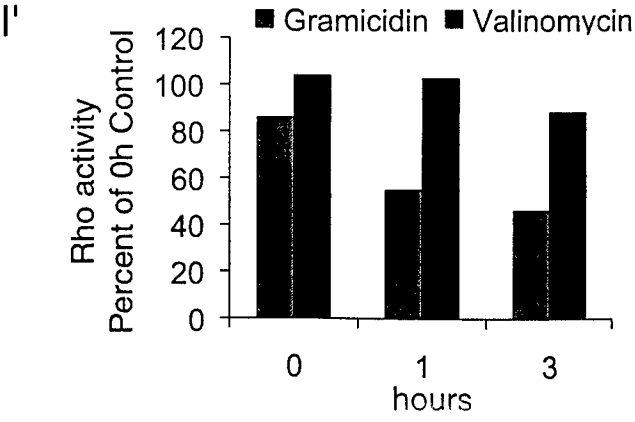
I'
Gramicidin
Valinomycin
Rho activity
Percent of 0h Control
120
100
80
60
40
20
0
0 1 3
hours

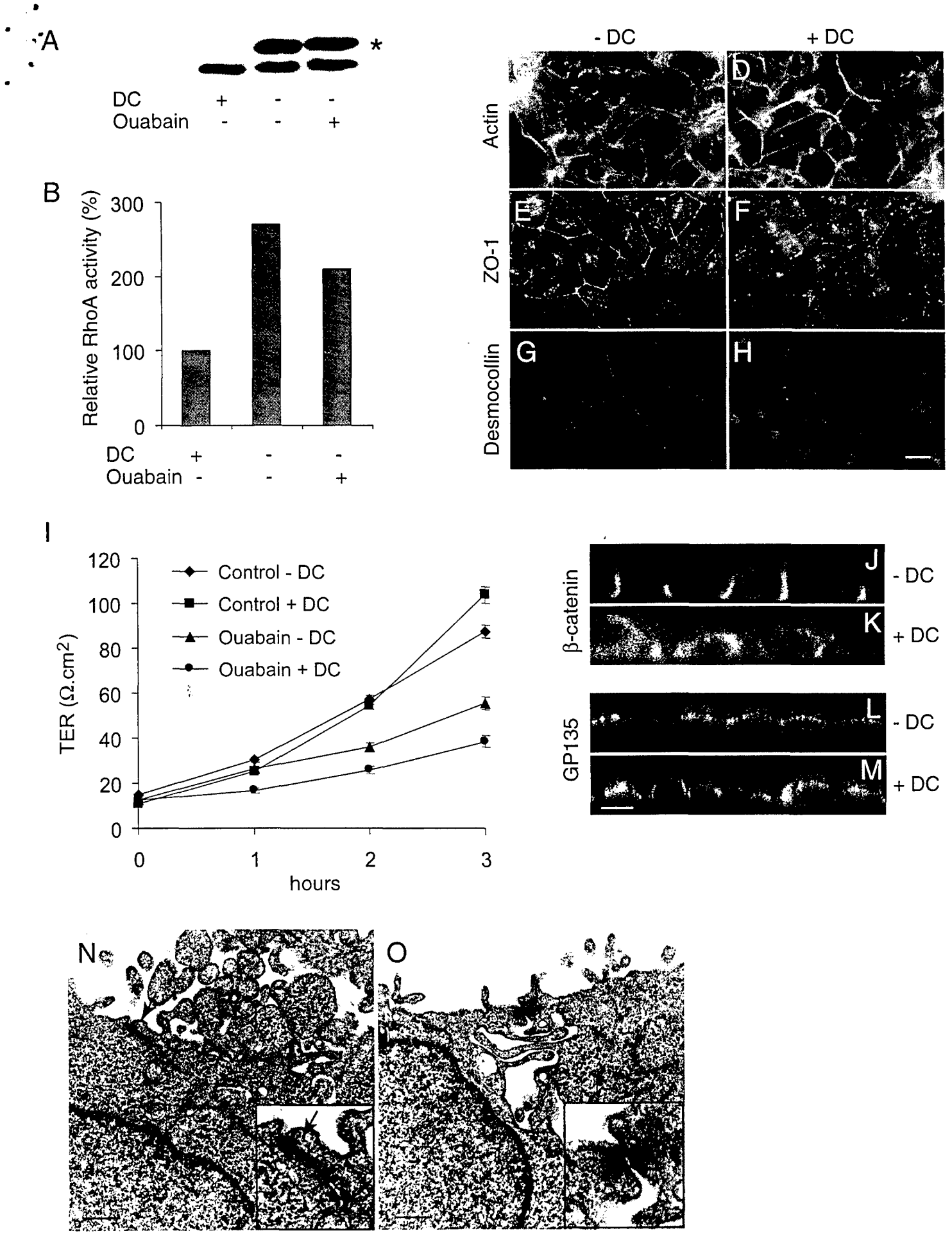
A
*
DC + - -
Ouabain - - +
B
Relative RhoA activity (%)
300
200
100
0
DC + - -
Ouabain - - +
- DC
+ DC
Actin
ZO-1
Desmocollin
D
E
F
G
H
I
TER (Ω.cm²)
120
100
80
60
40
20
0
Control - DC
Control + DC
Ouabain - DC
Ouabain + DC
0
1
2
3
hours
β-catenin
GP135
J
K
L
M
- DC
+ DC
- DC
+ DC
N
O

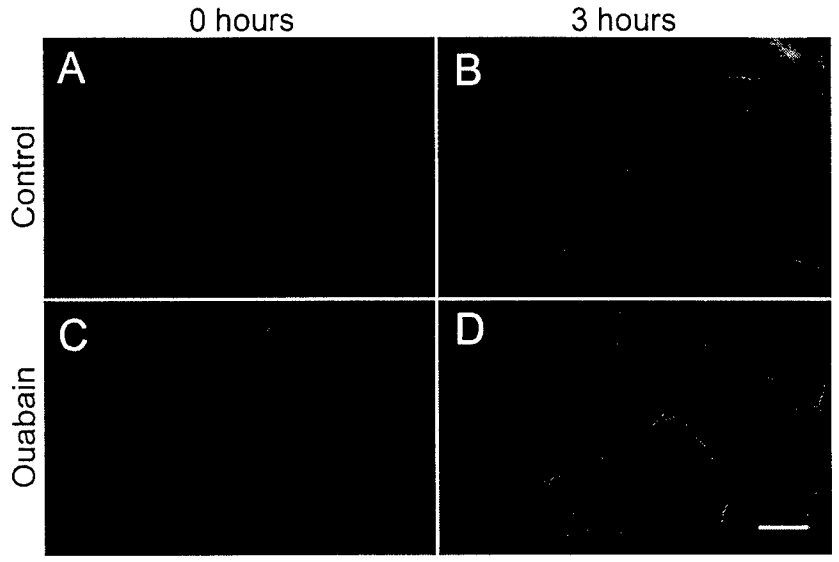
0 hours
3 hours
A
B
C
D
Control
Ouabain

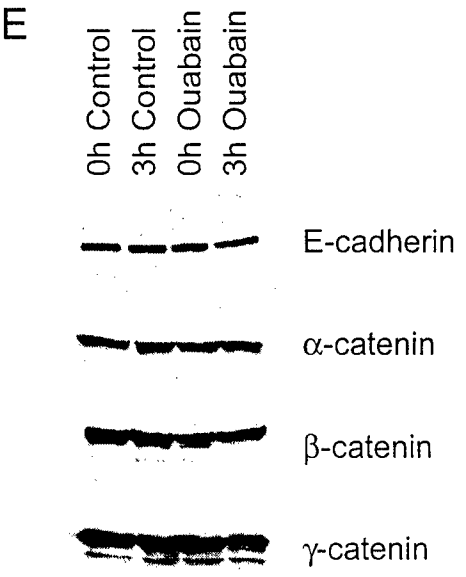
E
0h Control
3h Control
0h Ouabain
3h Ouabain
E-cadherin
α-catenin
β-catenin
γ-catenin

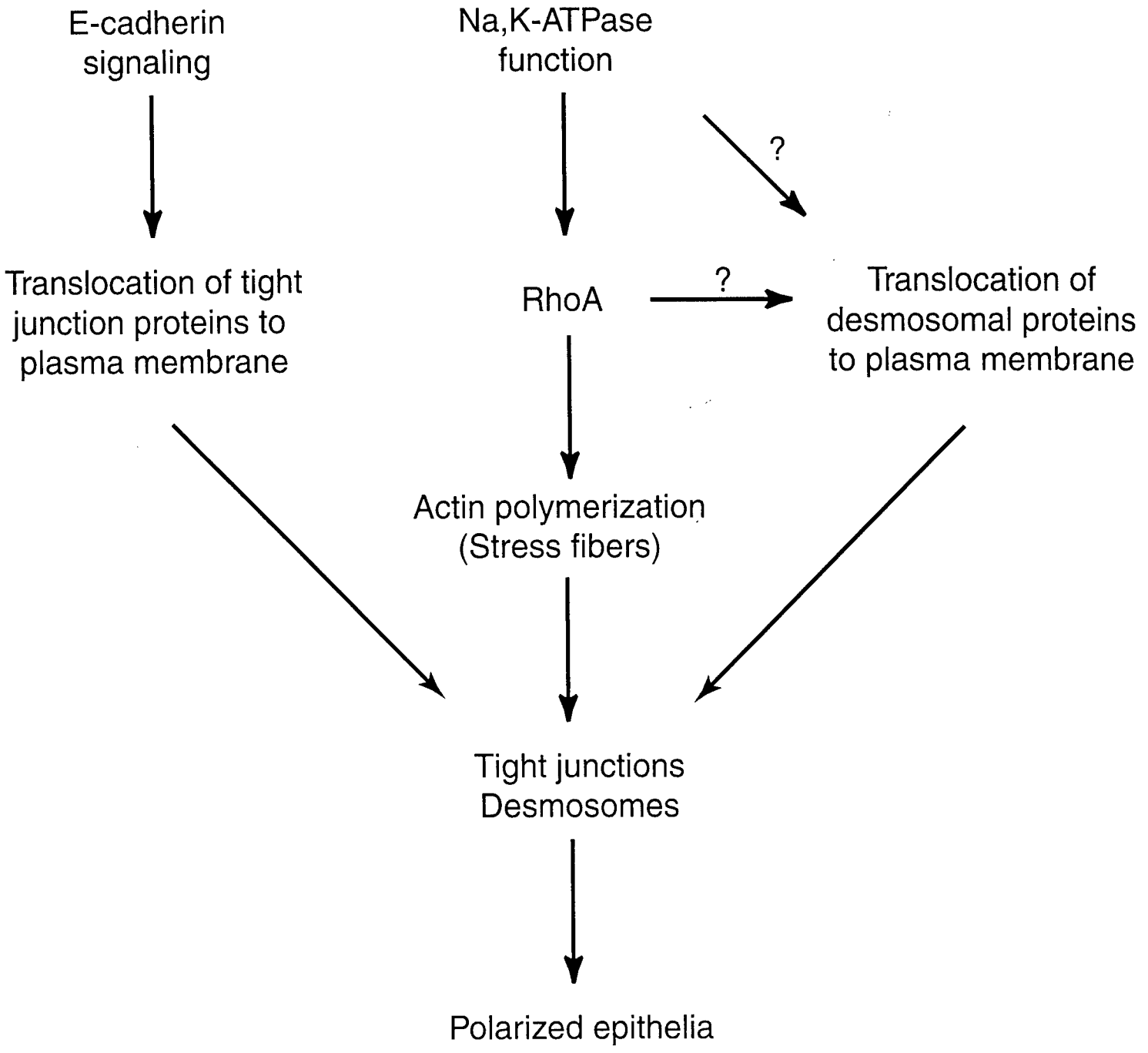
E-cadherin signaling
Na,K-ATPase function
?
Translocation of tight junction proteins to plasma membrane
RhoA
?
Translocation of desmosomal proteins to plasma membrane
Actin polymerization (Stress fibers)
Tight junctions Desmosomes
Polarized epithelia